MACROSCOPIC STUDY OF ROTATIONS OF DEFORMED EVEN-EVEN NUCLEI IN THE RARE-EARTH REGION

A Thesis Submitted

In Partial Fulfilment of the Requirements

for the Degree of

DOCTOR OF PHILOSOPHY

By

VITTAL RAO PRAKASH

to the

DEPARTMENT OF PHYSICS

INDIAN INSTITUTE OF TECHNOLOGY KANPUR

APRIL, 1974

DEDICATED

TO THE MEMORY OF

MY SISTER RUKMINI

STATEMENT

I hereby declare that the work presented in this thesis is the result of investigations carried out by me in the Department of Physics, Indian Institute of Technology, Kanpur, India under the supervision of Professor V.K. Deshpande.

In keeping with the general practice of reporting scientific observations, due acknowledgement has been made wherever the work described is based on the findings of other investigators.

V.R. Prakash

V.R. Prakash

CERTIFICATE

Certified that the work presented in this thesis entitled "Macroscopic Study of Rotations of Deformed Even-Even Nuclei in the Rare-Earth Region" has been carried out by Mr. V.R. Prakash under my supervision and that the same has not been submitted elsewhere for a degree.

V.K. Deshpande

V.K. Deshpande
Professor
Department of Physics
Indian Institute of Technology Kanpur

ACKNOWLEDGEMENTS

I thank Professor V.K. Deshpande for initiating me into the research problem, and for his valuable guidance on various occasions. I should like to be specially grateful to him for helping me to develop increasing awareness and insight not only in the area of research activity, but also in various other areas of general interest, through several stimulating discussions, constructive criticisms and valuable suggestions.

I am grateful to my friend and colleague, Mr. B.M. Bahal for his continued interest and assistance in the research problem.

The completion of writing of a thesis of this kind depends upon the assistance and cooperation of many persons. I am indebted to all of them, especially to Messrs. B.K. Srivastava, T.K. Sharma, H.R. Prabhakara, K. Naidu, K.K. Dwivedi, T. Raman, D.G. Kanhere and Miss Keya Sur. Thanks are due to Mr. M.H. Natu for neatly typing the text, and to Comrade R.S. Misra of Central Workshop for his generous help in cyclostyling of the same.

Last but not the least, I should like to express my most intimate thanks to Kum. Bharathi for her untiring forbearance and endurance. She has been a source of inspiration and encouragement all through. Finally, I wish to express my gratitude to Smt. Rukmini Devi and her children, Kums. Sarada and Sailaja, for their kind hospitality and encouragement.

V.R. Prakash

CONTENTS

LIST OF TABLES

LIST OF FIGURES

SYNOPSIS

1. TWO MASS-POINT MODEL

Gupta (1969) obtained satisfactory values of $E(L)/E(2)$, $L = 4,6$, etc., for the deformed nuclei in the region $150 < A < 1$ by representing a typical nucleus by a two mass-point system with a harmonic restoring force as a function of the distance between them and using semi-classical treatment. Although the model is not applicable to spherical nuclei, for deformed nuclei in the rare-earth region, it correlates the quadrupole moment and the moment of inertia data more satisfactorily than the rigi body or the hydrodynamic models. Such a representation of a nucleus is expected to be more appropriate for very large deformations, when the nucleus is about to undergo binary fissio However, what is rather interesting to note is that it is also applicable to nuclei with relatively small deformations.

Trainor and Gupta (1971) modified the above model to a governor model, so as to obtain zero moment of inertia for spherical nuclei, assuming that a central spherical portion of radius equal to the semi-minor axis of the spheroid does not participate in the rotational motion. The model was found to give satisfactory results.

In view of the above, it was felt that a quantum mechanical treatment of rotational-vibrational motion of the

two mass-point system with harmonic and with anharmonic potentials would yield better results as compared to the results of Gupta (1969). The energy expression thus obtained was found to contain in addition to the semi-classical terms (Gupta 1969), a beta vibrational energy term and a L-dependent zero point vibrational energy term, both contributing significantly to the energy of high angular momentum rotational states. Several quantities calculated on the basis of the model were found to be in better agreement with the corresponding experimental values. Besides, a number of features characteristic to these nuclei as obtained by Mariscotti et al (1969) and Mosel and Greiner (1968) are also observed for the two mass-point model. The variation of the stiffness with the proton and the neutron numbers is of particular interest (Prakash et al 1973).

Further, we have re-examined the governor model of Trainor and Gupta (1971), by choosing the radius of the rotationally invariant core as a variable, such that the two mass-point model and the governor model are obtained with appropriate limiting values of the radius of the core. The variation of relative densities inside and outside the spherical core as a function of its radius is rather interesting.

2. ROTATIONAL FLOW MODEL

As an improvement over the two mass-point model, we reconsidered the continuum model as proposed initially by Bohr

and Mottelson (1953). The flow of the continuum is known to be neither irrotational nor rigid. We, therefore, considered a rotational flow model (RFM) with a finite but uniform vorticity throughout the nuclear volume. The treatment was carried out in two dimensions with a subsequent generalization to flows in three dimensions. The velocity field for the case of pure rotation of the ellipsoidal boundary was uniquely found.

With the knowledge of the flow, the Hamiltonian of the system could be written down. It was shown that the Hamiltonian reduces to a rotational form $H = \sum_{j=1}^{3} (L_j^2/2I_{Ej})$ only if the vorticity components c_j are proportional to the rotational frequency w_j of the ellipsoidal boundary. It is thus concluded that in the continuum model, the intrinsic motion is strongly coupled with the rotational motion, and the adiabatic approximation is valid only if the proportionality constants (k_j) are much larger than unity. Assuming $c_j = k_j w_j$ an expression for the effective moment of inertia I_{Ej} as a function of k_j and the shape parameter $a_k/a_i = b_j$ was obtained. For $k_j = 0$ and 1, the flow corresponds to the rigid and the irrotational flow respectively, and it is found that the effective moment of inertia also goes over to the appropriate limiting values.

It was found that the experimental values of the moments of inertia and the quadrupole moments in the ground state rotational band of deformed even-even nuclei in the rare-earth

region could be accounted for by choosing the values of the vorticity constant (k_j) in the range 0.8 to 1.0. It was found that the value of the vorticity constant goes to 1, giving irrotational flow, as the nuclear deformation goes to zero. Thus, it is concluded that the nuclear flow which is rotational for deformed nuclei tends to become irrotational for spherical nuclei, with the consequent result that spherical nuclei do not show rotational spectrum.

The higher rotational bands have been analysed in terms of precessional motion of the ellipsoidal boundary with rotational flow. Small but finite values of moment of inertia about the longest axis in the ellipsoidal drop has been accounted for (Prakash et al. 1972, Prakash and Deshpande 197[illegible]).

Attempt is made to obtain a universal relationship between the vorticity and the shape parameter b_j valid for all rotational bands. Attempt is also made to write the Hamiltonian as a function of deformation from the determined flow pattern in order to estimate equilibrium deformation and vibrational stiffnes

REFERENCES

Gupta, R.K. (1969). Can. J. Phys. 47, 299.

Mariscotti, M.A.J., Goldhaber, G.S. and Buck, B. (1969). Phys. Rev. 178, 1864.

Mosel, U. and Greiner, W. (1968). Z. Phyk. 217, 256 and (1969). Nucl. Phys. A138, 241.

Prakash, V.R., Bahal, B.M. and Deshpande, V.K. (1972). Can. J. Phys. 50, 2957.

Prakash, V.R., Bahal, B.M. and Deshpande, V.K. (1973). Can. J. Phys. 51, No.23.

Prakash, V.R. and Deshpande, V.K. (1973). Can. J. Phys. 51, 1752.

C H A P T E R - I

INTRODUCTION

Phenomenological models have played a useful role in understanding nuclear structure ever since the introduction of the liquid drop model by Niels Bohr and Kalcker (1937). With the subsequent development of the single particle model independently by Mayer (1949) and Haxel, Jensen and Suess (1949), foundation was laid for the microscopic treatment of the nuclear system. While this model was eminently successful in accounting for the observed shell effects, processes like the fission continued to be studied in terms of the continuum model. While the understanding of the independent particle motion in terms of internucleon forces improved with the advent

of Brueckner's theory (1954), it was also becoming apparent that the nuclear system was capable of collective motion (Bohr 1952, Bohr and Mottelson 1953), such as rotations and vibrations. The relatively simple and common features of collective motion of a large number of nuclei permitted application of phenomenological models with advantage (Sood 1968). In such treatments it was not intended that the complicated motion of the nucleons be described. They were intended for classification and for inter-relating the large wealth of collective data. Such analysis brings out broad trends which are of interest in themselves and which provide guidelines for the microscopic treatments. In the recent past, significant advancement has been made in accounting for the collective behaviour of the nuclear system in terms of microscopic theories, while phenomenological treatments continued (Diamond et al 1964, Krutov 1968, Mariscotti et al 1969, Gupta 1969 and Trainor and Gupta 1971) to bring out inter-relating features.

The present work consists of exploration of some phenomenological macroscopic models to account for the rotational spectra of even-even nuclei primarily in the rare-earth region. In this region with $150 < A < 190$, rotational levels with spacing of the form $L(L+1)$ have been observed (Lieder et al 1971) up to $L = 22$. The simplest model which could be considered here is that of a rigid rotator. The broad features of

the observed spectra, such as L(L+1) dependence, and the existence of the higher precessional bands can indeed be accounted for, on the basis of this model. However, there is evidence that nuclei are not rigid. They can vibrate, and their moment of inertia increases (Sood 1968) with the spin L, so that there is noticeable departure from L(L+1) rule, as in the case of molecular rotation. The experimental value of the moment of inertia as obtained from absolute level spacing is found to be significantly smaller than the rigid body value obtained from nuclear mass and size. Finally, it is known that only the nuclei with finite deformation exhibit rotational spectra which is not true of rigid rotators.

Bohr and Mottelson (1953) considered the nucleus as a continuum, characterised by flows. Rigid rotation is then one possible flow of such a continuum. They assumed that the continuum is incompressible and that the flow is irrotational. The assumption of the irrotationality leads to possible shape vibrations but no rotation for nuclei with spherical equilibrium shape, in accordance with experimental observations. The Bohr-Mottelson treatment, however, led to vibrational frequencies which are too high and to values of moment of inertia which are too low. The experimental values of the moment of inertia, obtained from the observed rotational levels, therefore, lie between the rigid body values and the irrotational flow values.

While the Bohr-Mottelson continuum model over-estimated the absolute spacing, it provided a basis for the consideration of finer details of the relative spacing. Thus, the treatment assuming spheroidal shapes has been extended (Pal 1971) to ellipsoidal shapes. The increase in the moment of inertia with the angular momentum has been considered (Sood 1967, Gupta 1967, 1969) in terms of the centrifugal stretching of the non-rigid continuum.

Other phenomenological treatments have also been made. Thus, satisfactory fits have been obtained (Mariscotti et al 1969) by treating the moment of inertia as a variable parameter. Gupta (1968) has considered the deformed nucleus in terms of a two mass-point system. Trainor and Gupta (1971) have considered a governor model, where a deformed nucleus is considered as consisting of a non-rotational spherical core and the extra-spherical region responsible for the rotational moment of inertia.

The present work consists of two parts. In the first part, we have applied the two mass-point model to the even-even nuclei in the rare-earth region and have re-examined the governor model. In the second, we have considered the continuum model with flows of finite vorticity. The vorticity is assumed to be finite but uniform throughout the nuclear volume. The flow for the case of pure rotations is determined. The coupling of intrinsic flow (in the body fixed frame) with the rotational

motion is examined. An expression for the effective moment of inertia is obtained. Comparison with experimental results shows that the flow is rotational for deformed nuclei and it goes over to irrotational flow for spherical nuclei. Higher rotational bands have been analysed to account for the small but finite values of the moment of inertia about the longest axis of the ellipsoid. Attempt is made to obtain a relationship between the vorticity and the deformation and thus to write the Hamiltonian in terms of the deformation in order to estimate the equilibrium deformation and the vibrational stiffness.

In Chapter II, the available experimental data and the relevant theoretical methods to study the collective motion in even-even nuclei in the rare-earth region is discussed.

In Chapter III, the main features of the rigid body motion with its success and failures as applied to nuclear collective motion is presented.

In Chapter IV, the two mass-point representation of a deformed even-even nucleus is considered quantum mechanically.

In Chapter V, the general features of the continuum model are outlined.

Chapter VI presents the hydrodynamical model with a rotational flow and the last Chapter contains a summary of results.

REFERENCES

Bohr A. (1952). Kgl. Danske Videnskab. Selskab. Mat. Fys. Medd. 26, No. 14.

Bohr A. and Mottelson B.R. (1953). ibid., 27, No. 16.

Brueckner K.A. (1954). Phys. Rev. 96, 908.

Diamond R.M., Stephens F.S. and Swiatecki W.J. (1964). Phys. Letters. 11, 315.

Gupta R.K. (1967). Can. J. Phys. 45, 3521 and (1969). ibid., 47, 299.

Haxel O., Jensen J.H.D. and Suess H.E. (1949). Phys. Rev. 75, 1766.

Krutov V.A. (1968). Ann. Der. Physik. 7 Folge, Band 21, 263, 272, 281.

Lieder R.M., Beuscher H., Davidson W.F., Jahn P., Probst H.J. and Mayer-Böricke C. (1971). Private communication.

Mariscotti M.A.J., Goldhaber G.S. and Buck B. (1969). Phys. Rev. 178, 1864.

Mayer M. (1949). Phys. Rev. 75, 1969.

Niels Bohr and Kalcker F. (1937). Kgl. Danske. Videnskab. Selskab. Mat. Fys. Medd. 14, No. 10.

Pal M.K. (1971). Nucl. Phys. A183, 545.

Sood P.C. (1967). Phys. Rev. 161, 1063 and (1968). Nuclear Data Sect. A 4, 281.

Trainor L.E.H. and Gupta R.K. (1971). Can. J. Phys. 49, 133.

C H A P T E R - II

COLLECTIVE MOTION: EXPERIMENTAL AND THEORETICAL STATUS

The primary criterion for the success of a model proposed to account for the collective phenomenon in even-even nuclei in the rare-earth region, is to account satisfactorily for the available experimental data and their systematics. Hence, it will be appropriate, here, to discuss briefly some aspects of modern experimental methods employed in such studies, the systematics of the available experimental data and the theoretical methods to explain them.

II.1 Experimental Methods

The most promising tool, till date, for the exploration of the nuclear rotational and vibrational states is the Coulomb

excitation of a target nucleus by the electromagnetic field of charged projectiles which are not capable of penetrating into the region of nuclear forces. The information obtained out of such experiments regarding various nuclear properties such as spins and parities, transition rates, quadrupole moments, moments of inertia, magnetic moments, etc., are very accurate, for the theory of Coulomb excitation is accurately understood within the framework of electrodynamics. A collection of important papers and review articles on this subject is given by Alder and Winther (1966).

Recently, the use of heavy ion as a projectile has proved to be most useful in the study of collective phenomenon in nuclei. In this case, the electric field exerted by the projectile on the target is so large that higher order excitations occur. As the heavy ions carry large orbital angular momentum of the order of 50$\hbar$ to 100$\hbar$, excitation of rotational states of angular momentum as high as 20$\hbar$ has been possible. The process often results in multiple Coulomb excitations of the target nucleus, wherein the successive levels are excited by its predecessor, or eventually result in very high excitation of the target nucleus and then proceed to the evaporation of several neutrons or charged particles. This method has been very useful in the production and study of neutron deficient nuclei and has contributed immensely to the wealth of experimental data of such nuclei in the region $150 < A < 190$. An excellent review of heavy ion reaction has been given by Newton (1970).

Further, it has been found that the cross-sections and gamma ray angular distributions in Coulomb excitations depend to a measurable degree on the static quadrupole moments of nuclear levels. This is called the 're-orientation effect' and has recently become an important tool for measuring the static quadrupole moments of excited levels, especially, of some 'one-phonon' states in vibrational nuclei. A good review of this subject has been given by de Boer and Eichler (1968).

II.2 STUDY OF EXPERIMENTAL DATA

The experimental methods outlined above and many others finally provide us with the following experimental information:

(a) spins and parities of various levels

(b) electro-magnetic transition rates

(c) static and dynamic quadrupole moments

(d) magnetic moments

(e) energies of various states and corresponding moments of inertia.

II.2.1 Spins and Parities

In all even-even nuclei, following Pauli exclusion principle, the even number of protons and even number of neutrons will separately pair off among themselves to give a zero contribution to the total spin of the nucleus with a positive parity in its ground state. The ground state with $L^{\pi} = 0^{+}$ forms the head of a set of levels with sequence $L^{\pi} = 2^{+}, 4^{+}, 6^{+}$, etc., which constitute the ground state rotational band. Each time a spin repeats, it forms the head of a new excited band with a set of

levels built upon it with $\Delta L^{\pi} = 2^{+}$. At sufficiently high excitations ($\sim$ 1 MeV) a set of levels with $L^{\pi} = 1^{+}$, 2^{+}, 3^{+}, etc., have also been observed. $L^{\pi} = 1^{+}$ forms the head of yet another excited band and so on. The spin of the level forming the head of a particular band is usually denoted by K to distinguish it from the rest of its members. It will be shown later that K is nothing but the projection of L along the symmetry axis of a nucleus and is always less than or equal to L.

II.2.2 Electro-magnetic Transition Rates

The nuclei in the rare-earth region exhibit electric quadrupole transition rates which are about 100 times those of single particle estimates and hence is attributed to the collective excitation of a large number of nucleons. The reduced E2 transition probabilities for rotational excitations in even-even nuclei of spheroidal shape are given by (Bohr and Mottelson 1953)

$$B(E2) = \frac{15}{32\pi} e^2 Q_o^2 \frac{(L+1-K)(L+1+K)(L+2-K)(L+2+K)}{(L+1)(2L+3)(L+2)(2L+5)} \qquad (1)$$

for transitions of the type $L+2 \rightarrow L$ for a given K. Here Q_o is the intrinsic (static) quadrupole moment in the state L. For $L = K = 0$, eq.(1) gives a relationship between the B(E2) and Q_o^2 for the ground state of an even-even nucleus. In fact, B(E2) is related to the partial E2 gamma ray half-life ($T_{1/2}$) and the transition energy E_γ by the expression (Löbner et. al. 1970)

$$B(E2) = 56.56/(E_\gamma^5 T_{1/2}) \qquad (2)$$

for transitions of the type $2^+ \rightarrow 0^+$. Here $B(E2)$ is given in $e^2\ 10^{-48}\ cm^4$, $T_{1/2}$ in seconds, and E_γ in KeV.

Eq. (1) can be used to compare $B(E2)$ values between any two pairs of levels to obtain values of branching ratios.

II.2.3 Quadrupole Moments

The quadrupole moment of a nucleus arises out of the non-spherical distribution of charge and hence is a measure of the degree of departure of the nucleus from sphericity. The quadrupole moment defined with respect to an axis fixed in the body of the nucleus is called the intrinsic or the static quadrupole moment (Q_0) and that defined with respect to an axis fixed in space is called the dynamic or the spectroscopic quadrupole moment (Q). Hence, the value of Q for a given state is determined by the spin and the distribution of charge of the nucleus in that state, whereas Q_0 is determined only by the latter. In fact, for spheroidal nuclei, the two are related by the expression

$$Q = \frac{3K^2 - L(L+1)}{(L+1)(2L+3)} Q_0 \qquad (3)$$

Thus, in the ground state of a deformed even-even nucleus ($L = K = 0$) although Q is zero, Q_0 is not.

Assuming the nucleus to be a uniformly charged body of ellipsoidal shape with a_1, a_2, a_3 as the principal axes, the

following expression for Q_o is obtained (Kumar 1972)

$$Q_o/e = (Z/5)\left[(2a_3^2 - a_2^2 - a_1^2) + \sqrt{6}\,(a_2^2 - a_1^2)\right] \qquad (4)$$

The two terms within the square brackets respectively arise out of the axially symmetric deformation (β) and non-axially symmetric deformation (γ) of the nuclear surface

$$\sum_{j=1}^{3} (x_j^2/a_j^2) = 1$$

with $a_3 > a_2 > a_1$. Introducing polar coordinates and solving for $R(\theta,\phi)$, the parameters a_1, a_2, a_3 of the ellipsoid can be obtained in terms of the parameters β and γ (Kumar 1972).

$$a_j(\beta,\gamma) = \bar{R}_o(\beta,\gamma)\left[1+\sqrt{5/\pi}\,\beta\,\mathrm{Cos}\,(\gamma + 2\pi j/3)\right]^{1/2} \qquad (5)$$

where $\bar{R}_o(\beta,\gamma) = R_o\left[1 - (15/4\pi)\beta^2 + \frac{1}{2}\left(\frac{5}{\pi}\right)^{3/2}\beta^3\,\mathrm{Cos}3\gamma\right]^{-1/6}$

and $R_o^3 = a_1\,a_2\,a_3$.

Here R_o is the radius of the equal volume sphere. The ellipsoidal surface defined by eq. (5) is not identical to the quadrupole surface defined by Bohr and Mottelson (1953). However, for small spheroidal deformation ($\gamma = 0$), the parameter β is the same as that defined by Bohr and Mottelson. Assuming the nucleus to be a rigid prolate spheroid ($a_1 = a_2$ and $\gamma = 0$), for small symmetric deformation, eq. (3) combined with the eq. (5) approximately reduces to

$$Q_o/e \simeq (3/\sqrt{5\pi})\,ZR_o^2\,\beta(1+0.16\,\beta) \qquad (6)$$

The large values of B(E2) for all even-even nuclei in the region $150 < A < 190$ show that they are strongly deformed both in their ground and excited states. The values of β obtained from the known values of Q_o for the ground state range between 0.16 and 0.35, and is maximum for the nuclei in the middle of the region. The experimental data is available only for the ground state (0^+) and the first excited rotational state (2^+). The data for others is scarce.

It will be shown at the end of this section that there exists a definite correlation between the intrinsic quadrupole moment (Q_o) and the energy of the corresponding state. An excellent compilation of recent data on Q_o, obtained from various experiments has been given by Löbner et. al. (1970).

II.2.4 Magnetic Moments

The magnetic moment (μ) expressed in units of the nuclear magneton is

$$= \langle \bar{\mu}^o \cdot \bar{I} \rangle / (I + 1) \quad . \qquad (7)$$

where $\bar{\mu}_o = g_s \bar{s} + g_l \bar{l} + g_R \bar{R}$.

Here, g_s and g_l are respectively the g-factors for the intrinsic spin $\bar{s}$ and orbital angular momentum $\bar{l}$ of the nucleon, and g_R is that for the rotational angular momentum $\bar{R}$ of the nuclear surface. According to the above expression, all the even-even nuclei must have $\mu = 0$ in their ground state since their ground state spin is zero. This is true for all

even-even nuclei in the region $150 < A < 190$.

The experimental data available for nuclei of our interest is very sparse. In most of the determinations, the sign of μ is uncertain and only for three nuclei (^{152}Sm, ^{162}Dy, ^{164}Dy) the value of μ is known both in magnitude and sign. Hence, at present, it is hard to draw any conclusion regarding the systematics of μ. An excellent compilation of the experimental data on μ obtained from various experimental methods has been given by Fuller and Cohen (1969).

II.2.5 Systematics of Level Energies

We consider all the even-even nuclei lying between the closed shells $N = 82$, $Z = 50$ and $N = 126$, $Z = 82$. For nuclei near the closed shells, the first excited state is a singlet with spin-parity 2^+, the second is a triplet with spin parity 0^+, 2^+, 4^+, and it is experimentally found that the ratio of the energies between the two is about 2.2 thereby implying that these states may be vibrational in character. However, the degeneracy of the triplet state has been observed experimentally. As we move away from the closed shells, the energies of first and second excited states go progressively lower and the triplet state splitting becomes more and more prominent.

Nuclei in the region $158 < A < 186$ are found to have a set of low-lying excited states with spin-parity 0^+, 2^+, 4^+, 6^+, etc., with the energy of the lowest excited state (2^+) to be of the order of 100 KeV. The energies of these states, to a first

approximation, are found to be given by the familiar L(L+1) rule such that $E(4^+)/E(2^+) = 10/3$, $E(6^+)/E(2^+) = 7$, $E(8^+)/E(2^+) = 12$ and so on; implying that these states arise out of the rotations of the nucleus as a whole. However, for states with higher L the experimental energies go progressively below those expected from L(L+1) rule, indicating thereby that there is an increase in the moment of inertia of the nucleus, because a rotating nucleus can undergo centrifugal stretching. Usually, for a deformed nucleus the ground state moment of inertia (I_{expt}) is taken to be approximately equal to that calculated using the energy of 2^+ state and the L(L+1) rule. For large values of L the value of I_{expt}, thus calculated, is found to approach the rigid body value I_R.

A plot of the experimental values of quadrupole moments and energies of the 2^+ state as a function of neutron number (A-Z) for all even-even nuclei in the rare-earth region shown in Figure II.1 indicates that there is a definite correlation between the two data. Also, we see that for a given set of isotopes (same Z) in the region $84<(A-Z)<102$, the energy of 2^+ state is found to increase with the decrease in the neutron number whereas the corresponding quadrupole moment increases with the increase in the neutron number N. For nuclei in the region $102<(A-Z)<116$ the reverse of this case is observed. Also, it is clear from Figure II.1 that there is an asymmetry in some of the properties of the nuclei belonging to the two families.

Another rather interesting and important systematics recently found in these nuclei first by Johnson et. al. (1972) and subsequently by a number of others (Thieberger et. al. 1972; Lieder et. al. 1972) is that the variation of moment of inertia (I_{expt}) as a function of the square of rotational frequency ($\hbar\omega$) for all the states in the ground state rotational band follows a typical S-type curve for a given nucleus for which the energies of sufficiently high angular momentum states ($L^{\pi} > 14^{+}$) are known. The two quantities plotted in Figure II.2 for some of the rare-earth nuclei are given by (Appendix I)

$$(\hbar\omega)^2 = \frac{L^2-L+1}{(2L-1)^2}\left[E(L) - E(L-2)\right]^2 \text{ KeV}^2 \qquad (8)$$

$$(2I/\hbar^2) = \frac{2(2L-1)}{E(L)-E(L-2)} \text{ KeV}^{-1} \qquad (9)$$

where L can take the values 2,4,6, etc.

In addition to the low-lying levels described above, often groups of excited states (at energies around 1 MeV) with spin-parity $0^{+'}$, $2^{+'}$, $4^{+'}$, etc., and $0^{+'}$, $1^{+'}$, $2^{+'}$, etc., have also been experimentally observed. However, the experimental data in this part of the spectrum is so scarce that it is hard to draw any conclusion regarding their systematics. A very good compilation of the recent experimental energy level data for various rotational bands is given by Mitsuo Sakai (1970).

Thus, the spectrum exhibited by most nuclei near the closed shells is of vibrational type and as we go toward the

middle of the region there is a gradual transition from the vibrational type to the rotational type. However, the nuclei in the transition region, though a few in number, are found to exhibit both vibrational and rotational characteristics and hence are relatively complex to analyse.

II.3 THEORETICAL STUDIES

Basically there are two different approaches generally adopted in the study of nuclear collective motion: (i) microscopic and (ii) macroscopic.

The current microscopic investigations are mostly based on the shell model picture of the nucleus wherein it is assumed that each nucleon moves in a deformed effective field (this makes the model somewhat collective in nature) due to the rest, since the exact form of nucleon-nucleon interaction is not known. Although the model very successfully explained the experimental data and their trends in case of light nuclei ($A < 40$), it failed to do so for the nuclei in the region $150 < A < 190$ and $A > 220$. An excellent discussion of various microscopic theories of nuclear collective motion is given in the book by Rowe (1970).

Macroscopic studies of nuclear collective motion are based on the liquid drop model of the nucleus proposed by Niels Bohr and Kalckar (1937) and its subsequent developments. Perhaps, the most interesting aspect of its development has been its gradual merger with its chief competitor, the independent

particle model giving rise to the unified model (Bohr 1952, Bohr and Mottelson 1953), which could describe the collective and particle phenomena simultaneously. This idea has been developed considerably in recent years. In fact, the concept of particle interaction via the fields that they generate, which need not be static as in simple shell model, underlies virtually the whole of modern collective theory. Thus, the macroscopic models, although phenomenological in nature, have been instrumental in the development of microscopic theories.

As the work presented in this thesis is based on the phenomenological models of nuclear collective motion, it will be of use, here, to discuss the salient features of some of the important and recent phenomenological models.

II.4 STUDY OF MACROSCOPIC MODELS

For axially symmetric even-even nuclei in the rare-earth and actinide regions, the energies of rotational levels in the ground state band (K = 0) are approximately given by

$$E(L) = (\hbar^2/2I)\, L(L+1) \qquad (10)$$

where L = 0,2,4, etc., and I is rotational moment of inertia of the nucleus, the experimental value (I_{expt}) of which is obtained using the energy E(2) of the first excited L = 2 state. In quantum mechanics, the rotational moment of inertia of spherical systems is zero. In fact, since all directions in such a body are indistinguishable, it follows that it cannot be

brought into rotation (Nemirovskii 1960).

II.4.1 Rigid Spheroid Model

According to eq. (10) all the information about the rotating nucleus is contained in I. Hence, most of the phenomenological models aim at obtaining an analytical expression for I in terms of the shape parameters of the nucleus. Thus, for example, assuming the nucleus to be a rigid body of spheroidal shape, the value of I about an axis perpendicular to the symmetry axis is given by

$$I_R = (2/5)\, MR_o^2\, (1 + 0.31\beta + 0.42\beta^2 + \cdots) \qquad (11)$$

where M is the mass of the nucleus and $R_o = 1.2A^{1/3}$ fm., is the radius of equal volume sphere. It is found that the value of I_R is about twice that of I_{expt} and I_R does not go to zero as β goes to zero. Thus, the nucleus cannot be treated as a rigid body.

II.4.2 Irrotational Flow Model

Various other models have been developed assuming the nucleus to be a non-rigid body. The first of this kind of models is the irrotational flow model of Bohr and Mottelson (1953) based on the principles of hydrodynamics. They treated the vibrational-rotational motion of a deformed non-rigid liquid drop assuming the parameters β and γ to be time dependent, and the flow to be divergenceless and irrotational.

The value of moment of inertia thus obtained for a general non-rigid asymmetric rotator with quadrupole deformation is

$$I_{Hj} = 4B\beta^2 \sin^2(\gamma + 2\pi j/3) \qquad (12)$$

where $j = 1,2,3$ correspond to the three principal axes and B is the mass parameter given by

$$B = (3/8\pi) MR_o^2 \qquad (13)$$

For axially symmetric ($\gamma = 0$) spheroidal nuclei ($a_1 = a_2 < a_3$) we have

$$I_{H1} = I_{H2} = I_H = 3B\beta^2 \quad \text{and} \quad I_{H3} = 0 \qquad (14)$$

$I_{H3} = 0$ means that the spheroid does not rotate about its symmetry axis. Although I_H goes to zero as β goes to zero, the value of I_H is only one-third of I_{expt}. Thus, we have

$$I_R > I_{expt} > I_H \qquad (15)$$

and hence it follows that the nuclear flow is <u>neither irrotational nor rigid</u>.

II.4.3 <u>Centrifugal Stretching Models</u>

Following the above conclusion a number of rotational flow models have been proposed of which the centrifugal stretching model (Diamond et. al. 1964; Sood 1968; Gupta 1969; Trainor and Gupta 1971) is the most successful one.

The basic idea underlying the centrifugal stretching model is that a rotating non-rigid body undergoes a centrifugal stretching, and the displacement from its equilibrium position is controlled by restoring forces. The idea is based on the experimental evidence that for low-lying rotational levels the moment of inertia I increases with angular momentum L.

II.4.3a Model of Diamond et. al. (1964)

Diamond et. al. (1964) proposed a semi-classical model based on the assumption that the deformation (β) increases with the angular momentum (L), thus leading to an increase in the moment of inertia (I) with L. In the final calculations they used the following energy expression

$$E(L) = (\hbar^2/2I_L(\beta))L(L+1) + (C_d/2)(\beta_L - \beta_o)^2 \qquad (16)$$

along with the equilibrium condition $\partial E_L/\partial\beta_L = 0$ to obtain the value of the superfluous parameter β_L. With this model a good fit was obtained for rotational states in strongly deformed nuclei, assuming the relation $I \propto \beta^2$ given by the hydrodynamic model to be valid. However, the rotational states in the transition nuclei could not be fitted by this method with reasonable accuracy. Subsequently, various other forms of functions for the rotational moment of inertia $I(\beta)$ have been used in eq. (16) for obtaining better fits to the experimental data. Such calculations indicated that the increase in β is not large enough to explain the deviation from the L(L+1) rule.

II.4.3b Model of Sood

Sood (1968) applied the concept of centrifugal stretching to the study of rotational-vibrational motion of a strongly deformed even-even nucleus, assuming the nucleus to be a simple classical rotator (point-mass) and the restoring forces to be harmonic type. This simple model was successful in predicting the energies of low-lying rotational states only for the nuclei in the middle of the region $150 < A < 190$.

II.4.3c Model of Gupta

Gupta (1969) further developed the concept by considering an axially symmetric prolate deformed nucleus to consist of two parts obtained by dividing the nucleus by a plane containing the axis of symmetry. The center of mass for each of the two parts (see Figure IV.1) can be defined and the total separation r_o of the two centers of masses for equilibrium position is given by

$$r_o = (3/4)\, a_o \qquad (17)$$

where a_o is the semi-major axis corresponding to the ground state. The displacement $(r_L - r_o)$ from the equilibrium position due to centrifugal stretching was assumed to be balanced by harmonic restoring forces. The total energy $E(L)$ of rotation which is a sum of kinetic and potential energies is given by

$$E(L) = (\hbar^2/2I_L)\,(L(L+1) + (C_g/2)\,(r_L - r_o)^2 \qquad (18)$$

where C_g is the force constant and I_L is the moment of inertia in the state of angular momentum L. To carry out the final calculations, the rotational energy obtained in the form of an asymptotic series with I_o and C_g as parameters was used. The model gave better fits to the low-lying rotational levels when compared to other models. Also, an attempt was made to calculate the energies of β-vibrational levels. However, the agreement with the experiment was not satisfactory.

A quantum mechanical treatment of the model is expected to yield improved results. This is done in Chapter IV and it constitutes a part of the work presented in this thesis.

II.4.4 The Governor Model

The semi-classical models of Sood (1968) and Gupta (1969) give a non-vanishing value of I for spherical nuclei, which is contrary to the experimental observation. In order to include this, Trainor and Gupta (1971) modified the centrifugal stretching model of Gupta (1969) assuming that the effective mass contributing to the rotational moment of inertia lies outside a central geometric spherical core which is rotationally invariant. They refer to this model as the 'governor model'. Assuming the rotationally invariant core to be a sphere of radius equal to the semi-minor axis of a spheroidal nucleus ($a_1 = a_2 < a_3$), the following expression for the rotational moment of inertia I_G was obtained (Prakash 1973),

$$I_G = (1/5)\, M_s\, (a_3^2 + a_1 a_3 + 2a_1^2) \qquad (19)$$

where M_s is the effective mass participating in the rotations and is given by

$$M_s = (4\pi/3)\, a_1^2\, (a_3 - a_1)\, \rho_{eff} \qquad (20)$$

where ρ_{eff} is the effective density in the region outside the rotationally invariant core. Notice that I_G goes to zero for $a_1 = a_3$.

Both energy level and quadrupole moment data were used to obtain the values of the parameters involved in the final calculations. Significant improvement in the fitting was obtained for neutron deficient and transition nuclei.

A quantum mechanical treatment of the governor model with a variable rotationally invariant core is expected to improve the results obtained by Trainor and Gupta (1971). A brief discussion to this effect is included in the last section of Chapter IV.

II.4.5 Variable Moment of Inertia (VMI) Model

In view of the uncertainty of the dependence of I_L on β_L, Mariscotti et. al. (1969) have developed a variable moment of inertia (VMI) model by treating the moment of inertia itself as a variable in the semi-classical expression

$$E(L) = (\hbar^2/2I_L)\, L(L+1) + (C_m/2)\, (I_L - I_o)^2 \qquad (21)$$

where I_L is the moment of inertia in the state of angular momentum L obtained by setting $(\partial E_L/\partial I_L) = 0$. Since no model of moment of inertia is made, only empirical relation of the quadrupole moment with the moment of inertia is obtained. The VMI model has been most successful in predicting the energies of rotational states in the ground as well as in the excited rotational bands of deformed nuclei in the rare-earth and actinide regions.

In order to fit the rotational spectra of the nuclei in the transitional region characterized by the limit $1.82 < E(4)/E(2) < 2.23$ within the framework of VMI, it became necessary to use negative values of the parameters I_o which led to the concept of 'phase transition' in nuclei (Goldhaber and Goldhaber 1970). The nuclei in this region are characterized by considerably large E(2) values with a drastic reduction in level spacings for the higher states in the band. The qualitative explanation given for the negative values of I_o was based on the assumption that in the ground state these nuclei are not only rigid but also 'brittle', and hence these nuclei, when excited, first undergo some kind of rearrangement or 'melting' so that further excitations cost much less energy. The apparent phase change between the ground state and the higher states was qualitatively interpreted as a transition from 'super conducting' to 'normal' state associated with the symmetry breaking of pair excitations.

Recently, several attempts have been made to establish the equivalence of VMI model with other models, and to give a theoretical foundation to the VMI model. The equivalence of the VMI model with the Harris formula has been shown by Klein et. al. (1970). An application of VMI model for the study of of quasi-rotational spectra, and a derivation of the model which is general enough to account for its successful application to both deformed and spherical nuclei has been given by Das et. al. (1970a, 1970b and 1971).

REFERENCES

Alder, K. and Winther, A. (1966). 'Coulomb Excitation: A Collection of Reprints', Academic Press, New York.

Bohr, A. (1952). Kgl. Danske. Videnskab. Selskab. Mat. Fys. Medd. 26, No. 14.

Bohr, A. and Mottelson, B.R. (1953). ibid., 27, No.16.

Das, T.K., Dreizler, R.M. and Klein, A. (1970a). Phys. Rev. Letts. 25, 1629; (1970b). Phys. Rev. C2, 632; (1971). Phys. Letts. 34B, 235.

de Boer, J. and Eichler, J. (1968). 'The Reorientation Effect'. Advances in Nuclear Physics, edited by Baranger, M. and Vogt, E. Vol. 1, Plenum Press, New York.

Diamond, R.M., Stephens, F.S. and Swiateckii, W.J. (1964). Phys. Letts. 11, 315.

Fuller, C.F. and Cohen, V.W. (1969). Nuclear Data Tables A5, 433.

Goldhaber, A.S. and Goldhaber, G.S. (1970). Phys. Rev. Letts. 24, 1349.

Gupta, R.K. (1969). Can. J. Phys. 47, 299.

Johnson, A., Ryde, H. and Sztarkier, J. (1971). Phys. Letts. 34B, 605.

Klein, A., Dreizler, R.M. and Das, T.K. (1970). Phys. Letts. 31B, 333.

Kumar, K. (1972). Phys. Rev. Letts. 28, 249.

Lieder, R.M., Beuscher, H., Davidson, W.F., Jahn, P., Probst, H.J. and Mayer-Boricke, C. (1971). Private Communication, and (1972). Phys. Letts. 39B, 196.

Löbner, K.E.G., Vetter, M. and Hönig, V. (1970). Nuclear Data Tables A7, 495.

Mallmann, C.A. (1959). Phys. Rev. Letts. 2, 507.

Mariscotti, M.A.J., Goldhaber, G.S. and Buck, B. (1969). Phys. Rev. 178, 1864.

Mitsuo Sakai (1970). Nuclear Data Tables A8, 323.

Nemirovskii, P.E. (1963). 'Nuclear Models' E and F.N. Spon Limited, London, P. 104.

Newton, J.O. (1970). Prog. in Nucl. Phys. 11, 53.

Niels Bohr and Kalckar, F. (1937). Kgl. Danske. Videnskab. Selskab. Mat. Fys. Medd. 14, No. 10.

Prakash, V.R. (1973). Can. J. Phys. 51, 1794.

Rowe, D.J. (1970). 'Nuclear Collective Motion- Models and Theory'. Methuen and Co., Ltd., London, Part II.

Sood, P.C. (1968). Can. J. Phys. 46, 1419.

Thieberger, P., Sunyar, A.W., Rogers, P.C., Lark, N., Kistner, O.C., der Mateosian, E., Cochavi, S. and Auerbach, E.H. (1972). Phys. Rev. Letts. 28, 972.

Trainor, L.E.H. and Gupta, R.K. (1971). Can. J. Phys. 49, 133.

C H A P T E R - III

DYNAMICS OF RIGID BODIES

III.1.1 Definition of a Rigid Body

A rigid body is a system of particles bound together by internal forces which always keep the distance between any two particles a constant and act along the line joining the particles, irrespective of the external forces acting on the body.

Alternatively, a system of n-particles subject to the constraints

$$|\bar{r}_{ij}| = \sqrt{(x_i-x_j)^2 + (y_i-y_j)^2 + (z_i-z_j)^2} = \text{constant} \quad (1)$$

$$i,j = 1,2,\ldots\ldots,\ n,$$

where $x_i y_i z_i$ are rectangular coordinates of the i^{th} particle

and $|\bar{r}_{ij}|$ is the magnitude of the vector along the line joining the i^{th} and j^{th} particle, constitute a rigid body. (The rigid body is an idealization of the situation that occurs in practice and is useful when discussing the motion of a solid as a whole.)

III.1.2 Degrees of Freedom

A system of n independent particles will have 3n degrees of freedom. Since, by definition the particles in a rigid body do not move relative to each other, the most general motion that the body can perform is a rotation (3 degrees of freedom) and a translation (3 degrees of freedom), thus giving a total of six independent degrees of freedom for a rigid body and hence (3n-6) constraints.

III.2 AXIS OF ROTATION AND ANGULAR VELOCITY

Let the particles situated at O', A and B satisfy the rigidity condition. Fix any one of them (say O') and rotate the system about this point through an angle $d\phi$ as shown in Figure III.1.

The rigidity condition implies that the axis of rotation is the same for the particles at A and B and for any other particle located in the body. Thus, a rigid body moving with one point (O') fixed has an unique axis of rotation and an unique angular velocity $\bar{w} = (\bar{d\phi}/dt)$ about the fixed point. Further, it is easy to show that the angular velocity $\bar{w}$ of the rigid body is independent of the choice of the point fixed in the body.

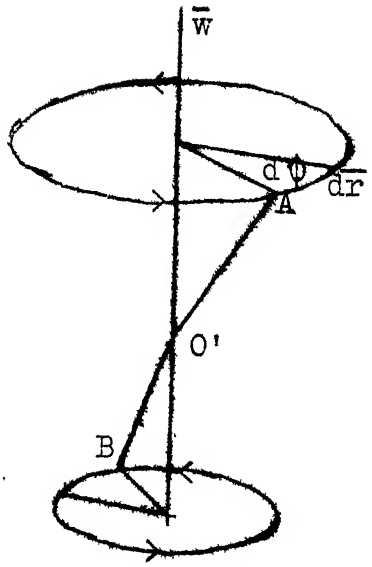

Fig. III.1

Rotation about a Fixed Point.

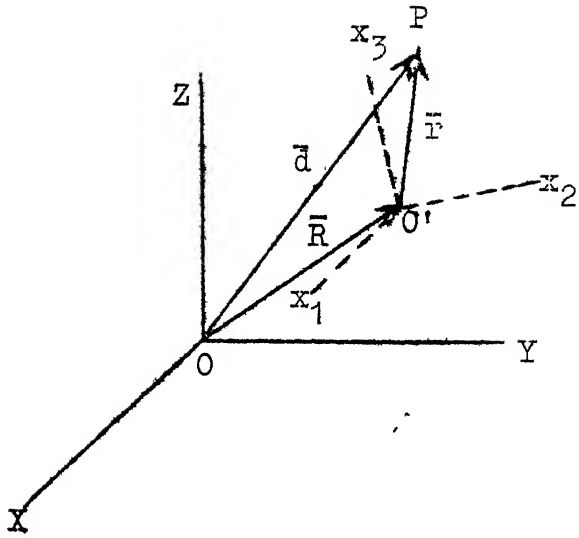

Fig. III.2

Motion of a Point (P) in Space and Body Fixed Co-ordinate Systems.

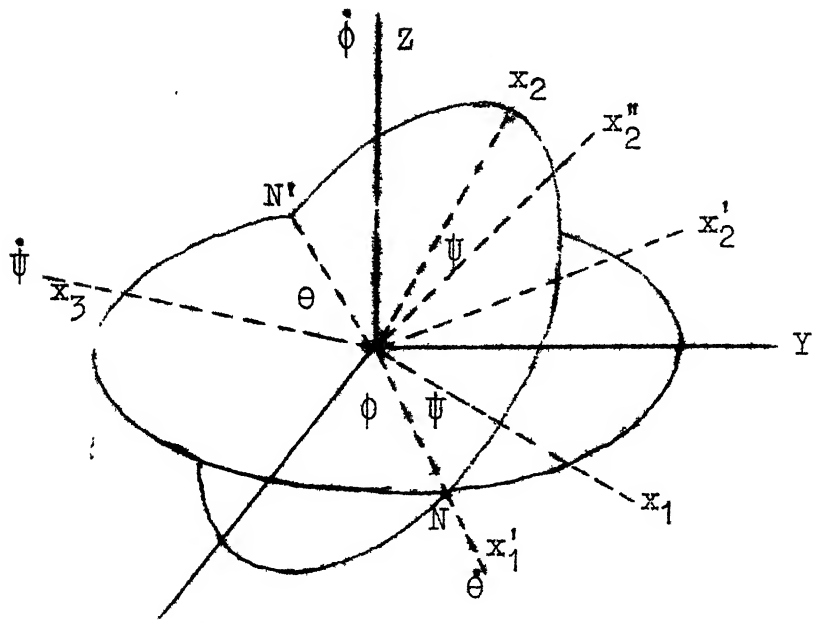

Fig. III.3: 'Euler Angles'.

Also, $d\bar{r} = \bar{d\phi} \times \bar{r}$.

III.3.1 Coordinate Systems and Euler Angles

The configuration of a rigid body is always specified with respect to a convenient set of coordinate axes. The choice of coordinate axes can as well be arbitrary. But, usually, a proper choice of coordinate system will simplify the problem tremendously. Generally, the following systems of coordinate axes are useful in the study of the dynamics of a rigid body.

(1) A system of coordinate axes fixed in space called the space fixed system, denoted by S(XYZ) or simply S.

(2) A system of coordinate axes fixed in the body called the body fixed system, denoted by $B(x_1x_2x_3)$ or simply B.

(3) A system of coordinate axes chosen to coincide with $B(x_1x_2x_3)$ at any instant of time called the instantaneous system of axes, denoted by $B'(x_1'x_2'x_3')$ or simply B'.

In Figure III.2, O and O' denote the origins of S and B respectively. P is any point in the body. Then

$$\bar{d} = \bar{R} + \bar{r} .$$

Taking the time derivative of this we have

$$\bar{u} = \bar{V} + \bar{w} \times \bar{r} \qquad (2)$$

where $\bar{u}$ and $\bar{V}$ are respectively the velocities of P and O' with respect to S and $(\bar{w} \times \bar{r})$ is the velocity of P with

respect to B.

Since $\bar{w}$ does not depend on the choice of O' in the body, O' can as well be the centre of mass of the rigid body in which case, $\bar{V}$ is the velocity of centre of mass with respect to O. Further, if O and O' are made to coincide with each other and with the centre of mass of the body then $\bar{u}$ is simply $\bar{w} \times \bar{r}$.

The various coordinate systems are related by certain spatial transformations. In discussing any spatial transformation there are two distinct points of view. In the first, the transformation is brought by a coordinate transformation, while each point P of space, along with all physical entities associated with it, remains fixed. In the second, the axes remains fixed while the physical system is itself transformed. Throughout this work the first of these viewpoints is adopted.

In the case where the origins O and O' are made to coincide with the centre of mass of the body, it is always possible to express a vectorial quantity either in terms of the coordinates in S(XYZ) or $B(x_1x_2x_3)$. The two are related by a coordinate transformation involving a rotation of any one of the set of axes, for which three parameters are essential. The most useful of them are the Euler angles (ϕ, θ, ψ) as shown in Figure III.3.

ϕ is the angle of rotation about the Z-axis which takes X to x_1' and Y to x_2' and $\dot{\phi}$ is the corresponding angular velocity along the Z-axis.

θ is the angle of rotation about x_1' axis which takes Z to x_3 and x_2' to x_2'' and $\dot{\theta}$ is the corresponding angular velocity along the x_1'-axis.

ψ is the angle of rotation about x_3-axis which takes x_1' to x_1 and x_2'' to x_2 and $\dot{\psi}$ is the corresponding angular velocity along the x_3-axis.

III.3.2 Resolutions of Angular Velocity $\bar{w}$ in Various Coordinate Systems

The angular velocity $\bar{w}$ has components $\dot{\phi}$, $\dot{\theta}$ and $\dot{\psi}$ along Z, x_1' and x_3 axes respectively which form a non-orthogonal system of axes. It is possible to obtain explicitly the components (w_1, w_2, w_3) and (w_X, w_Y, w_Z) of $\bar{w}$ along the two orthogonal system of axes $B(x_1x_2x_3)$ and $S(XYZ)$ respectively, in terms of $\dot{\theta}$, $\dot{\psi}$, $\dot{\phi}$. From Figure III.3, we get

$$\begin{pmatrix} w_1 \\ w_2 \\ w_3 \end{pmatrix} = \begin{pmatrix} \sin\theta & \sin\psi & \cos\psi & 0 \\ \sin\theta & \cos\psi & -\sin\psi & 0 \\ \cos\theta & & 0 & 1 \end{pmatrix} \begin{pmatrix} \dot{\phi} \\ \dot{\theta} \\ \dot{\psi} \end{pmatrix} = P \begin{pmatrix} \dot{\phi} \\ \dot{\theta} \\ \dot{\psi} \end{pmatrix} \quad (3a)$$

and

$$\begin{pmatrix} w_X \\ w_Y \\ w_Z \end{pmatrix} = \begin{pmatrix} 0 & \cos\phi & \sin\theta\sin\phi \\ 0 & \sin\phi & -\sin\theta\cos\phi \\ 1 & 0 & \cos\theta \end{pmatrix} \begin{pmatrix} \dot{\phi} \\ \dot{\theta} \\ \dot{\psi} \end{pmatrix} = Q \begin{pmatrix} \dot{\phi} \\ \dot{\theta} \\ \dot{\psi} \end{pmatrix} \quad (3b)$$

From these we get

$$\begin{pmatrix} w_1 \\ w_2 \\ w_3 \end{pmatrix} = R \begin{pmatrix} w_X \\ w_Y \\ w_Z \end{pmatrix} \quad \text{where} \quad R = P\,Q^{-1} \tag{3c}$$

The transformation matrix R explicitly given by

$$R = \begin{pmatrix} \cos\psi\cos\phi - \cos\theta\sin\phi\sin\psi & \cos\psi\sin\phi + \cos\theta\cos\phi\sin\psi & \sin\psi\sin\theta \\ -\sin\psi\cos\phi - \cos\theta\sin\phi\cos\psi & -\sin\psi\sin\phi + \cos\theta\cos\phi\cos\psi & \cos\psi\sin\theta \\ \sin\theta\sin\phi & -\sin\theta\cos\phi & \cos\theta \end{pmatrix} \tag{3d}$$

The transformation relation (3c) is true for any arbitrary vector $\bar{A}$ (Goldstein, 1950). Hence, R is the general transformation matrix which transforms the components of a given vector $\bar{A}$ in S to B and vice-versa. It is easy to show that R is a unitary real orthogonal matrix since $R^{+}R = I$ and the transpose of R is equal to its adjoint.

III.4.1 Angular Momentum of a Rigid Body in Motion

If m_i is the mass of i^{th} particle, $\bar{r}_i$ is its position vector and $\bar{u}_i$ is the corresponding velocity, then the angular momentum ($\bar{L}$) of a rigid body undergoing a rotational

motion about its centre of mass is

$$\bar{L} = \sum_{i=1}^{n} m_i(\bar{r}_i \times \bar{u}_i)$$

Using eq. (2) we have

$$\bar{L} = \Sigma\ m_i\left[\, r_i^2\, \bar{w} - (\bar{r}_i.\bar{w})\bar{r}_i \,\right] \qquad (4)$$

As with any vector equation, one may take the components of $\bar{L}$ in any desired system of coordinates. Thus, for instance, L_X in S(XYZ) is given by

$$L_X = \Sigma\ m_i\left[\, (Y_i^2 + Z_i^2)w_X - X_iY_iw_Y - X_iZ_iw_Z \,\right] \qquad (5)$$

with similar expressions for L_Y and L_Z. In $B(x_1x_2x_3)$ system we have

$$L_1 = \sum_{i=1}^{n} m_i\left[\, (x_{i2}^2 + x_{i3}^2)\, w_1 - x_{i1}y_{i2}w_2 - x_{i1}x_{i3}w_3 \,\right] \qquad (6)$$

with similar expressions for L_2 and L_3.

III.4.2 Kinetic Energy of a Rigid Body in Motion

Consider a rigid body in motion. If m_i is the mass of the i^{th} particle and $\bar{u}_i$ is its velocity in S, then the kinetic energy of the system is given by

$$T = \sum_{i=1}^{n} \frac{1}{2} m_i u_i^2 .$$

Using eq. (2) we get

$$T = \sum_{i=1}^{n} \frac{1}{2} m_i(\bar{V}+\bar{w}\times\bar{r}_i)^2 = \Sigma\, \frac{1}{2} m_iV^2 + \Sigma m_i\, \bar{V}\cdot(\bar{w}\times\bar{r}_i) + \Sigma\, \frac{1}{2} m_i\cdot$$

i.e., $T = \frac{1}{2} MV^2 + (\bar{V} \times \bar{w}) \cdot \Sigma m_i \bar{r}_i + \Sigma \frac{1}{2} m_i [\, w^2 r_i^2 - (\bar{w} \cdot \bar{r}_i)^2 \,]$.

Choosing the centre of mass of the body to be the origin of B and using eq. (4)

$$T = \frac{1}{2} MV^2 + \frac{1}{2} \bar{L} \cdot \bar{w} = T_{trans} + T_{rot} \qquad (7)$$

where M is the mass of the body and the vectors $\bar{L}$ and $\bar{w}$ can be expressed either in terms of the components in S(XYZ) or $B(x_1 x_2 x_3)$.

Thus, the kinetic energy of the system consists of two parts; (i) T_{trans}, the translation kinetic energy of the centre of mass in S and (ii) T_{rot}, the rotational kinetic energy of the body about the centre of mass. If one is interested in the study of only the rotational motion of the rigid body, it is useful to choose the centre of mass as the common origin of both S and B in which case,

$$T = T_{rot} = \frac{1}{2} (L_X w_X + L_Y w_Y + L_Z w_Z) = \frac{1}{2} (L_1 w_1 + L_2 w_2 + L_3 w_3) \qquad ...(8)$$

where (L_X, L_Y, L_Z) or (L_1, L_2, L_3) are respectively given by equations of the type (5) or (6). Using the latter, we have,

$$T = \frac{1}{2} \sum_{l,k=1}^{3} I_{lk} w_l w_k \qquad (9)$$

where the inertia coefficients I_{lk} are the elements of inertia tensor I given by (Goldstein, 1950)

i.e., $T = \frac{1}{2} MV^2 + (\bar{V} \times \bar{w}) \cdot \Sigma m_i \bar{r}_i + \Sigma \frac{1}{2} m_i [\, w^2 r_i^2 - (\bar{w} \cdot \bar{r}_i)^2 \,]$.

Choosing the centre of mass of the body to be the origin of B and using eq. (4)

$$T = \frac{1}{2} MV^2 + \frac{1}{2} \bar{L} \cdot \bar{w} = T_{trans} + T_{rot} \qquad (7)$$

where M is the mass of the body and the vectors $\bar{L}$ and $\bar{w}$ can be expressed either in terms of the components in S(XYZ) or $B(x_1 x_2 x_3)$.

Thus, the kinetic energy of the system consists of two parts; (i) T_{trans}, the translation kinetic energy of the centre of mass in S and (ii) T_{rot}, the rotational kinetic energy of the body about the centre of mass. If one is interested in the study of only the rotational motion of the rigid body, it is useful to choose the centre of mass as the common origin of both S and B in which case,

$$T = T_{rot} = \frac{1}{2} (L_X w_X + L_Y w_Y + L_Z w_Z) = \frac{1}{2} (L_1 w_1 + L_2 w_2 + L_3 w_3) \qquad \ldots(8)$$

where (L_X, L_Y, L_Z) or (L_1, L_2, L_3) are respectively given by equations of the type (5) or (6). Using the latter, we have,

$$T = \frac{1}{2} \sum_{l,k=1}^{3} I_{lk} w_l w_k \qquad (9)$$

where the inertia coefficients I_{lk} are the elements of inertia tensor I given by (Goldstein, 1950)

$$I = \begin{bmatrix} \Sigma\, m_i(x_{i2}^2 + x_{i3}^2) & -\Sigma\, m_i x_{i1} x_{i2} & -\Sigma\, m_i x_{i1} x_{i3} \\ -\Sigma\, m_i x_{i1} x_{i2} & \Sigma\, m_i(x_{i1}^2 + x_{i3}^2) & -\Sigma\, m_i x_{i2} x_{i3} \\ -\Sigma\, m_i x_{i1} x_{i3} & -\Sigma\, m_i x_{i2} x_{i3} & \Sigma\, m_i(x_{i1}^2 + x_{i2}^2) \end{bmatrix} \quad (10)$$

In the above, the diagonal elements are called principal moments of inertia and the off-diagonal elements are called products of inertia. Thus, there are only six independent inertial coefficients and they depend both upon the geometry of the solid and the origin of the axes chosen, and upon the orientation of these axes with respect to the solid. Had we chosen to express the energy in terms of the coordinates in S(XYZ), we would have landed up with equations exactly similar to (9) and (10) with (X,Y,Z) in place of (x_1, x_2, x_3).

In any solid, it is always possible to find a particular orientation of body axes, called the principal axes, for which the inertia tensor is diagonal. In this case,

$$T_{rot} = \frac{1}{2}\left(I_1 w_1^2 + I_2 w_2^2 + I_3 w_3^2 \right) \quad (11)$$

w_1 , w_2, w_3 are given by eq. (3a).
(I_i is written in place of I_{ii} for the case of principal axes.)

III.4.3 Hamiltonian of the System

In the absence of external forces, the rigid body undergoing a rotational motion has the Hamiltonian (eq. (8)),

$$H = \frac{1}{2}\left(L_X w_X + L_Y w_Y + L_Z w_Z \right) = \frac{1}{2}\left(L_1 w_1 + L_2 w_2 + L_3 w_3 \right) \quad \ldots(12)$$

In particular, by choosing the $B(x_1 x_2 x_3)$ axes parallel to the principal axes of the system we get the most useful form of H given by

$$H = \frac{1}{2} \sum_{j=1}^{3} (L_j^2)/(2I_j) \qquad (13)$$

where $L_j = I_j w_j$ as given by eqs. (6).

III.4.4 Conservation of $\bar{L}$ and H in case of the Motion of an Isolated Rigid Body

We have shown that for a rigid body in motion with no external forces, the rotational kinetic energy is given by eq. (12) and the corresponding angular momentum components are given by eq. (5) or (6). In the absence of any external force, the system will not experience any torque and hence $(d\bar{L}/dt) = 0$ which means that $\bar{L}$ is a constant of motion. But the conservation of kinetic energy and individual components of $\bar{L}$ depend on the conservation of $\bar{w}$ and its components which, in turn, depend on the geometry of the solid. Here, we will discuss three interesting and useful geometries of the solid. We will use H as given by eq. (13).

(a) Spherical Top: In this case we have $I_1 = I_2 = I_3 = I$. Hence $\bar{L} = I\,\bar{w}$ which implies that $\bar{w}$ is a constant of motion and the Hamiltonian H given by eq. (13) takes the form $H = L^2/2I$.

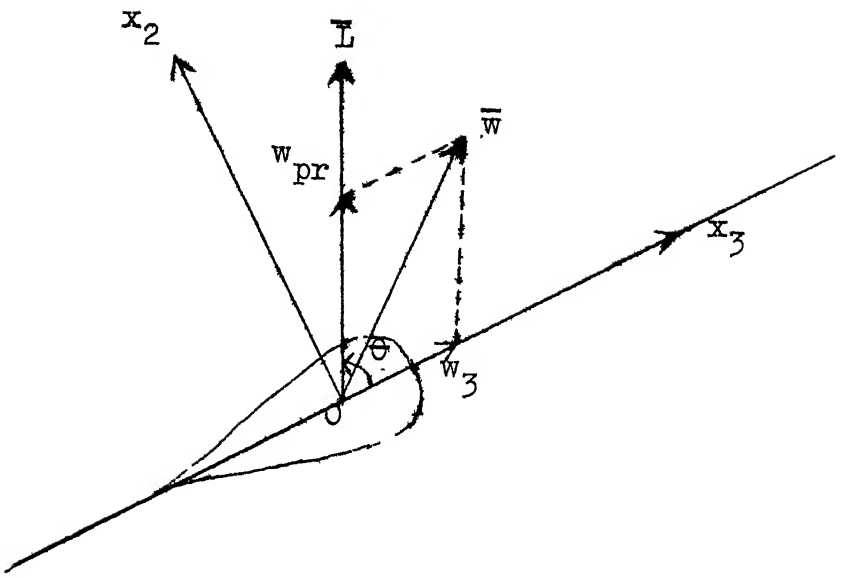

Figure III.4: Motion of a Symmetric Top.

(b) Symmetric Top: In this case we have $I_1 = I_2 \neq I_3$. Choose the Z-axis along the direction of $\bar{L}$ and the x_1-axis perpendicular to $\bar{L}$ so that the component L_1 of $\bar{L}$ along x_1-axis is zero and hence $w_1 = 0$. So $\bar{w}$ must lie in the plane containing axes (x_2, Z, x_3) i.e., in the plane of the paper as shown in Figure III.4.

If θ is the angle between Z and x_3-axes (refer to Fig. III.4), then

$$w_3 = (L_3/I_3) = L \cos\theta / I_3$$

and $$w_2 = (L_2/I_1) = w_{pr} \sin\theta = L \sin\theta/I_1$$

hence, $w_{pr} = (L/I_1)$.

So w_3 and w_{pr} are both constants of motion and hence $\bar{w}$ is again conserved. In this case eq. (13) for H takes the form

$$H = (L^2/2I_1) + (L_3^2 /2) (1/I_3 - 1/I_1) \qquad (14)$$

(c) Asymmetric Top: In this case we have $I_1 \neq I_2 \neq I_3$. Eq. (13) gives

$$L_1^2/I_1 + L_2^2/I_2 + L_3^2/I_3 = 2E$$

and $$L_1^2 + L_2^2 + L_3^2 = L^2.$$

Hence in $B(x_1x_2x_3)$, $\bar{L}$ moves along the path of intersection of the ellipsoid and the sphere defined by the above equations, which is necessarily a closed path. Hence, the motion of $\bar{L}$ in

B is periodic. It can be shown (Landau and Lifshitz, 1969) that θ and ψ will have the same period, but ϕ will be a combination of two periodic motions. Thus, while $\bar{L}$ is a constant of motion, the top never exactly returns to its original position.

III.4.5 Euler's Equations of Motion

It can be shown (Goldstein, 1950) that the time derivative of an arbitrary vector in S is related to its time derivative in B, together with its vector product with $\bar{w}$, the instantaneous angular velocity of B, by the operator equation

$$(d/dt)_S = (d/dt)_B + \bar{w} \times \tag{15}$$

Operating (15) on the total angular momentum $\bar{L}$, we have

$$(d\bar{L}/dt)_S = (d\bar{L}/dt)_B + \bar{w} \times \bar{L} \tag{16}$$

Choosing $B(x_1x_2x_3)$ along the principal axes of the solid we have $L_j = I_j w_j$ and

$$(d\bar{L}/dt)_B = (dL_1/dt)\bar{e}_1 + (dL_2/dt)\bar{e}_2 + (dL_3/dt)\bar{e}_3$$

where $(\bar{e}_1, \bar{e}_2, \bar{e}_3)$ are unit vectors along the principal axes.

In the absence of any external forces we have $(d\bar{L}/dt)_S = 0$ and hence eq. (16) reduces to

$$\frac{dw_j}{dt} + \frac{I_l - I_k}{I_j} w_k w_l = 0 \tag{17}$$

with two more expressions obtained by the cyclic combination of j,k,l (j,k,l correspond to 1,2,3). Eqs. (17) give the description of the motion of an isolated rigid body with one point fixed in B and are called as Euler's equations of motion of a rigid body.

III.5 QUANTIZATION OF THE RIGID BODY MOTION

In III.4.3, we have seen that the rotational motion of a rigid body can be described by an Hamiltonian of the type given either by eq. (12) or by eq. (13). Of these, the latter is relatively simple and convenient to handle. The solution of the associated Schrödinger equation will yield energy eigenvalues and state functions which are very useful in the calculation of other physical properties of the system. Hence, to study the quantum mechanics of a rigid body it is essential to know the total angular momentum ($\bar{L}$) and its components in B and in S (L_1, L_2, L_3 and L_X, L_Y, L_Z respectively) in their operator form and their various quantum mechanical properties.

In III.3.2, we obtained the transformation relations for transforming various components of $\bar{w}$ from a given set of axes to another. Thus, eqs. (3a) to (3b) imply

$$(w_1 , w_2 , w_3) \longleftrightarrow (\dot{\phi}, \dot{\theta}, \dot{\psi}) \longleftrightarrow (w_X, w_Y, w_Z).$$

III.5.1 Orthogonal Coordinates

The Euler angles (ϕ,θ,ψ) are coordinates of the system referred to the set of axes (Z, x_1', x_3) which is non-orthogonal

(refer to Figure III.2). The Schrödinger equation for describing any system can be written only in terms of an orthogonal (like the Cartesian) set of coordinates. In our study, both $B(x_1x_2x_3)$ and $S(XYZ)$ form two independent orthogonal set of axes. If α_1, α_2, α_3 and α_X, α_Y, α_Z are the angles of rotation about the coordinate axes in B and in S respectively, these will then constitute two independent orthogonal set of generalised coordinates for describing the system. It is necessary to express these angles in terms of the Euler angles $(\phi\theta\psi)$ for explicitly obtaining angular momentum operators which requires

$$(\alpha_1\alpha_2\alpha_3) \longleftrightarrow (\phi\ \theta\ \psi) \longleftrightarrow (\alpha_X\alpha_Y\alpha_Z)$$

III.5.2 Angular Momentum Operators

Since $\alpha_1,\alpha_2,\alpha_3$ and α_X, α_Y, α_Z represent angles of rotation about the coordinate axes in B and in S respectively, we have

$$w_j = \dot{\alpha}_j \quad (j = 1,2,3) \quad \text{and} \quad w_{X,Y,Z} = \dot{\alpha}_{X,Y,Z}$$

and, according to eq. (11)

$$H = \frac{1}{2} \sum_{j=1}^{3} I_j \dot{\alpha}_j^2$$

Thus, the quantities that are canonically conjugate to the α_j's are given by

$$\partial H/\partial\dot{\alpha}_j = I_j \dot{\alpha}_j = I_j w_j = L_j$$

The L_j's are then represented in the Schrödinger picture by the differential operators

$$L_j = -i\hbar\,(\partial/\partial\alpha_j) \tag{18a}$$

Now, the partial derivatives with respect to α_j are related to those with respect to ϕ, θ, ψ by the following equations (Appendix II.1)

$$\begin{aligned}
\frac{\partial}{\partial\alpha_1} &= \frac{\sin\psi}{\sin\theta}\frac{\partial}{\partial\phi} + \cos\psi\frac{\partial}{\partial\theta} - \sin\psi\cot\theta\frac{\partial}{\partial\psi} \\
\frac{\partial}{\partial\alpha_2} &= \frac{\cos\psi}{\sin\theta}\frac{\partial}{\partial\phi} - \sin\psi\frac{\partial}{\partial\theta} - \cos\psi\cot\theta\frac{\partial}{\partial\psi} \\
\frac{\partial}{\partial\alpha_3} &= \frac{\partial}{\partial\psi}\,.
\end{aligned} \tag{19a}$$

Using these in eq. (18a) we obtain L_1, L_2, L_3 explicitly in their operator form.

Working along the same line with α_X, α_Y, α_Z we get

$$L_{X,Y,Z} = -i\hbar\,(\partial/\partial\alpha_{X,Y,Z}) \tag{18b}$$

Again, the partial derivatives with respect to $\alpha_{X,Y,Z}$ are related to those with respect to ϕ, θ, ψ by the following three equations (Appendix II.1)

$$\begin{aligned}
\frac{\partial}{\partial\alpha_X} &= -\sin\phi\cot\theta\frac{\partial}{\partial\phi} + \cos\phi\frac{\partial}{\partial\theta} + \frac{\sin\phi}{\sin\theta}\frac{\partial}{\partial\psi} \\
\frac{\partial}{\partial\alpha_Y} &= \cos\phi\cot\theta\frac{\partial}{\partial\phi} + \sin\phi\frac{\partial}{\partial\theta} - \frac{\cos\phi}{\sin\theta}\frac{\partial}{\partial\psi} \\
\frac{\partial}{\partial\alpha_Z} &= \frac{\partial}{\partial\phi}\,.
\end{aligned} \tag{19b}$$

Using these in eq. (18b), we get L_X, L_Y, L_Z explicitly in their operator form.

Thus, we have for the operator

$$\bar{L} = (L_1, L_2, L_3) = -i\hbar\left(\frac{\partial}{\partial\alpha_1}, \frac{\partial}{\partial\alpha_2}, \frac{\partial}{\partial\alpha_3}\right) = (L_X, L_Y, L_Z) = -i\hbar\left(\frac{\partial}{\partial\alpha_X}, \frac{\partial}{\partial\alpha_Y}, \frac{\partial}{\partial\alpha_Z}\right).$$

It is easy to verify that

$$\bar{L}^2 = L_1^2 + L_2^2 + L_3^2 = L_X^2 + L_Y^2 + L_Z^2 ,$$

and each is equal to (Appendix II.1),

$$L^2 = -\hbar^2 \left[\frac{1}{\sin^2\theta} \frac{\partial^2}{\partial\phi^2} + \frac{1}{\sin\theta} \frac{\partial}{\partial\theta}\left(\sin\theta \frac{\partial}{\partial\theta}\right) + \frac{1}{\sin^2\theta} \frac{\partial^2}{\partial\psi^2} \right] \qquad \ldots(20)$$

Explicit expressions for (L_1, L_2, L_3) and (L_X, L_Y, L_Z) in terms of the Euler angles yield the following commutation relations

$$\begin{aligned} &[L_1, L_2] = -i\hbar L_3 \quad \text{and cyclic in } 1,2,3 ; \\ \text{and} \quad &[L_X, L_Y] = +i\hbar L_Z \quad \text{and cyclic in } X,Y,Z . \end{aligned} \qquad (21)$$

The above are the usual commutation relations for angular momentum operators. It is easy to verify that the operators L_1, L_2, L_3 and L_X, L_Y, L_Z are Hermetian. Other important commutation relations are listed in Appendix II.2.

III.5.3 Angular Momentum Eigen-Functions

In the last section we have obtained the components of angular momentum $\bar{L}$ in their operator form. In Appendix II.2,

we have listed the various commutation relations satisfied by these operators. It is now essential to study the angular momentum eigen-functions and their properties in order to obtain eigenvalues and eigen-functions of the Hamiltonian given by eq. (13).

From the commutation relations (Appendix II.2), it is clear that the operators $\bar{L}^2$, L_Z and L_3 commute with each other. Hence, it must be possible to find simultaneous eigen-functions $|LMK\rangle$ of these operators which render $\bar{L}^2$, L_Z and L_3 diagonal with eigenvalues $L(L+1)$, M and K respectively. Thus,

$$\bar{L}^2|LMK\rangle = L(L+1)\hbar^2|LMK\rangle \qquad (22a)$$

$$L_Z|LMK\rangle = M\hbar\,|LMK\rangle \qquad (22b)$$

$$L_3|LMK\rangle = K\hbar\,|LMK\rangle \qquad (22c)$$

Our task, at present, is to find the explicit form of $|LMK\rangle$.

The Euler angles (ϕ,θ,ψ) are the dynamical variables which completely specify the orientation of the B-frame relative to the S-frame. The rotation of the B-frame relative to the S-frame can be generated by a rotational operator $R(\phi,\theta,\psi)$ which according to the definition of Euler angles is

$$R(\phi,\theta,\psi) = R(\psi)\,R(\theta)\,R(\phi)$$

The explicit form of the operator R has been obtained in

Appendix II.3 (Elliott, 1958)

$$R(\phi,\theta,\psi) = e^{\frac{-i\phi}{\hbar} L_Z} e^{\frac{-i\theta}{\hbar} L_X} e^{\frac{-i\psi}{\hbar} L_Z} \qquad (23)$$

where L_X, L_Y, L_Z are the components of the angular momentum $\bar{L}$ with respect to the S-frame. Clearly, the operator R is unitary. Since equation (23) contains only angular momentum operators L_Z, L_X, it is clear that the operator $R(\phi,\theta,\psi)$ can only couple a $\psi(LM)$, in the usual angular momentum representation to other $\psi(LM')$ with the same L value.

Writing this formally

$$\psi_{\gamma}(LM') = R(\phi,\theta,\psi)\,\psi(LM) = \sum_{M'} \langle LM'|R(\gamma)|LM\rangle\,\psi(LM') \qquad (24)$$

Here ψ_{γ} is the same function as ψ but of coordinates referred to the rotated frame (B-frame). γ stands for the three Euler angles ϕ,θ,ψ.

Following Wigner, we define the matrix element on the right hand side of the above expression as

$$D^{L*}_{M'M}(\gamma) = \langle LM'|R(\gamma)|LM\rangle \qquad (25)$$

D^L is the familiar rotation matrix. Hence,

$$\psi(LM') = \sum_{M'} D^{L*}_{M'M}(\gamma)\,\psi(LM')$$

Multiplying both sides by $D^L_{MM'}(\gamma)$ and using the unitary property of D-matrices (since R is unitary),

$$\psi(LM) = \sum_{M'} D^{L}_{MM'}(\gamma)\ \psi_{\gamma}(LM') \qquad (26)$$

Let R_1, R_2, R_3 and R_X, R_Y, R_Z be the Cartesian components of $\bar{R}$ and, R'_0, $R'_{\pm 1}$ and $R_0, R_{\pm 1}$ be the corresponding spherical components of $\bar{R}$ along $B(x_1, x_2, x_3)$ axes and $S(XYZ)$ axes respectively. Now, consider a system of particles whose coordinates may be referred either to B or S. The rotation (α) of the <u>system</u> with the reference frame fixed is entirely equivalent to a rotation ($-\alpha$) of the axes of reference frame during which the system does not change, provided the axis of rotation is the same in both the operations. Let $\bar{L}$ be the angular momentum operator associated with the rotations of the system of particles, and ψ be the wave function of the system referred to S, while ψ_{γ} is the <u>same</u> function but of coordinates referred to B. Since imposing the same rotation on the system of particles and on the axes of reference B has no effect on the description of the system, the infinitesimal change in the wave function of the system caused by such an operation must be zero (Elliott, 1957),

$$(\bar{R} + \bar{L})\ \psi_{\gamma} = 0 \qquad (27)$$

Also, since ψ referred to S is independent of rotation $\bar{R}$ of B, we have

$$\bar{R}\,\psi = 0 \qquad (28)$$

Using the equation (26) in (28) we have

$$0 = \bar{R}\,\psi = \sum_{M'} \bar{R}\, D^{L}_{MM'}(\gamma)\, \psi_{\gamma}(LM') \qquad (29)$$

$\bar{R}$ being the generator of the rotations of B, operates both on $D^{L}_{MM'}(\gamma)$ and on ψ_{γ}. Accordingly, since $\bar{R}$ is a linear differential operator

$$\begin{aligned} 0 = \bar{R}\psi &= \sum_{M'} \left[(\bar{R}\, D^{L}_{MM'}(\gamma)) + D^{L}_{MM'}(\gamma)\bar{R}\right]\psi_{\gamma}(LM') \\ &= \sum_{M'} \left[(\bar{R}\, D^{L}_{MM'}(\gamma)) - D^{L}_{MM'}(\gamma)\bar{L}\right]\psi_{\gamma}(LM') \quad \text{(using (3c))} \end{aligned} \qquad (30)$$

$(\bar{R}\, D^{L}_{MM'}(\gamma))$ denotes the result of operation of $\bar{R}$ on $D^{L}_{MM'}(\gamma)$ and hence is a simple function of γ and not an operator.

We now study eq. (30) for particular spherical components of $\bar{R}$, either R'_0, $R'_{\pm 1}$ referred to B or $R_0, R_{\pm 1}$ referred to S.

First consider R'_0 (same as R_z) where upon, because L_z $L_z\,\psi_{\gamma}(LM') = \hbar M'\ \psi_{\gamma}(LM')$, eq. (30) becomes

$$\sum_{M'} \left[(R'_0\, D^{L}_{MM'}(\gamma) - \hbar M'\, D^{L}_{MM'}(\gamma)\right]\psi_{\gamma}(LM') = 0.$$

Since $\psi_{\gamma}(LM')$ are linearly independent, coefficients of $\psi_{\gamma}(LM')$ may be equated separately to zero. Thus

$$R_0\, D^{L}_{MM'}(\gamma) = R_e\, D^{L}_{MM'}(\gamma) = \hbar M'\, D^{L}_{MM'}(\gamma) \qquad (31a)$$

Note that the auxiliary function ψ_{γ} do not appear in eq. (31a),

Similarly taking the $R'_{\pm 1}$ spherical components (related to the Cartesian components by $R'_{\pm 1} = \mp \frac{1}{\sqrt{2}}(R_1 \pm iR_2)$) are used to obtain (Elliott, 1957)

$$R'_{\mp 1}\, D^{L}_{MM'}(\gamma) = \pm\hbar \left[\frac{(L \mp M')\,(L \pm M' + 1)}{2}\right]^{\frac{1}{2}} D^{L}_{M,M' \pm 1}(\gamma) \qquad (32a)$$

In obtaining the above, we have made use of the known eigenvalues of the operators $L'_{\pm} = (L_1 \pm iL_2)$ and the relation $L'_{\pm 1} = \mp \frac{1}{\sqrt{2}} L'_{\pm}$ (Rose, 1957). It is of interest to notice that the commutation relations of the operators $R'_{\pm 1}$ are

$$\left[R'_{+1},\, R'_{-1}\right] = \hbar R'_{o} \qquad (33)$$

or, in Cartesian form $[R_1, R_2] = -i\hbar R_3$ (1,2,3, cyclic). These differ from the customary relations by the appearance of a negative sign. Also, compare eq. (33) with eq. (21). To examine the components R_o, $R_{\pm 1}$ of $\bar{R}$ in S-frame, it is necessary to perform the sum over M' in the second term in eq. (30) explicitly because, the effect of L_o, $L_{\pm 1}$ on $\psi_{\gamma}(LM')$ is not obvious.

Doing this, we get

$$\sum_{M'} \left[(\bar{R}\, D^{L}_{MM'}(\gamma))\,\psi_{\gamma}(LM')\right] - \bar{L}\,\psi(LM) = 0 \qquad (34)$$

The operator $\bar{L}$ operates only on the particle coordinates. Now, taking the spherical component R_o (same as R_Z) in (34)

$$\sum_{M'} \left[(R_o\, D^{L}_{MM'}(\gamma))\,\psi\ (LM')\right] - \hbar\, M\, \psi(LM) = 0$$

and, expanding $\psi(LM)$ again, we have

$$\sum_{M'} \left[(R_o \, D^L_{MM'}(\gamma)) - M\hbar \, D^L_{MM'}(\gamma) \right] \psi_\gamma (LM') = 0$$

Equating coefficients of $\psi_\gamma (LM')$ to zero yields

$$R_o \, D^L_{MM'}(\gamma) = M\hbar \, D^L_{MM'}(\gamma) \tag{31b}$$

Following the same procedure for $R_{\pm 1}$ starting from eq. (34), we get

$$R_{\pm 1} \, D^L_{MM'}(\gamma) = \mp \hbar \left[\frac{(L \mp M)(L \pm M + 1)}{2} \right]^{1/2} D^L_{M \pm 1, M}(\gamma) \tag{32b}$$

In obtaining the above expression, we have made use of the known eigenvalues of the operator $L_\pm = (L_X \pm iL_Y)$ and the relations $L_{\pm 1} = \mp \frac{1}{\sqrt{2}} L_\pm$.

From eqs. (31a), (31b), (32a) and (32b) it is easy to deduce the result of the operation of R^2 on $D^L_{MM'}(\gamma)$. We find - as expected - that

$$R^2 \, D^L_{MM'}(\gamma) = L(L+1)\hbar^2 \, D^L_{MM'}(\gamma) \tag{35}$$

Comparison of eqs. (31a), (31b) and (35) with eqs. (22) shows that the function $D^L_{MM'}(\gamma)$ is a simultaneous eigenfunction of $\bar{R}^2$, R_3 and R_Z and in the S-frame of reference it behaves like an eigenfunction of angular momentum $\bar{L}$, with Z-component M and in the rotated frame (B-frame), $D^L_{MM'}(\gamma)$ is an eigenfunction of angular momentum $\bar{L}$ (but for the negative in (33)), with 3-component M' which corresponds to K in

$|LMK\rangle$. Important properties of $D^{L}_{MK}(\Omega)$ are listed in Appendix II.4.

In the rotational motion of a rigid body, the operators $\bar{R}$ are associated with the rotational angular momentum of the body with components R_1, R_2, R_3 in the B-frame and R_X, R_Y, R_Z in the S-frame. Thus, in the rotational motion of a rigid body, the angular momentum $\bar{L}$ associated with the motion of the system of particles is the same as the angular momentum $\bar{R}$ associated with a frame fixed in its body.

In the case of a non-rigid body the total angular momentum associated with the rotational motion is a sum of the angular momentum associated with B-frame and the angular momentum associated with the intrinsic motion of the system of particles.

III.5.4 Eigenvalues and Eigenfunctions of H

Thus, having studied the angular momentum operators and their eigenfunctions, we are now in a position to solve the eigenvalue problem of a deformed rigid rotator quantum mechanically the Hamiltonian of which is given by eq. (13). That is

$$H = \sum_{j=1}^{3} (L_j^2/2I_j) \qquad (13)$$

where I_j are the principal moments of inertia.

We shall discuss the eigenvalue problem for two physically important cases of ellipsoidal type of geometry.

(a) Symmetric Top: The case of axially symmetric rotator is interesting to study as it is possible to obtain the solution in a closed form. Choosing the x_3-axis in $B(x_1,x_2,x_3)$ as the symmetry axis, which implies $I_1 = I_2 \neq I_3$, the Schrödinger equation with the Hamiltonian given by equation (13) is (Davidson, 1968)

$$H|LMK\rangle = E_{sym}|LMK\rangle \tag{36}$$

with $$E_{sym} = \frac{\hbar^2}{2}\left[\frac{L(L+1)}{I_1} + \left(\frac{1}{I_3} - \frac{1}{I_1}\right)K^2\right] \tag{37}$$

Thus, the state functions $|LMK\rangle$ of eqs. (22) are also the eigenfunctions of the Hamiltonian for the symmetric top. We have already shown that the state functions $|LMK\rangle$ are nothing but $D^{L^*}_{MK}(\phi,\theta,\psi)$. Various properties of these functions are discussed in Appendix II.4.

(b) Asymmetric Top ($I_1 \neq I_2 \neq I_3$): A general rotator does not possess an axis of symmetry and hence K is not a good quantum number. Also, this is clear from the fact that although L_3 commutes with $\vec{L}^2$ and L_Z, it does not commute with the Hamiltonian H for a general rotator given by eq. (13). However, since $\vec{L}^2$, L_Z and L_3 commute with each other, it is possible to represent the state functions $|LM\rangle$ of an asymmetric top as a linear combination of states of a symmetric top (Davidson, 1968). Thus,

$$|LM\rangle = \sum_{K=-L}^{+L} A_K|LMK\rangle \tag{38}$$

With $|LMK\rangle$ as the basic set of wavefunctions, the eigenvalues of H can then be obtained by treating the asymmetry as a small perturbation over the symmetry which is a fairly good approximation for ellipsoidal type of solids. The Hamiltonian for such a system is

$$H = \frac{L^2 - L_3^2}{2I_1} + \frac{L_3^2}{2I_3} + (1/I_2 - 1/I_1)\,(L_2^2/2) = H_{sym} + H_{per} \qquad \ldots (39)$$

The above expression is obtained by adding and subtracting the term $(L_2^2/2I_1)$ in eq. (13). Clearly for small deviations from axial symmetry ($I_1 \simeq I_2$) the last term can be treated as a perturbation. Using $|LMK\rangle$ as the unperturbed state functions, the energy eigenvalues for an asymmetric top are given by

$$E = E_{sym} + \Delta E$$

where ΔE is given by

$$\Delta E = \langle LMK|L_2^2|LMK\rangle \left(1/2I_2 - 1/2I_1 \right)$$

to a first order. The diagonal elements of L_j^2 in $|LMK\rangle$ representation are

$$\langle LMK|L_{1,2}^2|LMK\rangle = (\hbar^2/2)\,(L(L+1) - K^2)$$

$$\langle LMK|L_3^2|LMK\rangle = \hbar^2 K^2 .$$

Thus, the energy eivenvalues for a slightly asymmetric top to a first order are

$$E = \frac{\hbar^2}{4}\left(\frac{1}{I_1}+\frac{1}{I_2}\right)\left[L(L+1) - K^2\right] + \frac{\hbar^2 K^2}{2I_3} \qquad (40)$$

Note that for $I_1 = I_2$, the above equation gives the eigenvalues for a symmetric top. Further details are discussed in the book by Davidson (1968).

III.5.5 Symmetry Properties of the State Function $|LM\rangle$

For ellipsoidal type of geometry of the solid, the state function $|LM\rangle$ exhibit a number of useful symmetries. Most important of these is the rotational symmetry which introduces arbitrariness in the choice of $B(x_1x_2x_3)$ axes. By rotational symmetry we mean that under certain rotational operations all the physical quantities describing the system remain invariant. In fact, as we shall see, there are 24 such operations providing we use only right-handed system (there are also 24 left-handed systems). In order to investigate the symmetries arising out of such operations, we define the relabeling transformations T_1, T_2 and T_3 (Bohr, 1952);

(i) T_1 produces the interchange 1 <—> -1, 3 <—> -3. It is equivalent to a rotation of π about the 2-axis such that $T_1^2 = 1$.

(ii) T_2 produces the interchange 1 <—> 2, 2 <—> -1. It is equivalent to a rotation of $\pi/2$ about the 3-axis such that $T_2^4 = 1$.

(iii) T_3 produces the interchange 1 <—> 2 <—> 3 <—> 1 such that $T_3^3 = 1$.

Hence, the most general relabeling transformation that does not involve a change of handedness is $T_1^p\, T_2^q\, T_3^r$. Here $p = 1,2$; $q = 1,2,3,4$; $r = 1,2,3$; giving rise to 24 different principal axis systems.

The symmetry properties of the state function $|LM\rangle$ under the operations T_1 and T_2^2, which have the eigenvalues ± 1, are

$$T_1 \,|LM\rangle = \pm\, |LM\rangle$$

$$T_2^2 \,|LM\rangle = \pm\, |LM\rangle \,.$$

Thus, there are four classes of rigid rotator state functions. Since, the basic state functions in our case are the symmetric top state functions, it is interesting to study the operation of T_1 and T_2^2 on $|LMK\rangle$. This leads to the following result (Appendix II.5)

$$T_1 |LMK\rangle = e^{i\pi(L+K)} \; |LM\,-K\rangle$$

$$T_2^2 |LMK\rangle = e^{i\pi K} \; |LMK\rangle$$

It is useful to write equation (38) in the form

$$|LM\rangle = \sum_{K=0}^{L} \left[A_K \,|LMK\rangle + A_{-K} \,|LM\,-K\rangle \right] \qquad (41)$$

Clearly the operation of T_2^2 on $|LM\rangle$ shows that K can either be only even or only odd. Further, operating T_1 on $|LM\rangle$ and relating the expansion coefficients in eq. (41)

with negative K to those with positive K we get

K - even

(i) $A_{-K} = (-1)^{L} A_K$ state function is $+|LM\rangle$

(ii) $A_{-K} = -(-1)^{L} A_K$ state function is $-|LM\rangle$

K - odd

(iii) $A_{-K} = -(-1)^{L} A_K$ state function is $-|LM\rangle$

(iv) $A_{-K} = (-1)^{L} A_K$ state function is $+|LM\rangle$

From eq. (40) for the energy of an asymmetric top, it is clear that each level is characterised by two quantum numbers L and K. The above symmetry conditions on the state function $|LM\rangle$ helps in obtaining the possible energy level structure in each of the above four cases. For example, consider the system belonging to case (i), K-even class of symmetry. This system will have one level with $L = 0$, no levels with $L = 1$ (since the state functions vanish), two levels with $L = 2$, one with $L = 3$, three with $L = 4$ and so on.

REFERENCES

Bohr, A. (1952). Kgl. Danske. Videnskab. Selskab. Mat. Fys. Medd. 26, No. 14.

Davidson, J.P. (1968). 'Collective Models of Nucleus', Academic Press, New York.

Elliott, J.P. (1958). 'Lectures on Collective Motion in Nuclei', compiled by Macfarlane, M.H., Department of Physics, University of Rochester, Rochester, New York.

Goldstein, H. (1950). 'Classical Mechanics', Addison Wesley, New York.

Landau, L.D. and Lifshitz, E.M. (1969). 'Mechanics', Oxford, Pergamon Press, 2nd ed.

Rose, M.E. (1957). 'Elementary Theory of Angular Momentum', John Wiley and Sons, Inc., New York.

C H A P T E R - IV

THE TWO MASS-POINT CENTRIFUGAL STRETCHING MODEL

In Chapter II, it was pointed out that the two mass-point centrifugal stretching model of Gupta (1969) gives a satisfactory description of high spin states up to L = 14 in the ground state rotational band of deformed even-even nuclei in terms of only two parameters, viz., the distance (r_o) between the two mass-points in the ground state, and the stiffness C of the potential. However, the treatment of Gupta (1969) was somewhat semi-empirical and semi-classical, and the rotational energy was obtained in the form of an asymptotic series whose convergence was sensitive to the magnitude of the total angular momentum ($\bar{L}$).

It will be shown in this Chapter that it is possible to obtain the energy of the rotational-vibrational motion of the

two mass-points in a closed form, by treating the two mass-point non-rigid system quantum mechanically with suitable phenomenological potentials. Thus, use of a harmonic potential is found to yield an energy expression as a function of the parameters r_o and C, and is found to contain, in addition to terms occurring in eq. (18) of Chapter II, an L-dependent zero point vibrational energy term for a given nucleus.

Essentially, the purpose of our present investigation is to examine whether the nuclear flow, which is known to be neither irrotational nor rigid, is 'equivalent' to the motion of two mass-points.

The formulation, calculations and the discussion of the results are presented in the following sections.

IV.1 FORMULATION

The model is formulated by representing the rotational-vibrational motion of an axially symmetric prolate deformed even-even nucleus equivalently by the motion of two mass-points, situated at the centres of mass of the two fragments, with a phenomenological potential as a function of the distance (r) between them. The two fragments are obtained by dividing the deformed nucleus into two equal parts by a plane containing the axis of rotation and perpendicular to the symmetry axis. In such a representation, the increase in the moment of inertia of the nucleus due to centrifugal stretching resulting from an

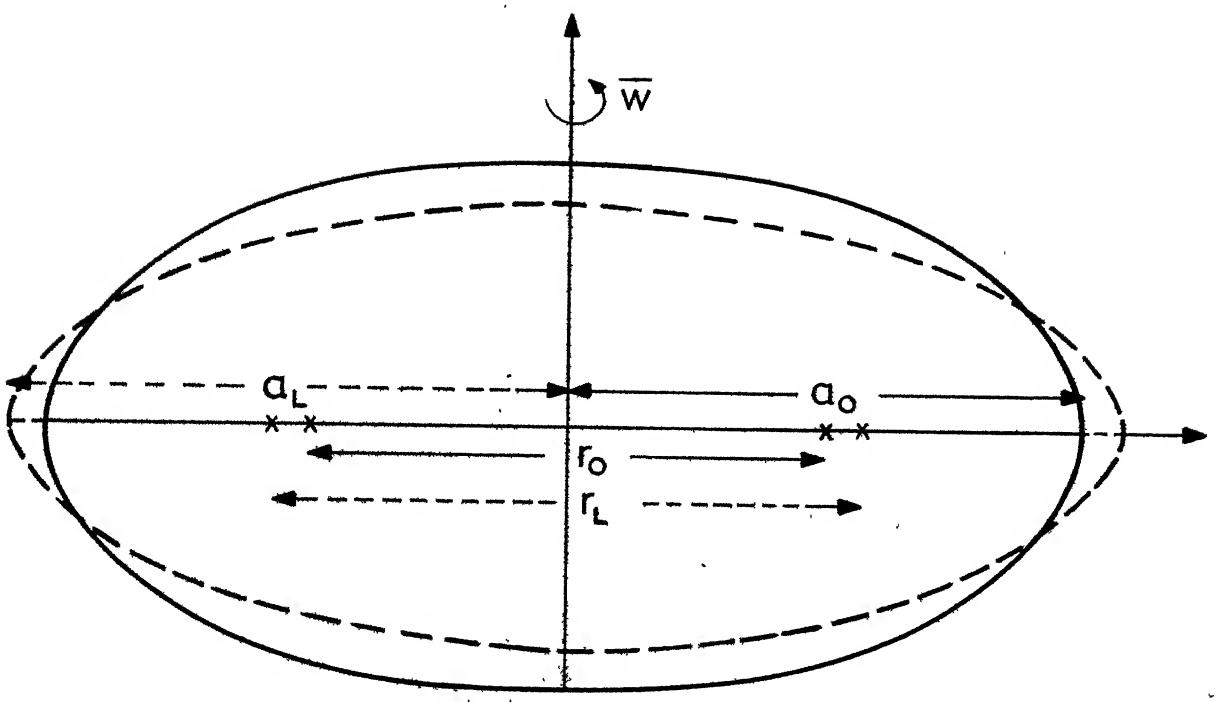

Fig. IV.1 A spheroidal nucleus undergoing rotation and centrifugal stretching.

increase in the rotational frequency is accounted for, by an increase in the distance between the two mass-points. Here, we consider only such vibrations (β-type) which preserve the prolate shape and the volume of the nucleus under centrifugal stretching which means that the centres of mass of the two fragments will vibrate only along the nuclear symmetry axis, and hence no γ-vibrations are considered. Such a system will have a reduced mass (m) equal to one quarter of the mass (M) of the nucleus and a moment of inertia (I_T) given by (Davydov and Fillippov, 1957)

$$I_T = Mr^2/4 \qquad (1)$$

By simple geometry (Figure IV.1) it can be shown that the total separation r of the two-centres of mass in their equilibrium position is given by

$$r_L = (3/4)\, a_L \qquad (2)$$

where a_L is the semi-major axis of the spheroid in its equilibrium position and the subscript L is used to characterize the state of the system. For a prolate spheroid with quadrupole deformation we have (Bohr and Mottelson 1953)

$$a_L = R_o\,(1 + \sqrt{5/4\pi}\,\beta_L) \qquad (3)$$

Thus, the equilibrium distance (r_L) between the two mass-points is determined by the deformation and the total volume. Notice

that eq. (2) is independent of semi-minor axis (b_L).

For a rotating nucleus, the two-centres of mass would shift due to centrifugal stretching such that the amount of stretching is given by the displacement ($r_L - r_o$). The centrifugal force

$$F = m w^2 r_L = L^2/(m r_L^3) \qquad (4)$$

causing the displacement ($r_L - r_o$) are balanced, in our investigation, either by harmonic or by anharmonic restoring forces. In eq. (4) w is the rotational angular frequency of the nucleus.

Alternatively, one can also consider the stretching of the nucleus in terms of individual nucleons. Naturally, when such a system rotates, due to centrifugal forces, the inter-nucleon distance (r_i) would increase with the increase in w. If m_i is the mass of each nucleon, the total centrifugal force F is

$$F = \sum_{i=1}^{A} m_i r_i w^2 = m w^2 \sum_{i=1}^{A} r_i \qquad (5)$$

where again the integral over r_i defines the distance r_L between the centres of mass and eq. (5) is same as eq. (4).

IV.2 CHOICE OF THE POTENTIAL

A likely form of the potential is the curve A of Figure IV.2 which is characterized by a strong repulsion when the nucleus is squeezed in from its equilibrium position at r_o and

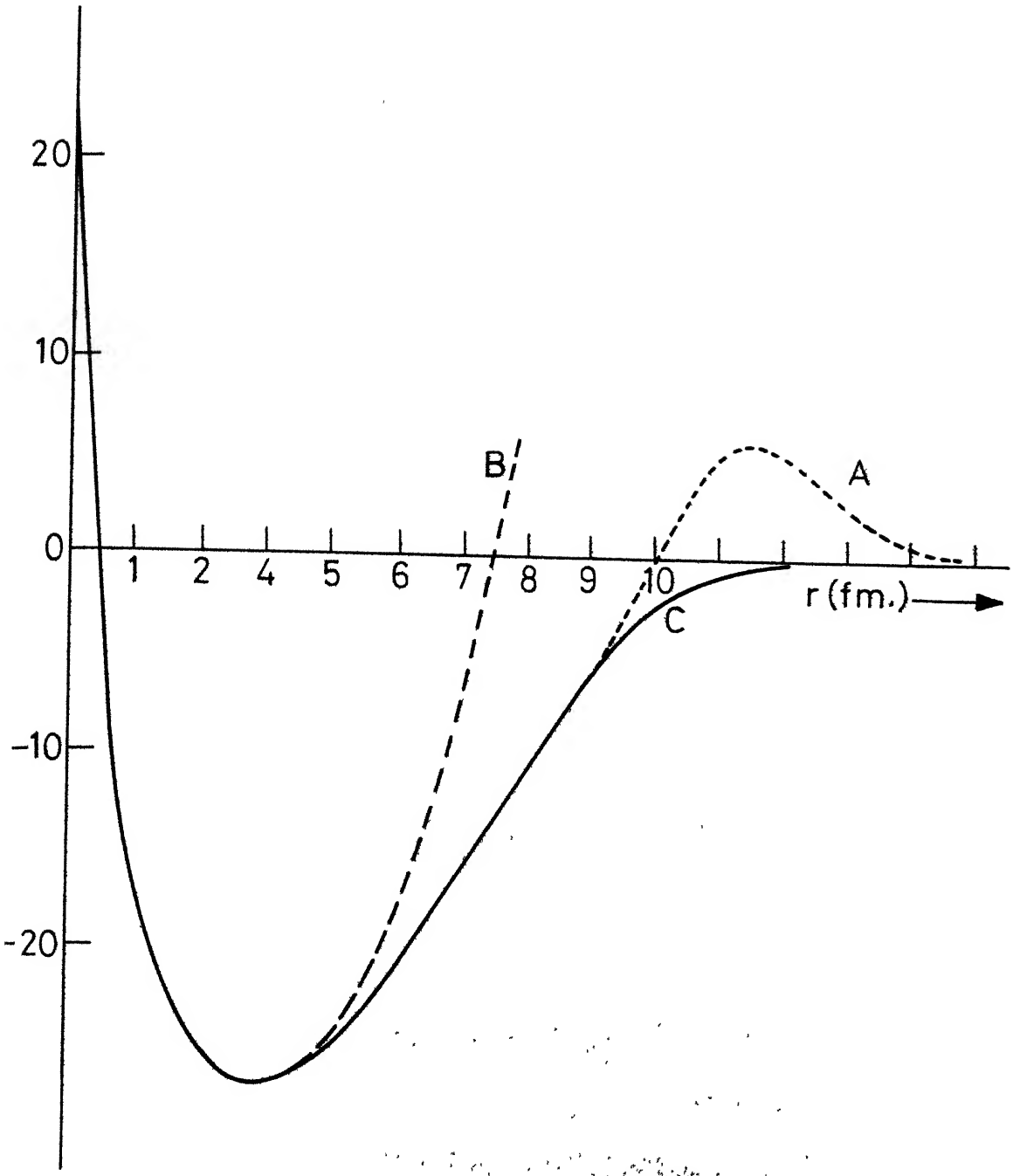

Fig. IV.2 Choice of the potential

a potential barrier before fission. Although a more appropriate form of the potential to be used is a single particle potential with two-centres of attraction each situated at the centre of mass of each of the fragments (Holzer et. al. 1969), we, for simplicity and in analogy with the model of Gupta (1969), have used a single particle potential with one centre of attraction as our interest, at present, is only in the low-lying rotational states. For such states, we have approximated the actual potential in the neighbourhood of the equilibrium minimum, by the harmonic potential (curve B of Figure IV.2) given by

$$V_H(r) = (s/2)\,(r - r_o)^2 \qquad (6)$$

where s is the stiffness of the potential.

In order to investigate the anharmonicity effect we have used the Morse potential (Morse 1929) which is extensively used in the study of diatomic molecules and is given by

$$V_M(r) = D\left[1 - \exp\{-\alpha(r - r_o')\}\right]^2 - D \qquad (7)$$

where the parameters D and r_o' respectively correspond to the depth and the width of the potential (curve C of Figure IV.2). This potential has the general shape of curve A, though not the potential barrier feature. While the right potential to be used for the entire spectrum is not the Morse potential, we have used it only to study the anharmonicity effect on rotational states which lie much lower in energy than the potential barrier.

IV.3 THEORY AND ITS COMPARISON WITH OTHER MODELS

IV.3.1 With Harmonic Oscillator Potential

Using for example, the harmonic oscillator potential, the Hamiltonian (H) representing the relative motion of the system is

$$H = (-\hbar^2/2m)\ \nabla^2(r,\theta,\phi) + (s/2)\ (r-r_o)^2 \qquad (8)$$

where r, θ, ϕ are relative coordinates. The energy eigenvalues and eigenfunctions of the system are obtained by solving the Schrödinger equation

$$H\psi_{NLM}\ (r,\ \theta,\ \phi) = E(N,L)\ \psi_{NLM}\ (r,\theta,\phi) \qquad (9)$$

where N,L,M are the usual quantum numbers characterizing the state of the system. Following the usual procedure, the total wave function (ψ_{NLM}) is separated into the radial and angular parts by writing

$$\psi_{NLM}(r,\theta,\phi) = \frac{u_{NL}(r)}{r}\ y_{LM}(\theta,\phi) \qquad (10)$$

Since the potential is centrally symmetric, use of eqs. (8) and (10) in eq. (9) yields the following radial equation for the motion of the reduced mass (m) of the system

$$\left[\ \frac{-\hbar^2}{2m}\ \frac{d^2}{dr^2} + V_{eff}(r) - E(N,L)\ \right]\ u_{NL}(r) = 0 \qquad (11)$$

where V_{eff} is the effective potential that the particle experiences and is given by

IV.3 THEORY AND ITS COMPARISON WITH OTHER MODELS

IV.3.1 With Harmonic Oscillator Potential

Using for example, the harmonic oscillator potential, the Hamiltonian (H) representing the relative motion of the system is

$$H = (-\hbar^2/2m)\ \nabla^2(r,\theta,\phi) + (s/2)\ (r-r_o)^2 \qquad (8)$$

where r, θ, ϕ are relative coordinates. The energy eigenvalues and eigenfunctions of the system are obtained by solving the Schrödinger equation

$$H\psi_{NLM}\ (r,\ \theta,\ \phi) = E(N,L)\ \psi_{NLM}\ (r,\theta,\phi) \qquad (9)$$

where N,L,M are the usual quantum numbers characterizing the state of the system. Following the usual procedure, the total wave function (ψ_{NLM}) is separated into the radial and angular parts by writing

$$\psi_{NLM}(r,\theta,\phi) = \frac{u_{NL}(r)}{r}\ y_{LM}(\theta,\phi) \qquad (10)$$

Since the potential is centrally symmetric, use of eqs. (8) and (10) in eq. (9) yields the following radial equation for the motion of the reduced mass (m) of the system

$$\left[\ \frac{-\hbar^2}{2m}\ \ \frac{d^2}{dr^2} + V_{eff}(r) - E(N,L)\ \right]\ u_{NL}(r) = 0 \qquad (11)$$

where V_{eff} is the effective potential that the particle experiences and is given by

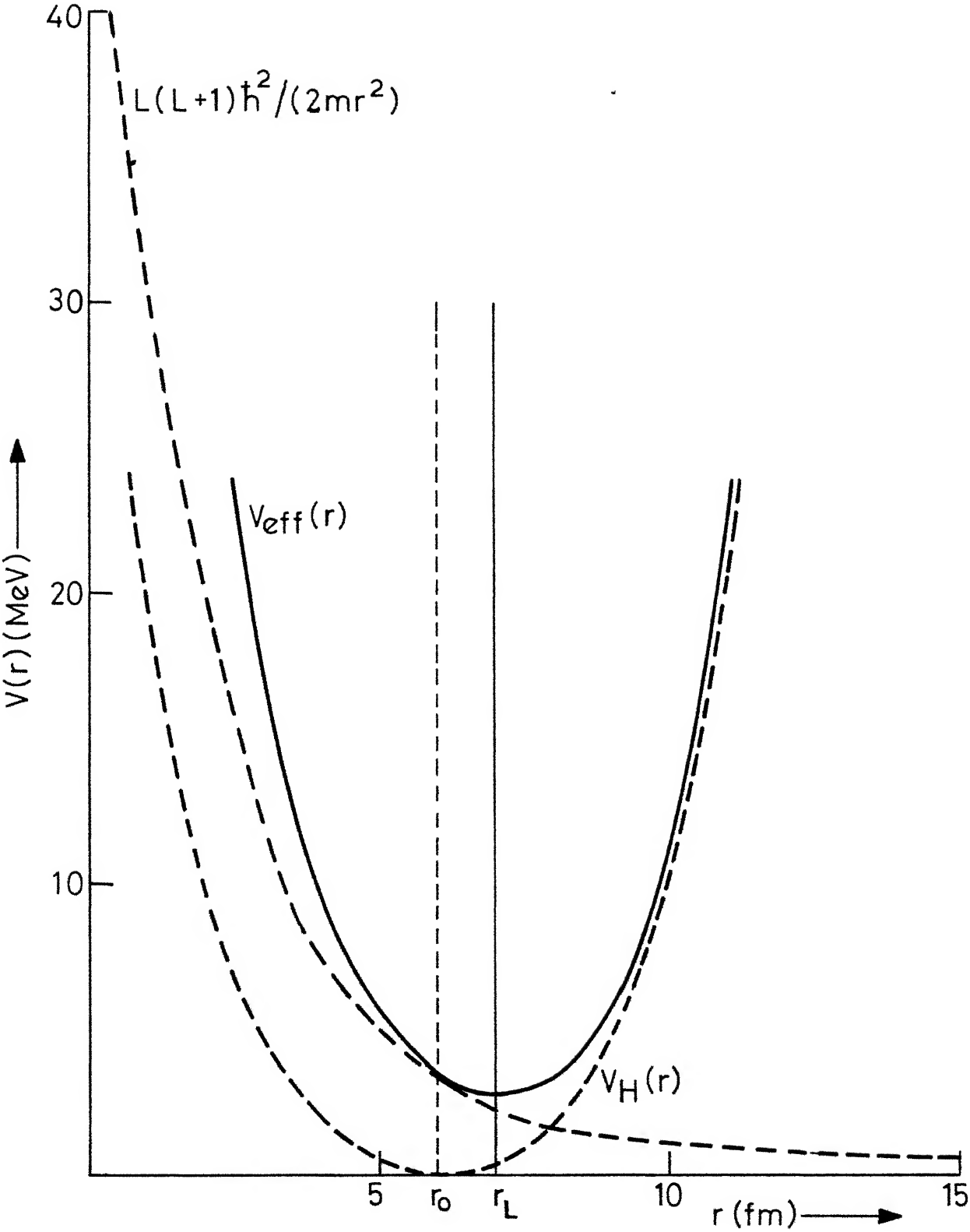

Fig. IV.3 Plots of the harmonic (V_H) and the centrifugal terms and their sum (V_{eff}) as a function of the distance (r).

$$V_{eff}(r) = L(L+1)\hbar^2/(2mr^2) + (s/2)(r-r_o)^2. \qquad (12)$$

A plot of the individual terms on the right hand side of eq. (12) and their sum (V_{eff}) as a function of the distance r is shown in Figure IV.3. It is important to note that the effective potential is different for different L-values, with a characteristic equilibrium minimum at $r = r_L$ for each L.

Making a Taylor expansion of $V_{eff}(r)$ around the equilibrium position r_L we have

$$V_{eff}(r) = V_{eff}(r_L) + \frac{\partial V_{eff}}{\partial r}\Big|_{r=r_L}(r-r_L) + \frac{1}{2}\frac{\partial^2 V_{eff}}{\partial r^2}\Big|_{r=r_L}(r-r_L)^2+\cdots \qquad \ldots(13)$$

Using the condition that $\frac{\partial V_{eff}}{\partial r} = 0$ at $r = r_L$ and neglecting the effect of higher order terms we have

$$V_{eff}(r) = (s_L/2)(r-r_L)^2 + V_{eff}(r_L).$$

Hence, eq. (11) becomes

$$\left[-\frac{\hbar^2}{2m}\frac{d^2}{dr^2} + (s_L/2)(r-r_L)^2 - E'\right] u_{NL}(r) = 0 \qquad (14)$$

where $E' = E(N,L) - V_{eff}(r_L)$ and $s_L = s + \frac{3L(L+1)\hbar^2}{mr_L^4}$.

Eq. (14) is supplemented by the following boundary conditions; the eigenfunctions $u_{NL}(r)$ goes to zero for $r \to 0$ or ∞. For $|r| >> r_L$, eq. (14) approaches the Schrödinger equation for one dimensional harmonic oscillator and hence, the eigenvalues of eq. (14) can approximately be written as

$$E' = (N + 1/2)\hbar \sqrt{(s_L/m)}$$

$$\text{or} \quad E(N,L) = (N + 1/2)\hbar \sqrt{\left[s + 3L(L+1)\hbar^2/(mr_L^4) \right](1/m)}$$

$$+ \frac{s}{2} (r_L - r_o)^2 + \frac{L(L+1)\hbar^2}{2mr_L^2} \qquad \ldots(15)$$

where $r_L = r_o + \frac{L(L+1)\hbar^2}{msr_L^3}$

and N, in general, is not an integer (Merzbächer 1961). However, for values of parameters characteristic of even-even nuclei in the rare-earth region, use of integral values of N leads to negligible errors.

Eq. (15) gives, in general, the energy of vibrational-rotational motion of the two mass-point system. The ground state zero-point vibrational energy E(0,0) of the system is obtained by putting N = 0 and L = 0 in eq. (15). The energies of rotational states in the ground state rotational band is obtained by putting N = 0 in eq. (15) and subtracting out the zero-point vibrational energy E(0,0) from the resulting expression. The energy expression thus obtained is

$$E(L) = \frac{\hbar^2}{2I_T} L(L+1) + \frac{s}{2} (r_L - r_o)^2 + E_c \qquad (16a)$$

$$\text{where} \quad E_c = (\tfrac{\hbar}{2}) \left[\sqrt{(s/m) + 3L(L+1)\hbar^2/(m^2 r_L^4)} - \sqrt{(s/m)} \right] \qquad (16b)$$

$$\text{and} \quad r_L = r_o + L(L+1)\hbar^2/(msr_L^3) \qquad (16c)$$

$$I_T = mr_L^2 . \qquad (16d)$$

We now make a comparison of the expressions obtained above with the corresponding expressions obtained by others on the basis of various models.

A direct comparison of eq. (16a) with the energy expression obtained by Gupta (1969) (eq. (18) of Chapter II) shows that

(i) the two differ by the quantity E_c corresponding to the zero-point energy given by eq. (16b)

(ii) the energy $E(L)$ is obtained in a closed form aided by the auxiliary eq. (16c) for the equilibrium position

(iii) there is no breakdown in rotational structure at high spin states.

Further, use of eqs. (2) and (3) in eq. (16a) and a subsequent simplification, shows that eq. (16a) is of the same form as eq. (16) of Chapter II (Diamond et. al. 1964), with the difference that there is a zero-point energy term (E_c) and the moment of inertia I_T is now given by mr_L^2 which is determined by values of the parameters r_o and s.

Lastly, using $r = (3/4)R_o\ (1 + \sqrt{5/4\pi}\ \beta)$ for the instantaneous value of r (refer to eqs. (2) and (3)) together with eq. (12) in eq. (11), the radial equation in the two mass-point centrifugal stretching model for the harmonic potential becomes

$$\left[\frac{-\hbar^2}{2B_T} \frac{d^2}{d\beta^2} + \frac{\hbar^2}{2I_T} L(L+1) + \frac{C_T}{2} (\beta-\beta_o)^2 - E(N,L) \right] u_{NL}(\beta) = 0 \quad (17)$$

where $B_T = (15/32)\ (3MR_o^2/8\pi)$ (17a)

$$I_T = (45/128)\ (2MR_o^2/5)\ (1 + \sqrt{5/4\pi}\ \beta)^2 \quad (17b)$$

$$C_T/B_T = s/m\ . \quad (17c)$$

An expression similar to eq. (17) has already been obtained by Davydov and Chaban (1960) on the basis of the irrotational flow model of Bohr and Mottelson (1953) and is given by

$$\left[\frac{-\hbar^2}{2B_H} \frac{d^2}{d\beta^2} + \frac{\hbar^2}{2I_H} L(L+1) + \frac{C_H}{2} (\beta-\beta_o)^2 - E \right] u_{NL}(\beta) = 0 \quad (18)$$

where $B_H = (3MR_o^2/8\pi)$ (18a)

$$I_H = (9/8\pi)MR_o^2\ \beta^2 \quad (18b)$$

$$C_H/B_H = s/m\ . \quad (18c)$$

A direct comparison of eq. (17) with eq. (18) reveals that eq. (17) is of the same form as eq. (18), and that the specific differences in the values of various quantities may be due to the difference in the specific flow pattern in the two cases. Besides, it is rather interesting to note that although the mass parameter B_T is about half of B_H, the two mass-point moment of inertia (I_T) is about six times the

hydrodynamic value (I_H), and is about a third of the rigid spheroid value (I_R), for values of $\beta \simeq 0.3$. Also, notice that unlike I_H, I_T does not go to zero with β. However, the frequency of vibration is the same in both the cases.

Thus, the two mass-point model, based on the simple classical considerations of symmetry, represents a flow which is neither irrotational nor rigid, leading to the above values of the parameters.

IV.3.2 With Morse Potential

The expression for the eigenvalues with the Morse potential is well known (Pekeris 1934, Pauling and Wilson 1935) and is given by

$$E(N,L) = c_o - \frac{(D-c_1/2)^2}{(D+c_2)} + \frac{2\alpha(D-c_1/2)}{\sqrt{2m(D+c_2)}}\hbar(N+\tfrac{1}{2}) - \frac{\alpha^2}{2m}\hbar^2(N+\tfrac{1}{2})^2 \qquad \ldots(19)$$

where
$$c_o = A_L\left(1 - \frac{3}{\alpha r_o'} + \frac{3}{\alpha^2 r_o'^2}\right)$$

$$c_1 = A_L\left(\frac{4}{\alpha r_o'} - \frac{6}{\alpha^2 r_o'^2}\right)$$

$$c_2 = A_L\left(-\frac{1}{\alpha r_o'} + \frac{3}{\alpha^2 r_o'^2}\right)$$

and
$$A_L = \frac{\hbar^2}{2I_o'} L(L+1) \; ; \quad \text{where } I_o' = mr_o'^2 .$$

D, α, r_o' are the parameters of the potential. Eq. (19) differs from eq. (16a) for higher values of L. The energies

of rotational states in the ground state rotational band is obtained by putting $N = 0$ in eq. (19) and then subtracting out the zero-point vibrational energy $E(0,0)$ obtained by putting $N = 0$ and $L = 0$ in eq. (19). The resulting equation is

$$E(L) = c_o - \frac{(D-c_1/2)^2}{D+c_2} + \frac{\alpha(D-c_1/2)}{\sqrt{2m(D+c_2)}} - \frac{\alpha^2\hbar^2}{2m} - E(0,0) \qquad (20)$$

where $$E(0,0) = -E + \frac{\alpha\hbar D}{\sqrt{2mD}} + \frac{\alpha^2\hbar^2}{8m} .$$

IV.4 CORRELATION OF THE INTRINSIC QUADRUPOLE MOMENT WITH THE MOMENT OF INERTIA ON THE BASIS OF VARIOUS MODELS

A simple analysis of the available experimental data on the basis of various models shows that the two mass-point model of Gupta (1969) successfully correlates the intrinsic quadrupole moment data with the moment of inertia data more satisfactorily than the rigid spheroid or the hydrodynamic models.

The value of R_o occurring in various expressions is not well determined by a formula of the type $R_o = 1.2\ A^{1/3}$ fm., since nuclei in the rare-earth region are expected to have large skin depths (Hofstadter 1957) of the order of two fermis. However, it is interesting to note that for spheroidal nuclei, the ratio of model moment of inertia (I_M) for the rigid spheroid, the hydrodynamic and the two mass-point models, to the quadrupole moment given by eq. (6) of Chapter II is independent of R_o. Thus,

TABLE IV.1

β obtained for various models using experimental values of (I/Q)

Nucleus	Q_{expt} (barns)	I_{expt} (10^{-19} keV sec^2)	Value of deformation obtained using experimental values of (I/Q)		
			β_T	β_R	β_H
$^{152}_{62}Sm$	5.85	95.9	0.372	1.052	2.003
^{154}Sm	6.81	142.5	0.270	0.728	2.751
$^{154}_{64}Gd$	6.08	94.9	0.390	1.116	1.924
^{156}Gd	6.86	131.3	0.296	0.806	2.490
^{158}Gd	7.30	146.9	0.282	0.763	2.626
^{160}Gd	7.55	155.1	0.279	0.754	2.656
$^{156}_{66}Dy$	6.17	84.6	0.464	1.442	1.668
^{158}Dy	6.85	118.0	0.335	0.925	2.09
^{160}Dy	6.91	134.7	0.287	0.778	2.576
^{162}Dy	7.13	144.2	0.278	0.751	2.666
^{164}Dy	7.49	159.2	0.264	0.712	2.812
$^{162}_{68}Er$	7.01	115.6	0.354	0.988	2.098
^{164}Er	7.23	128.4	0.324	0.891	2.278
^{166}Er	7.62	144.9	0.300	0.816	2.464
^{168}Er	7.64	146.4	0.302	0.821	2.448
^{170}Er	7.46	147.9	0.293	0.795	2.524
$^{168}_{70}Yb$	7.39	134.3	0.312	0.853	2.367
^{170}Yb	7.56	138.7	0.313	0.855	2.361
^{172}Yb	7.77	148.4	0.301	0.818	2.456

Table IV.1 (Contd.)

^{174}Yb	7.57	152.7	0.283	0.768	2.609
^{176}Yb	7.40	142.3	0.307	0.839	2.401
$^{174}_{72}Hf$	7.27	128.5	0.327	0.901	2.58
^{176}Hf	7.37	132.3	0.325	0.895	2.270
^{178}Hf	6.78	125.3	0.317	0.869	2.327
^{180}Hf	6.73	125.2	0.319	0.876	2.311
$^{180}_{74}W$	6.65	114.5	0.343	0.951	2.161
^{182}W	6.46	116.7	0.325	0.895	2.271
^{184}W	6.08	105.4	0.352	0.892	2.1[illegible]
^{186}W	6.00	95.4	0.405	1.175	1.861
$^{186}_{76}Os$	5.59	85.1	0.415	1.215	1.823
^{188}Os	5.26	75.4	0.465	1.450	1.663
^{190}Os	5.06	62.6	0.612		1.367

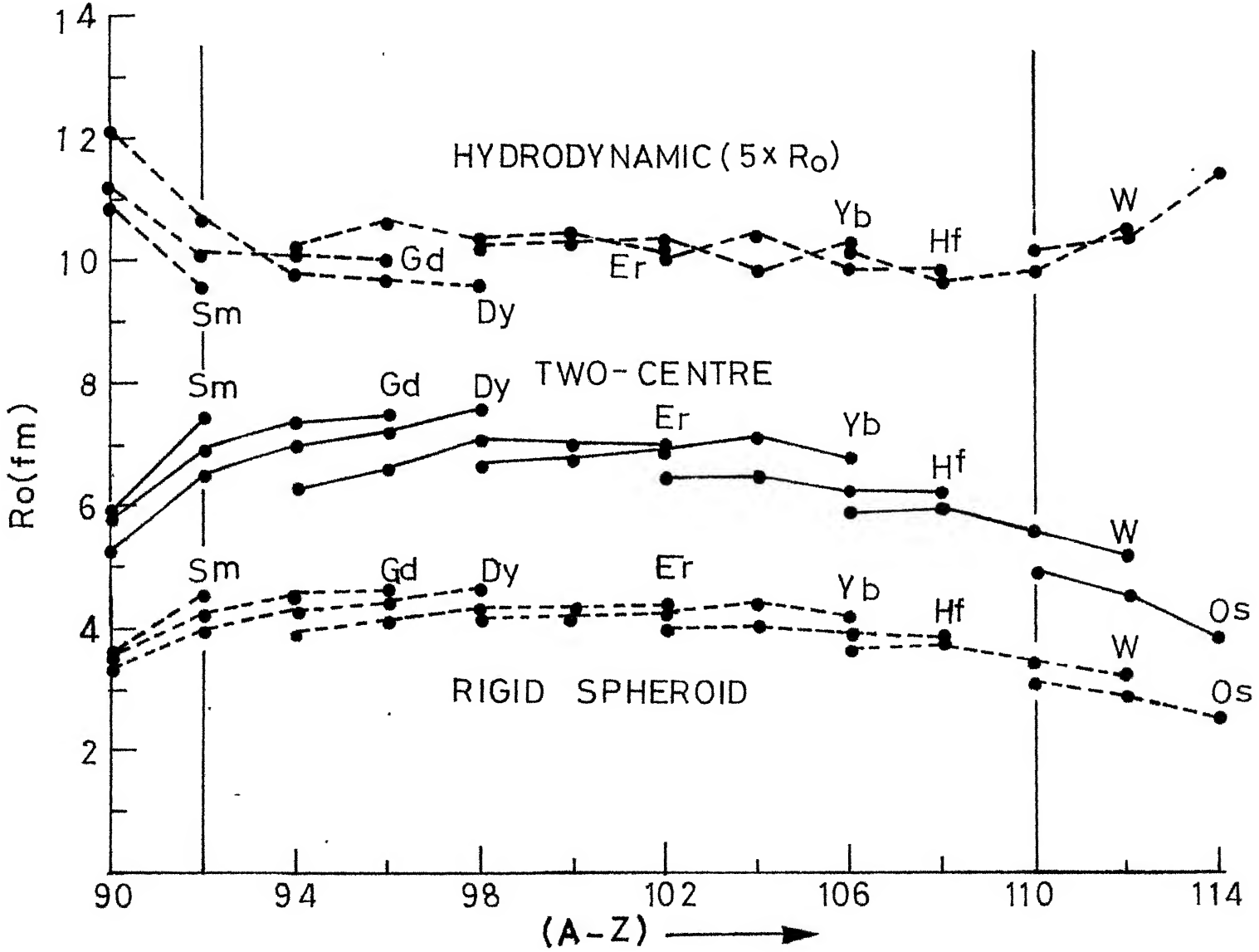

Fig.IV.4: Variation of R_o as a function of the neutron number (A-Z) for various models.

$$(I_M/Q_o) = F_M(M,Z,\beta) \qquad (21)$$

where F_M is a model dependent function. For the two mass-point model, I_M is given by eq. (17b) and corresponding model dependent function is

$$F_M = F_T = (\sqrt{45\pi}/64)(M/Ze)(1 + 0.63\,\beta)^2/(\beta + 0.16\,\beta^2). \qquad (22)$$

Expressions similar to eq. (22) can be obtained for the rigid spheroid and the hydrodynamic models using corresponding model moments of inertia. However, such an analysis is not appropriate for the case of governor model since the effective nuclear density is treated as a parameter (Trainor and Gupta 1971).

Calculations are done for thirty-two even-even nuclei in the rare-earth region for which experimental values (Mariscotti et. al. 1969) of quadrupole moments were available. Their moments of inertia are obtained from the known energies of the levels with $L = 2$. Using these values of (I/Q_o) in eq. (21), the values of β obtained for each model are tabulated in Table IV.1. These values of β are in turn used to calculate the values of R_o for the two mass-point, the rigid spheroid and the hydrodynamic models, and are plotted as a function of the neutron number $(A-Z)$ in Figure IV.4. It is clear that only the two mass-point model gives satisfactory values of β and R_o: For $90 < (A-Z) < 110$, the values of R_o for the two mass-point model are close to those given by the equation $R_o = 1.2\,A^{1/3}$ fm. In this region, $\beta \simeq 0.35$ and $R_o \simeq 6.5$ fm.,

for the two mass-point model, $\beta \simeq 0.85$ and $R_0 \simeq 4.5$ fm., for the rigid spheroid model and $\beta \simeq 2.2$ and $R_0 \simeq 2$ fm., for the hydrodynamic model.

IV.5 CALCULATIONS

IV.5.1 Level Energies

For calculating the energies of rotational levels in the ground state band, we have used eqs. (16) in the case of harmonic potential with s and r_0 as parameters, and eqs. (20) in the case of Morse potential with D, α and r_0' as parameters.

For fitting the energy levels there were two alternatives. Either to adopt the least squares fitting procedure or to fit the low lying levels exactly to uniquely determine the parameters and then calculate the higher levels. While apparently, satisfactory fits to the levels of a large number of nuclei could be obtained with the least squares fitting procedure as has been done earlier by Mariscotti et. al. (1969) and many others, the latter procedure is used to bring out systematic departures, if any.

In actual calculations, in the case of harmonic potential eqs. (16) are used to fit exactly the lowest 2^+ and 4^+ levels of about fifty even-even nuclei in the rare-earth region to uniquely determine the parameters s and r_0 for each nucleus. Notice that r_L is only an auxiliary parameter. These values of s and r_0 are used to calculate the energies of levels up to $L = 18$. The

maximum departure of the calculated value from the experimental value (Mariscotti et. al. 1969) usually occurs for the highest known level. The values of C, I_o the maximum percentage departure $(\Delta E)_{max}$ and the level to level comparison of calculated energies are given in Table IV.2.

Plots of variation of the stiffness C with the neutron number and the proton number are shown in Figures IV.6 and IV.7 respectively.

The stiffness s' characteristic of the equilibrium position r'_o of the Morse potential is

$$s' = (\partial^2 V_M(r)/\partial r^2)_{r=r'_o} = 2\alpha^2 D . \qquad (23)$$

In order to study the effect of anharmonicity, it is necessary to make a direct comparison of the results obtained using Morse potential with those obtained using harmonic potential Such a comparison is possible provided we reduce the three independent parameters D, α and r'_o to essentially two.

For low lying levels in the ground state the shape of the Morse potential closely resembles that of the harmonic potential and hence it is reasonable to assume that the stiffness s' of the Morse potential to be same as that of the harmonic potential, thus reducing the number of parameters to essentially two with the aid of eq. (23). The values of these two parameters are determined using eq. (20) and by fitting the known energies of

2^+ and 4^+ states exactly. These values of the parameters are used to calculate the energies of rotational levels up to L = 18. The values of the parameters, the maximum percentage departure $(\Delta E)_{max}$ and a level to level comparison of calculated energies with the experiment are given in Table IV.3. Although the ground state moment of inertia I'_o obtained with the Morse potential is about the same as that obtained with the harmonic potential, no noticeable improvement in the level fitting is observed.

Further, the energy of the excited β-vibrational state ($0^{+'}$) is calculated using the parameters needed to fit the lowest rotational levels exactly. A comparison of the calculated vibrational energies with the experiment is done in Figure IV.5. However, a least squares fit to all the rotational levels and $0^{+'}$ level gives fits to within a maximum departure of 6 per cent as shown in Table IV.4.

IV.5.2 Quadrupole Moment (Q_{oL}) and the Value of $B(E2;\ 4^+ \rightarrow 2^+)/B(E2;\ 2^+ \rightarrow 0^+)$

The reduced transition probability for transitions of the type $L+2 \rightarrow L$ is given by (Bohr and Mottelson 1953)

$$B(E2;\ L+2 \rightarrow L) = \frac{15}{32\pi} e^2 Q_{oL}^2 \frac{(L+1)(L+2)}{(2L+3)(2L+5)} \qquad (24)$$

where Q_{oL} is the intrinsic quadrupole moment of the nucleus in the state of angular momentum L given by eq. (6) of Chapter II

with the corresponding deformation β_L for spheroidal shape. Eq. (24) can be used to obtain

$$\frac{B(E2;\ 4^+ \rightarrow 2^+)}{B(E2;\ 2^+ \rightarrow 0^+)} = (10/7)(Q_{04}/Q_{02})^2 \ . \qquad (25)$$

The value of the superfluous parameter r_L obtained during the energy level fitting is used to obtain deformation β_L using eqs. (2) and (3). A comparison of the calculated values of Q_{02} and the value of the ratio $B(E2;\ 4^+ \rightarrow 2^+)/B(E2;\ 2^+ \rightarrow 0^+)$ with those of the experimental values is done in Table IV.5.

A comparison of the various results obtained above with experiments and other models is done in the following sections.

IV.6 COMPARISON OF RESULTS WITH EXPERIMENTS AND OTHER MODELS

The experimental values of the deformation β and the equal volume radius R_o for a typical spheroidal nucleus located around the middle of the region $150 < A < 190$, are approximately equal to 0.3 and 6.5 fm., respectively. It is clear from Table IV.1 and Figure IV.4 that the best values of β and R_o are obtained only for the two mass-point moment of inertia and hence the model correlates the quadrupole moment data with the moment of inertia data more satisfactorily than the rigid spheroid or the hydrodynamic models.

In Table IV.2, for fifty even-even nuclei in the rare-earth region, we have tabulated the values of the parameters C and I_o, the experimental and the calculated energies up to

L = 18, and the maximum percentage departure $(\Delta E)_{max}$ of the calculated energy from the experimental value for the case of harmonic potential. $(\Delta E)_{max}$ usually occurs for the highest known level and is less than 1 per cent for 27 nuclei, less than 2 per cent for 7 nuclei and more than 2 per cent for 16 nuclei, whereas, for the 32 nuclei analysed by Gupta (1969), $(\Delta E)_{max}$ was less than 1 per cent for 17 nuclei, less than 2 per cent for 7 nuclei and more than 2 per cent for 8 nuclei, considering levels up to L = 14 only. A least squares fit would give results as good as those obtained by Mariscotti et.al. (1970). The values of moment of inertia obtained using the values of the parameter r_o in eq. (16d) are in agreement with the experimental values to within a maximum departure of 1 per cent, except for a few neutron deficient nuclei and ^{190}Os nucleus.

The stiffness constants(C) that we obtain are about 50 per cent larger than those obtained by Mariscotti et. al. (1970) and are considerably smaller than those obtained by Mosel and Greiner (1968). However, a number of prominent features characteristic to these nuclei as obtained by Mariscotti et. al. (1970) on the basis of the Variable Moment of Inertia model are also observed for the two mass-point model.

From Table IV.2, it is clear that the values of the parameters I_o and C vary rather smoothly from one isotope to the other. It is readily seen that, as a rule, large values

TABLE IV.2

Calculated and Experimental Values of Energies, and the Values of Parameters for the Harmonic Potential

Nucleus	L^{π}	2^+	4^+	6^+	8^+	10^+	12^+	14^+	16^+	18^+	C (MeV)	I_o (10^{-19} KeV. Sec^2)	$(\Delta E)_m$ (%)
^{150}Nd	1:	132.0	397.0	760.0									
	2:	132.0	397.0	749.1	1161	1617	2107	2625	3165	3723	1.639	94.6	1.4
	3:	5.435	5.829	6.263	6.692	7.104	7.497	7.871	8.228	8.570			
^{152}Sm	1:	121.8	366.4	712.0	1122	1615							
	2:	121.7	366.6	692.6	1074	1497	1952	2432	2933	3451	1.551	102.6	5.0
	3:	5.618	6.020	6.465	6.905	7.328	7.732	8.117	8.484	8.835			
^{154}Sm	1:	81.99	267.0	545.0	927.0								
	2:	81.96	267.1	543.6	808.4	1320	1797	2322	2889	3492	3.891	149.3	3.0
	3:	6.508	6.629	6.797	6.995	7.210	7.434	7.660	7.886	8.110			
^{154}Gd	1:	123.1	371.2	718.1	1146	1644	(2189)						
	2:	123.0	371.3	702.5	1091	1522	1985	2474	2985	3515	1.561	101.5	7.2
	3:	5.546	5.936	6.369	6.799	7.213	7.608	7.985	8.345	8.688			
^{156}Gd	1:	88.97	288.2	584.5	966.0	1417	1924						
	2:	88.97	288.2	587.0	967.2	1417	1924	2482	3081	3718	4.205	137.8	0.4
	3:	6.217	6.344	6.519	6.722	6.941	7.167	7.621	7.845				

TABLE IV.2 (Contd.)

	1:	79.51	261.4	539.0	898.2								
^{158}Gd	2:	79.54	261.5	538.1	899.9	1337	1840	2402	3015	3674	6.125	152.7	0.4
	3:	6.475	6.552	6.664	6.801	6.956	7.122	7.295	7.471	7.648			
	1:	75.3	247.0	509.0	863.0								
^{160}Gd	2:	75.3	248.0	511.7	858.3	1279	1766	2311	2909	3553	6.745	161.0	0.4
	3:	6.601	6.670	6.770	6.894	7.036	7.189	7.350	7.514	7.682			
	1:	138.0	403.0	766.0	1212								
^{156}Dy	2:	138.0	404.6	749.2	1147	1582	2045	2532	3038	3560	1.434	90.3	2.5
	3:	5.276	5.740	6.227	6.697	7.142	7.562	7.960	8.338	8.698			
	1:	99.0	317.0	633.0	1037	1512 (2037)							
^{158}Dy	2:	98.7	316.7	633.7	1030	1490	2002	2558	3150	3775	3.392	125.1	0.4
	3:	5.916	6.091	6.320	6.575	6.841	7.108	7.372	7.630	7.883			
	1:	86.7	284.0	582.0	972.0	1442							
^{160}Dy	2:	86.7	284.0	582.1	968.9	1433	1964	2552	3192	3876	6.176	140.6	0.6
	3:	6.181	6.271	6.398	6.552	6.723	6.903	7.089	7.276	7.463			
	1:	81.0	266.0	548.0	923.0								
^{162}Dy	2:	80.7	266.0	549.5	923.1	1378	1905	2497	3147	3849	8.622	150.0	0.3
	3:	6.330	6.391	6.480	6.591	6.719	6.858	7.004	7.155	7.308			
	1:	73.39	242.2	501.3	839.0								
^{164}Dy	2:	73.39	242.2	500.8	840.2	1258	1742	2285	2382	3529	7.727	164.7	0.2
	3:	6.593	6.653	6.741	6.851	6.979	7.118	7.264	7.416	7.571			

TABLE IV.2 (Contd.)

	1:	192.1	528.4	972.0	1496	2076	2684					
^{158}Er	2:	192.1	528.4	940.1	1400	1893	2412	2952	3508	4078	1.461	63.2	10.0
	3:	4.580	5.152	5.701	6.208	6.677	7.114	7.523	7.909	8.275			
	1:	126.2	390.5	766.8	1231	1763	2343					
^{160}Er	2:	126.3	390.3	752.3	1185	1671	2199	2760	3349	3962	2.471	98.7	6.8
	3:	5.307	5.603	5.948	6.302	6.650	6.986	7.309	7.619	7.917			
	1:	101.0	327.0	662.0	1090	1595							
^{162}Er	2:	101.0	327.0	661.0	1084	1582	2141	2753	3409	4104	4.982	121.6	0.8
	3:	5.740	5.873	6.053	6.259	6.479	6.704	6.929	7.152	7.371			
	1:	91.0	298.0	608.0	1014	1512							
^{164}Er	2:	91.2	299.3	614.5	1025	1518	2084	2713	3397	4131	7.729	133.4	1.0
	3:	5.944	6.024	6.139	6.279	6.434	6.600	6.770	6.944	7.117			
	1:	80.6	264.9	545.0	910.0	(1343)							
^{166}Er	2:	80.6	264.8	544.1	908.5	1348	1852	2414	3026	3683	6.525	150.7	0.1
	3:	6.280	6.361	6.476	6.617	6.776	6.944	7.119	7.300	7.475			
	1:	79.8	264.0	549.0									
^{168}Er	2:	79.8	264.0	548.5	927.2	1393	1940	2560	3248	3996	13.740	150.9	0.1
	3:	6.226	6.267	6.326	6.403	6.494	6.595	6.704	6.818	6.937			
	1:	79.0	261.0	542.0									
^{170}Er	2:	79.0	261.0	541.5	913.6	1370	1903	2506	3173	3896	11.880	152.7	0.1
	3:	6.228	6.274	6.343	6.430	6.532	6.644	6.764	6.890	7.019			

TABLE IV.2 (Contd.)

	1:	166.5	486.7	922.9	1444	2013							
^{162}Yb	2:	166.4	486.7	900.1	1375	1895	2449	3030	3634	4256	2.108	74.8	6.2
	3:	4.179	5.141	5.583	6.008	6.410	6.789	7.148	7.489	7.814			
	1:	122.5	384.0	758.0	1219	1748	2354	(2928)					
^{164}Yb	2:	122.5	384.1	750.8	1196	1701	2253	2845	3469	4121	3.188	101.1	4.0
	3:	5.282	5.523	5.816	6.125	6.433	6.734	7.027	7.309	7.581			
	1:	101.8	329.7	667.1	1097	1604	2172	(2774)	(3402)				
^{166}Yb	2:	101.8	329.9	667.3	1096	1600	2168	2789	3457	4163	6.454	120.7	0.2
	3:	5.646	5.773	5.946	6.145	6.357	6.574	6.792	7.008	7.221			
	1:	87.9	287.0	582.0	967.0	1427	(1932)						
^{168}Yb	2:	87.9	287.0	585.8	971.1	1430	1953	2529	3153	3819	5.795	139.0	0.9
	3:	6.005	6.107	6.249	6.418	6.603	6.797	6.994	7.192	7.389			
	1:	84.2	277.7	572.0	962.0	1439	(1986)						
^{170}Yb	2:	84.2	277.6	573.8	964.2	1440	1991	2612	3292	4028	10.400	143.7	0.4
	3:	6.049	6.106	6.189	6.294	6.414	6.545	6.682	6.824	6.970			
	1:	78.7	260.3	540.0	910.0	1352							
^{172}Yb	2:	78.8	260.2	538.8	907.1	1357	1881	2472	3122	3827	10.510	153.3	0.6
	3:	6.207	6.260	6.337	6.434	6.547	6.671	6.802	6.938	7.077			
	1:	76.5	252.0	527.0	892.0								
^{174}Yb	2:	76.5	252.1	521.2	876.1	1309	1811	2375	2995	3664	9.040	158.2	1.8
	3:	6.273	6.330	6.416	6.523	6.646	6.780	6.922	7.068	7.217			
	1:	82.1	270.0	564.0	947.0								

TABLE IV.2 (Contd.)

	1:	158.7	470.7	897.6	1407	1971	2565	(3178)					
^{166}Hf	2:	158.7	470.6	878.5	1351	1871	2427	3013	3622	4251	2.337	78.6	5.0
	3:	4.743	5.129	5.543	5.946	6.329	6.692	7.037	7.365	7.679			
	1:	123.9	385.0	756.1	1212	1734	2304	(2910)					
^{168}Hf	2:	123.9	385.0	745.5	1179	1667	2198	2765	3360	3981	2.828	100.5	4.8
	3:	5.214	5.486	5.808	6.141	6.470	6.790	7.097	7.393	7.678			
	1:	100.0	320.0	641.1	1041	1503	2013	2564	3147	3761			
^{170}Hf	2:	100.0	320.6	640.2	1039	1501	2015	2571	3164	3788	3.760	123.5	0.5
	3:	5.669	5.844	6.070	6.322	6.583	6.844	7.102	7.354	7.600			
	1:	94.5	307.9	627.0	1036	1519	2063	2651	3273	(3915)			
^{172}Hf	2:	94.5	307.8	625.8	1033	1516	2063	2663	3311	4000	5.987	129.6	1.6
	3:	5.737	5.848	6.001	6.180	6.374	6.575	6.778	6.981	7.182			
	1:	90.9	298.0	609.0	1010	1502							
^{174}Hf	2:	91.0	297.6	608.4	1010	1490	2037	2643	3299	3999	7.032	134.1	0.9
	3:	5.793	5.885	6.015	6.171	6.342	6.522	6.706	6.891	7.076			
	1:	88.3	290.4	596.6	998.0								
^{176}Hf	2:	88.4	290.4	597.4	998.6	1483	2040	2662	3340	4068	9.110	137.5	0.1
	3:	5.822	5.893	5.996	6.121	6.263	6.414	6.571	6.731	6.891			
	1:	93.2	306.8	632.5	1059								
^{178}Hf	2:	93.2	306.6	631.9	1058	1575	2171	2838	3567	4351	11.420	130.2	0.3
	3:	5.631	5.694	5.785	5.897	6.025	6.162	6.305	6.452	6.600			

TABLE IV.2 (Contd.)

	1:	93.3	308.6	641.1	1085								
^{180}Hf	2:	93.3	308.7	641.1	1084	1628	2265	2989	3790	4662	20.560	129.0	0.1
	3:	5.563	5.600	5.655	5.725	5.808	5.900	5.999	6.103	6.210			
	1:	122.9	376.9	727.2	1147	1616	2129	2677	(3252)	(3849)			
^{172}W	2:	122.7	377.2	724.0	1137	1599	2099	2631	3188	3768	2.393	101.5	1.7
	3:	5.207	5.514	5.868	6.229	6.581	6.920	7.246	7.558	7.858			
	1:	111.9	355.0	704.2	1137	1635	2186	(2780)					
^{174}W	2:	111.9	355.0	701.7	1128	1617	2156	2737	3352	3996	3.767	110.8	1.4
	3:	5.329	5.530	5.784	6.057	6.336	6.611	6.880	7.141	7.395			
	1:	108.7	348.5	699.4	1140	1648	2206	(2801)	(3425)				
^{176}W	2:	108.7	348.9	698.7	1137	1646	2213	2830	3487	4180	2.430	113.7	0.3
	3:	5.340	5.494	5.697	5.923	6.160	6.397	6.633	6.864	7.089			
	1:	104.0	342.0	697.0	1152	1679	2264	2894					
^{178}W	2:	104.0	342.1	696.7	1152	1693	2306	2981	3710	4486	8.262	116.6	3.0
	3:	5.347	5.446	5.582	5.743	5.918	6.100	6.289	6.468	6.651			
	1:	103.6	337.5	690.0	1147	1667	2252						
^{180}W	2:	103.6	337.6	687.6	1137	1671	2276	2943	3663	4429	8.224	118.2	0.3
	3:	5.353	5.451	5.587	5.748	5.923	6.104	6.289	6.473	6.655			
	1:	100.1	329.4	680.4	1144	(1712)							
^{182}W	2:	100.1	329.4	679.5	1139	1697	2343	3065	3856	4709	14.500	121.2	0.1
	3:	5.371	5.427	5.510	5.612	5.729	5.855	5.987	6.123	6.260			

TABLE IV.2 (Contd.)

	1:	111.2	364.0	748.2								
^{184}W	2:	111.2	364.0	745.1	1239	1830	2505	3253	4065	4932	12.170	100.7	0.4
	3:	5.093	5.170	5.279	5.411	5.556	5.709	5.866	6.024	6.182			
	1:	122.5	399.0	818.0								
^{186}W	2:	122.4	399.6	816.5	1354	1996	2726	3534	4408	5340	13.660	99.9	0.2
	3:	4.837	4.916	5.028	5.162	5.309	5.462	5.619	5.776	5.933			
	1:	131.6	397.7	760.8	1194	1682	2218						
^{178}Os	2:	131.6	397.7	753.2	1170	1633	2132	2658	3208	3778	1.816	94.9	4.0
	3:	4.984	5.332	5.717	6.101	6.471	6.824	7.161	7.482	7.790			
	1:	132.2	408.5	795.2	1257	1767	2308	2875					
^{180}Os	2:	132.2	409.0	789.8	1246	1758	2315	2908	3531	4179	3.392	94.3	0.9
	3:	4.888	5.154	5.467	5.788	6.104	6.410	6.705	6.988	7.260			
	1:	126.9	400.2	793.9	1277	1810							
^{182}Os	2:	126.9	400.2	786.2	1258	1795	2385	3019	3688	4388	4.557	97.9	1.8
	3:	4.910	5.117	5.371	5.642	5.915	6.183	6.444	6.697	6.941			
	1:	119.8	383.6	773.9	1275	1871							
^{184}Os	2:	119.8	383.5	764.8	1240	1789	2400	3060	3763	4503	5.944	103.2	5.0
	3:	4.984	5.141	5.345	5.571	5.804	6.037	6.267	6.492	6.711			
	1:	137.2	433.9	868.7	1420	(2068)							
^{186}Os	2:	137.2	433.9	854.4	1369	1958	2605	3301	4037	4807	5.855	90.5	3.6
	3:	4.666	4.853	5.087	5.337	5.590	5.840	6.082	6.318	6.546			

TABLE IV.2 (Concluded)

	1:	155.0	477.9	939.5	1514	2170						
$^{188}_{0s}$	2:	155.0	477.9	919.6	1447	2038	2679	3361	4076	4820	4.708	80.5	6.2
	3:	4.425	4.677	4.970	5.270	5.563	5.847	6.119	6.380	6.631			
	1:	186.7	547.8	1050	1662								
$^{190}_{0s}$	2:	186.6	548.0	1016	1556	2148	2778	3441	4129	4840	4.708	80.5	6.5
	3:	4.108	4.465	4.842	5.205	5.550	5.875	6.183	6.476	6.756			

(In the above the rows 1, 2 and 3 respectively denote the experimental energies, calculated energies and the value of the superfluous parameter r_L for various values of L^π for each nucleus.)

TABLE IV.3

Calculated and Experimental Values of Energies, and the Values of Parameters for the Morse Potential

Nucleus		L^π 2^+	4^+	6^+	8^+	10^+	12^+	14^+	16^+	18^+	Stiffness $s'=s$ (10^{29} $\frac{KeV}{cm^2}$)	α (10^{12} cm^{-1})	(E) (%)	D (MeV)	r'_o (fm)
^{150}Nd	1:	132.0	397.0	760.0											
	2:	132.0	397.1	749.6	1174	1671	2246	2902	3643	4470	0.180	2.24	1.4	1.8	4.856
^{152}Sm	1:	121.8	366.4	712.0	1122	1615									
	2:	121.8	366.3	690.7	1080	1534	2059	2658	3333	4087	0.158	2.20	5.0	1.6	5.012
^{154}Sm	1:	81.99	267.0	545.0	927.0										
	2:	81.99	267.0	541.8	889.9	1295	1745	2229	2742	3281	0.420	2.29	4.0	4.0	6.188
^{154}Gd	1:	123.1	371.2	718.1	1146	1644	(2189)								
	2:	123.1	371.2	701.3	1097	1560	2093	2701	3386	4151	0.168	2.22	4.9	1.7	4.962
^{156}Gd	1:	88.97	288.2	584.5	966.0	1417	1924								
	2:	89.00	288.2	579.8	941.0	1349	1783	2230	2678	3123	0.450	3.13	6.9	2.3	5.803
^{158}Gd	1:	79.51	261.4	539.0	898.2										
	2:	79.53	261.4	537.5	897.0	1328	1820	2364	2952	3579	0.650	1.90	0.3	9.0	6.270
^{160}Gd	1:	75.30	247.0	509.0	863.0										
	2:	75.30	247.2	506.8	840.8	1232	1659	2100	2529	2923	0.710	4.21	2.5	2.0	6.182
^{156}Dy	1:	138.0	403.0	766.0	1212										
	2:	137.9	403.1	749.5	1170	1671	2257	2933	3699	4559	0.150	2.50	3.5	1.2	4.572

TABLE IV.3 (Contd.)

^{158}Dy	1:	99.00	317.0	633.0	1037	1512	(2037)							
	2:	99.00	317.1	630.2	1013	1447	1922	2431	2976	3557	0.360	2.45	4.3	3.0	5.528
^{160}Dy	1:	86.70	284.0	581.3	967.2	1429	1952	2515	3192	(3773)					
	2:	86.70	284.1	581.6	965.4	1421	1936	2500	3106	3748	0.650	2.16	2.7	7.0	5.946
^{162}Dy	1:	80.70	266.0	548.0	923.0										
	2:	80.70	266.0	549.4	921.4	1371	1388	2462	3083	3745	0.900	2.24	0.2	9.0	6.131
^{164}Dy	1:	73.39	242.2	501.3	839.0										
	2:	73.39	242.2	501.1	842.6	1258	1740	2279	2870	3507	0.800	1.53	0.4	17.0	6.444
^{160}Er	1:	126.2	390.5	766.8	1231	1763	2343								
	2:	126.2	390.6	752.9	1190	1696	2272	2922	3649	4456	0.260	2.10	3.1	3.0	4.884
^{162}Er	1:	101.0	327.0	662.0	1090	1595									
	2:	101.0	327.1	659.3	1076	1558	2094	2675	3297	3962	0.520	2.28	2.3	5.0	5.454.
^{164}Er	1:	91.20	299.0	608.0	1014	1512									
	2:	91.20	299.1	613.2	1020	1503	2050	2648	3288	3965	0.800	2.39	0.8	7.0	5.717
^{166}Er	1:	80.60	264.9	545.0	910.0	(1343)									
	2:	80.60	264.9	544.9	910.0	1350	1854	2416	3029		0.670	1.40	0.1	17.0	6.126
^{168}Er	1:	79.80	264.0	549.0											
	2:	79.80	264.0	548.5	927.2	1393	1937	2551	3230	3964	1.400	1.83	0.1	21.0	6.098
^{170}Er	1:	79.00	261.0	542.0											
	2:	79.00	261.1	541.4	912.6	1366	1892	2481	3125	3815	1.200	2.33	0.1	11.0	6.054

TABLE IV.3 (Contd.)

^{162}Yb	1:	166.5	486.7	922.9	1444	2013									
	2:	166.5	486.7	906.8	1420	2032	2751	3579	4520	5574	0.220	2.71	1.7	1.50	4.095
^{164}Yb	1:	122.5	384.0	758.0	1219	1748	2354	(2928)	(3398)						
	2:	122.5	384.1	746.8	1183	1680	2237	2855	3537	4288	0.330	2.34	5.0	3.00	4.882
^{166}Yb	1:	101.8	329.7	667.1	1097	1604	2172	(2774)	(3402)						
	2:	101.8	329.7	664.4	1084	1567	2101	2676	3288	3935	0.560	2.52	3.2	4.40	5.348
^{168}Yb	1:	87.90	287.0	582.0	967.0	1427	(1932)								
	2:	87.90	287.0	584.5	964.2	1410	1907	2445	3018	3920	0.590	2.43	1.2	5.00	5.734
^{170}Yb	1:	84.20	277.7	572.0	962.0	1439	(1986)								
	2:	84.20	277.7	573.5	962.2	1432	1973	2572	3220	3910	1.050	2.41	0.5	9.00	5.854
^{172}Yb	1:	78.70	260.3	540.0	910.0	1352									
	2:	78.70	260.1	538.9	908.0	1360	1885	2478	3132	3842	1.050	1.13	0.6	41.00	6.112
^{174}Yb	1:	76.50	252.0	527.0	892.0										
	2:	76.50	252.0	519.0	866.7	1281	1747	2247	2764	3231	0.900	3.87	2.9	3.00	5.944
^{176}Yb	1:	82.10	270.0	564.0	947.0										
	2:	82.10	270.1	556.6	931.5	1384	1904	2482	3113	3792	0.830	1.66	1.6	15.00	5.880
^{166}Hf	1:	158.7	470.7	897.6	1407	1971	2565	(3178)							
	2:	158.8	470.7	881.9	1380	1970	2657	3446	4340	5340	0.240	2.62	1.9	1.75	4.178
^{168}Hf	1:	123.9	385.0	756.1	1212	1734	2304	(2854)							
	2:	123.8	385.1	744.5	1178	1677	2242	2877	3585	4369	0.288	2.19	3.1	3.00	4.810

TABLE IV.3 (Contd.)

^{170}Hf	1:	100.0	320.6	641.1	1041	1503	2013	2564	3149	(3915)				
	2:	100.0	320.7	640.0	1036	1493	2004	2566	3180	3847	0.380	1.95	1.0	5.00	5.376
^{172}Hf	1:	78.70	260.3	540.0	910.0	1352									
	2:	78.70	260.1	539.1	908.7	1361	1889	2485	3143	3860	1.050	0.90	0.7	65.00	6.128
^{174}Hf	1:	90.90	298.0	609.0	1010	1502									
	2:	90.95	298.0	610.6	1016	1502	2059	2681	3364	4106	0.700	1.06	0.6	31.00	5.670
^{176}Hf	1:	88.30	290.4	596.6	998.0										
	2:	88.34	290.4	597.3	997.4	1478	2027	2634	3292	3996	0.900	2.02	0.1	11.00	5.644
^{178}Hf	1:	93.20	306.8	632.5	1059										
	2:	93.20	306.8	632.4	1059	1574	2167	2827	3547	4321	1.120	1.81	0.1	17.00	5.486
^{180}Hf	1:	93.33	308.6	641.1	1085										
	2:	93.33	308.6	640.9	1082	1624	2256	2967	3749	4592	2.000	2.42	0.3	17.00	5.428
^{172}W	1:	122.7	377.2	727.2	1147	1616	2129	2677	(3252)	(3849)					
	2:	122.6	377.1	722.8	1138	1620	2169	2791	3488	4263	0.240	2.21	4.2	2.45	4.758
^{174}W	1:	111.9	355.0	704.2	1137	1635	2186	(2780)							
	2:	111.9	355.1	699.7	1107	1600	2136	2726	3374	4081	0.375	2.24	2.6	3.75	4.990
^{176}W	1:	108.7	348.9	699.4	1140	1648	2206	(2801)	(3425)						
	2:	108.8	343.5	678.1	1097	1596	2175	2835	3578	4405	0.240	0.52	3.7	45.00	5.244
^{178}W	1:	104.0	342.0	697.0	1152	1679	2264	2894							
	2:	104.0	340.1	694.5	1152	1697	2320	3015	3779	4609	0.810	1.18	4.2	29.00	5.240

TABLE IV.3 (Contd.)

^{180}W	1:	103.6	337.5	690.0	1147	1667	2252							
	2:	103.6	337.6	685.4	1126	1640	2209	2822	3470	4150	0.800	2.83	1.9	5.00	5.088
^{182}W	1:	100.1	329.4	680.4	1144	(1712)									
	2:	100.1	329.4	678.8	1136	1685	2313	3005	3750	4538	1.400	2.79	0.7	9.00	5.182
^{184}W	1:	111.2	364.0	748.2											
	2:	111.2	364.0	743.6	1231	1805	2449	3148	3890	4670	1.170	2.95	0.6	6.70	4.870
^{186}W	1:	122.5	399.6	818.0											
	2:	122.5	399.6	812.9	1338	1949	2624	3343	4092	4864	1.300	3.57	0.6	5.10	4.582
^{178}Os	1:	131.6	397.7	760.8	1194	1682	2218								
	2:	131.6	397.7	752.9	1180	1679	2254	2909	3648	4472	0.226	2.42	1.6	1.93	4.476
^{180}Os	1:	132.2	408.5	795.1	1257	1767	2308	2875							
	2:	132.2	408.3	783.4	1231	1742	2320	2967	3688	4486	0.330	2.60	3.2	2.45	4.458
^{182}Os	1:	126.9	400.2	793.9	1277	1810									
	2:	126.9	400.2	783.2	1257	1776	2368	3023	3744	4535	0.440	2.45	1.9	3.65	4.520
^{184}Os	1:	119.8	383.6	773.9	1275	1871									
	2:	119.8	383.7	763.5	1232	1770	2368	3024	3738	4513	0.570	2.39	5.3	5.00	4.702
^{186}Os	1:	137.2	433.9	868.7	1420	(2068)									
	2:	137.2	433.9	851.5	1359	1939	2586	3302	4089	4951	0.555	2.56	4.3	1.25	4.354
^{188}Os	1:	155.0	477.9	939.8	1514	2170									
	2:	155.0	477.8	916.7	1443	2049	2738	3515	4383	5347	0.445	2.70	5.5	3.05	4.042

TABLE IV.3 (Concluded)

^{190}Os	1:	186.6	547.8	1050	1662								
	2:	186.6	547.7	1022	1599	2286	3090	4017	5068	6246	0.340	3.10	3.9	1.78	3.580

(In the above 1 and 2 denote the experimental and calculated values of energies in KeV, and 3 denotes the value of the equilibrium deformation parameter β_I. Values within the parentheses involve a lot of uncertainty and (E) corresponds to (E)$_{max}$ of the text.)

TABLE IV.4

Values of the Harmonic and the Morse Potential Parameters and $(\Delta E)_{max}$ obtained by a least squares fit to all the rotational levels and $E(0^{+'})$.

Nucleus	s (10^{29} keV/cm^2)	r_o (fm.)	$(\Delta E)_{max}$ (%)	D (MeV)	α (10^{12} cm^{-1})	r_o' (fm.)	$(\Delta E)_{max}$ (%)
^{150}Nd	0.39	5.275	4.6	10.5	1.4	5.170	5.0
^{152}Sm	0.38	5.475	5.9	9.0	1.5	5.320	6.1
^{154}Sm	1.08	6.455	1.7	45.5	1.1	6.380	1.8
^{154}Gd	0.39	5.410	4.7	8.0	1.6	5.280	6.2
^{156}Gd	0.96	6.197	2.6	40.5	1.1	6.130	2.7
^{158}Dy	0.84	5.886	5.0	36.5	1.1	5.800	4.0
^{160}Dy	1.47	6.175	2.5	52.5	1.2	6.110	2.5
^{164}Er	1.46	5.945	2.4	51.5	1.2	5.880	2.4
^{166}Er	2.02	6.270	2.4	72.0	1.2	6.200	2.0
^{168}Yb	1.27	6.015	3.1	33.5	1.4	5.950	2.8
^{170}Yb	1.15	6.028	0.4	48.0	1.1	5.960	0.7
^{172}Yb	1.11	6.135	0.6	40.0	1.2	6.110	0.5
^{174}Yb	1.81	5.610	0.5	47.0	1.4	6.160	0.6
^{174}Hf	0.71	5.750	0.6	36.0	1.0	5.680	0.6
^{178}Hf	1.50	5.610	0.8	45.5	1.3	5.540	0.9
^{182}W	1.50	5.346	0.5	63.0	1.1	5.285	0.3
^{188}Os	1.21	4.350	4.7	51.0	1.1	4.320	5.0

TABLE IV.5

Comparison of Calculated Values of Q_{o2} and $B(E2, 4^+ \rightarrow 2^+)/B(E2; 2^+ \rightarrow 0^+)$ with the Experimental Values

Nucleus	Q_{o2} (barns)		$B(E2; 4^+ \rightarrow 2^+)/B(E2; 2^+ \rightarrow 0^+)$	
	Experimental	Calculated	Experimental*	Calculated
^{152}Sm	5.93	5.22	1.11	3.25
^{154}Sm	6.65	11.07	1.44	1.65
^{154}Gd	6.15	4.78	1.41	3.45
^{156}Gd	6.91	9.26	1.42	1.72
^{158}Gd	7.20	10.90	1.31	1.58
^{160}Dy	7.13	9.08	1.43	1.64
^{162}Dy	7.18	10.05	1.47	1.56
^{160}Er	6.52	3.00	1.36	4.17
^{166}Er	7.58	9.75	1.45	1.61
^{168}Er	7.60	9.23	1.50	1.52
^{172}Yb	7.81	9.12	1.28	1.56
^{180}Hf	6.83	3.77	1.56	1.66
^{182}W	6.40	2.18	1.42	2.09

*from Abou-Leila et al.(1971). Nucl. Phys. 175A, 663.

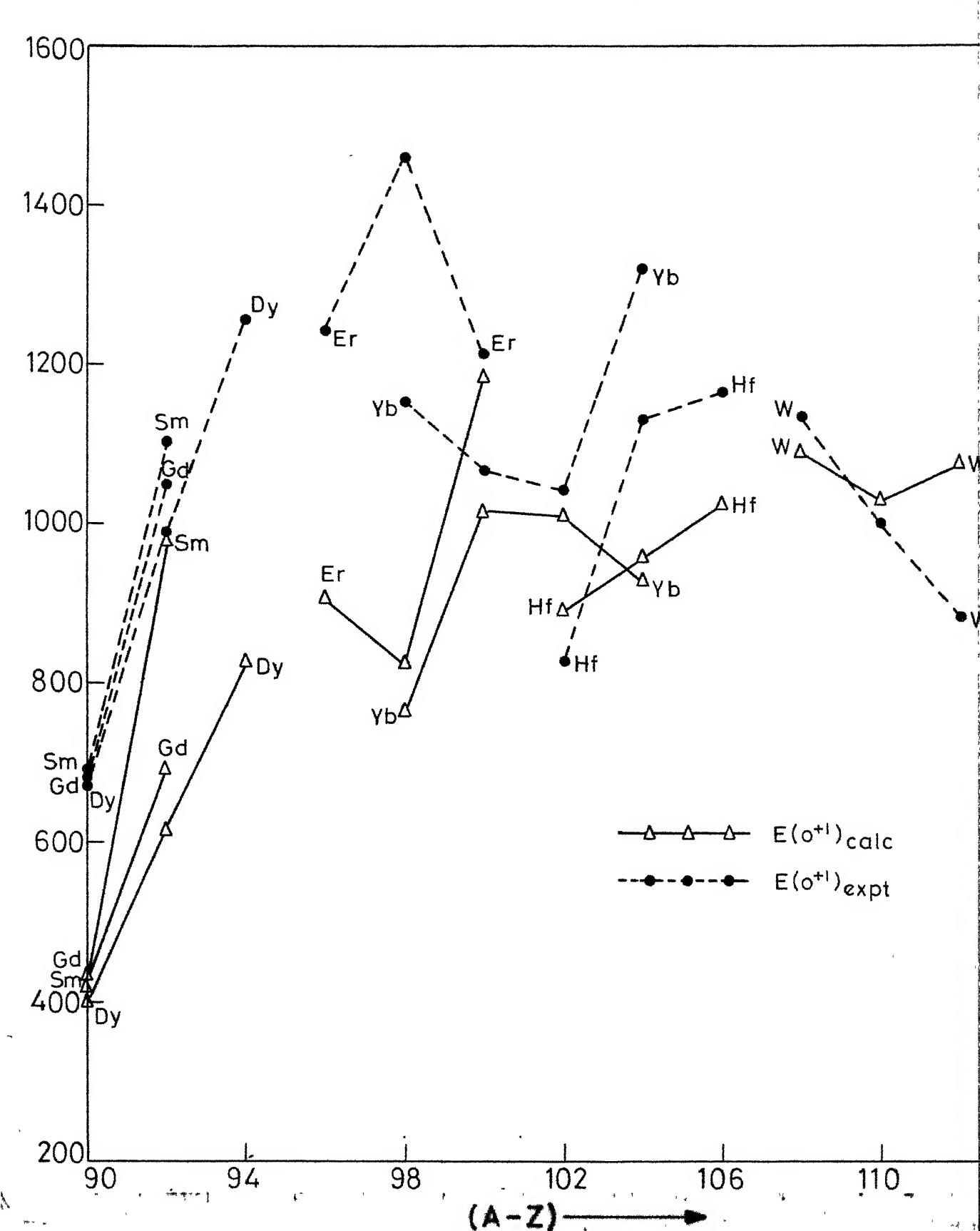

Fig. IV. 5 : Variation of the calculated and experimental valu of $E(o^{+'})$ with the neutron number (A-Z)

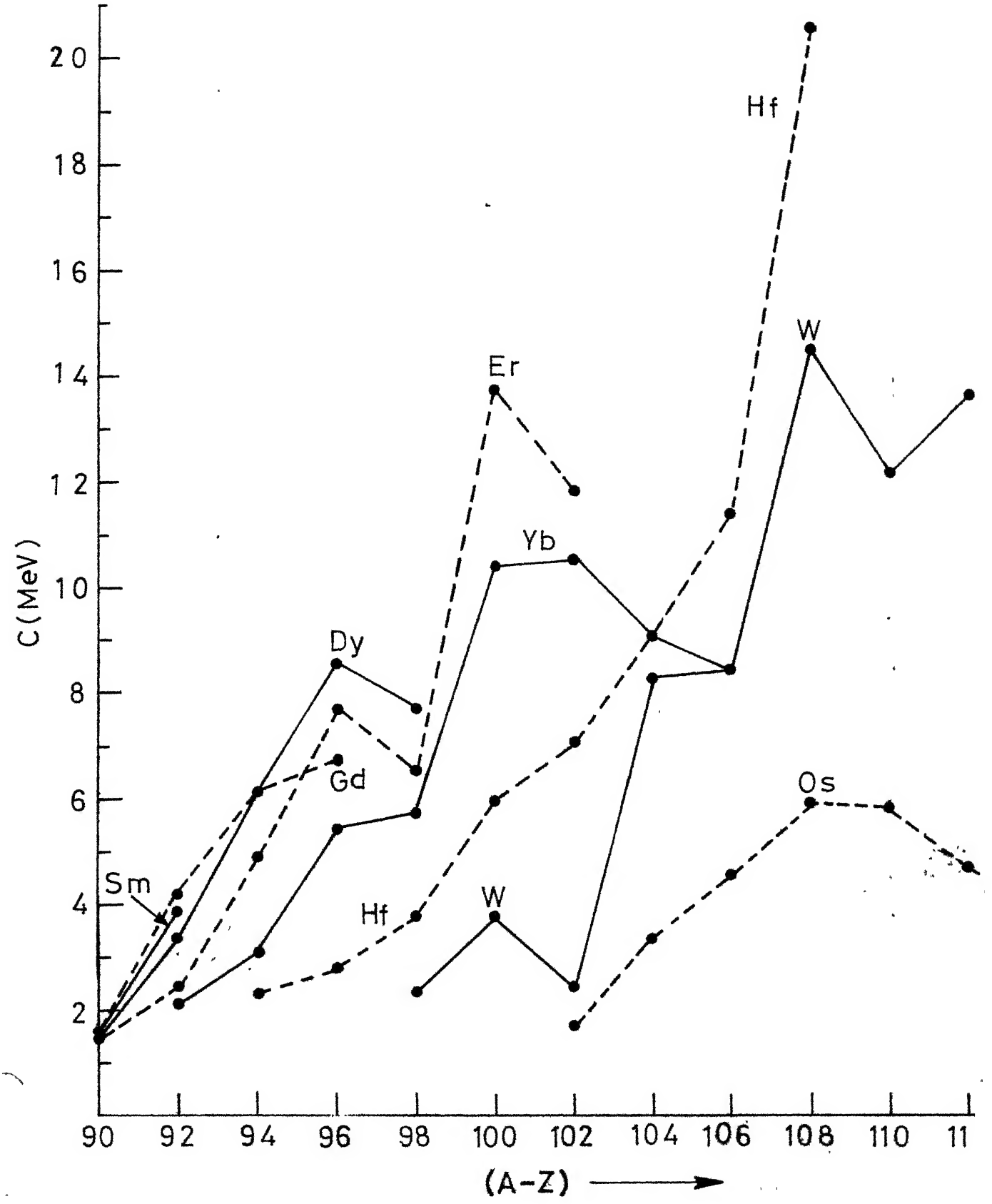

Fig. IV. 6: Variation of stiffness (C) with neutron number (A-
for the harmonic potential.

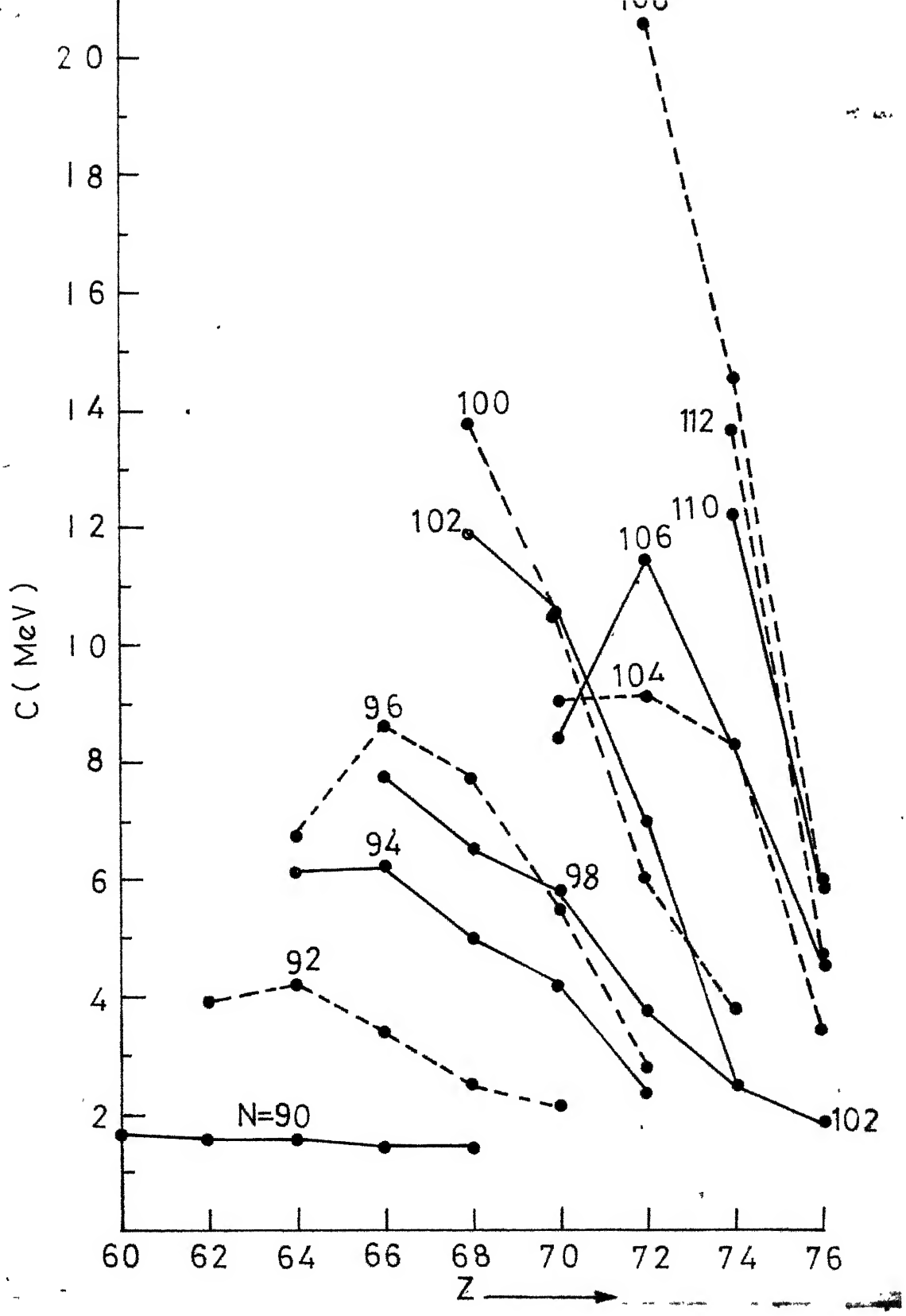

Fig. IV.7: Variation of stiffness (C) with the proton number (Z) for the harmonic potential.

of I_o correspond to large values of C. However, certain values appear to deviate from this rule. The glaring cases are ^{178}Hf, ^{180}Hf, ^{184}W and ^{186}W. Relatively high values of I_o are observed for (A-Z) = 98 and (A-Z) = 108 isotones except for ^{180}Hf. In particular, I_o has the maximum value for ^{182}W and ^{184}Os and decreases sharply for nuclei in their respective neighbourhood. The anomalous behaviour at (A-Z) = 98 had previously been observed by Stephens et. al. (1964), who speculated, as a possible explanation for this effect, that the pairing correlations are reduced (implying large moments of inertia) because of the large gap in the Nilsson diagram for such nuclei. More recently, Duckworth (1967) has shown that breaks are also seen at (A-Z) = 98 and (A-Z) = 108 in a plot of the double-neutron separation energy as a function of the neutron number (A-Z).

Table IV.3 gives the calculated values of the parameters s, D, α, r_o' ; the level energies and the value of $(\Delta E)_{max}$ for the Morse potential. $(\Delta E)_{max}$ is less than 1 per cent for 18 nuclei, less than 2 per cent for 8 nuclei and more than 2 per cent for 23 nuclei. The values of the parameter I_o' are in general about 2 per cent less than those obtained with harmonic potential. The value of the depth parameter (D), although small, increases with the addition of neutrons and decreases with the addition of protons which is an expected behaviour. All other features exhibited by the Morse potential are very much the same as those of the harmonic potential.

Thus, no noticeable improvement in the level fitting was observed when the anharmonic Morse potential with exactly same stiffness as that of the harmonic potential is used. For obvious reasons, much better fits are obtainable with the Morse potential when the parameters of the potential are treated as independent parameters obtainable by fitting the energies of 2^+, 4^+ and 6^+ states.

A few striking facts may be gathered from the results given in Tables IV.2 and IV.3.

(i) The largest value of stiffness (C) (but not I_o) occurs for ^{180}Hf, an almost 'rigid rotor.'

(ii) A sharp change in I_o between 90 and 92 neutron numbers in Sm, Gd, Dy and Er isotopes results in a similar change in the value of the stiffness C. This is contrary to the conclusion drawn by Mariscotti et. al. (1970) on the basis of the Variable Moment of Inertia model.

The energy $E(0^{+'})$ of the first excited β-vibrational state calculated using the value of stiffness C needed to fit the lowest rotational states exactly were on an average found to be lower than the experimental values by about 55 per cent. The variation of $E(0^{+'})$ with the neutron number (A-Z) as shown in Figure IV.5 has more or less the same trend as the experimental value, except for the case of Er and Yb isotopes.

thus rendering a good support to the observed variation of C with the neutron number (refer to Figure IV.6). It is also found that a least squares fit to the rotational levels and $0^{+'}$ level gives results which are in agreement with experiments to within a maximum departure of 6 per cent as shown in Table IV.4.

Table IV.5 gives a comparison of the values of the intrinsic quadrupole moment of the first 2^+ state, and the ratio $B(E2; 4^+ \rightarrow 2^+)/B(E2; 2^+ \rightarrow 0^+)$ calculated using eq. (25) for about a dozen nuclei, with the experimental values (Abou-Leila and Darwish 1971). Except for a few neutron deficient nuclei and the nuclei in the transition regions, the agreement appears to be quite satisfactory.

IV.7 DISCUSSION

IV.7.1 Variation of the Stiffness of the Harmonic Potential with the Neutron and the Proton Numbers

The variation of stiffness C with the neutron number (A-Z) and the proton number (Z) shown in Figures IV.6 and IV.7 respectively, on the whole, show the same general trend as those obtained by Mariscotti et. al. (1970) and Mosel and Greiner (1968). With the addition of neutrons, the stiffness increases sharply for neutron deficient nuclei and tends to decrease smoothly for neutron excess nuclei. This peculiar variation is rather interesting and may be understood in the following ways.

Since the β-vibrations, in our case, are of harmonic type, it is reasonable to expect $E(0^{+'})$ to be proportional to the square root of C. A comparison of the points in Figure IV.5 with the corresponding points in Figure IV.6 for various nuclei appear to render a good support to the above argument.

Also, comparing Figure IV.5 with Figure II.1, it is easy to notice that the variation of $E(0^{+'})$ with (A-Z) has a close resemblance with the variation of quadrupole moment with (A-Z). Using this, the variation of C with (A-Z) may be understood in the following way.

Experimentally it is known that the intrinsic quadrupole moment increases with the addition of neutrons for the nuclei in the first half of the region $150 < A < 190$, and decreases in the latter half (see Figure II.1) resulting in a corresponding increase or decrease in the deformation β and hence the moment of inertia (I_o) of the nucleus increases or decreases. Whereas, a decrease in the value of moment of inertia (away from the rigid body value) makes the nucleus 'softer' resulting in a decrease in the stiffness of the nucleus (neutron deficient nuclei), the increase in the value of moment of inertia (approaching the rigid body value) makes the nucleus 'harder' resulting in an increase in the stiffness of the nucleus, and when I_o approaches the rigid body value (neutron excess nuclei), C attain

the maximum value and becomes fairly constant thereon. Thus, the nucleus ^{180}Hf, which is known to be one of the best approximations to an ideal 'rigid rotator' has the largest value of stiffness. The same result has been obtained for ^{180}Hf by Mariscotti et. al. (1970) and by Mosel and Greiner (1968) independently.

The variation of the stiffness may also be understood in terms of the increase or decrease in the value of pairing energy (Mosel and Greiner 1968) when more and more neutron pairs are added to or taken out of the nucleus.

The variation of stiffness C with the proton number Z is shown in Figure IV.7. Although, on the whole, the stiffness decreases with the addition of protons, the trend for a given set of isotones, in general, is very similar to those obtained by Mariscotti et. al. (1970), the only exception being for 90 and 92 neutron numbers. The stiffness is almost constant for $(A-Z) = 90$ and is approximately equal to 1.7 MeV.

Such a variation could be attributed to the competition between the Coulomb and pairing forces in the nucleus when more and more proton pairs are added (Mosel and Greiner 1968). However, as we have not taken the effect of these forces into consideration, it is hard to draw any such conclusion.

IV.7.2 Generalization of the Two Mass-Point Model

We have seen that the simple two mass-point model explains most of the experimental data quite satisfactorily. However, the main drawback of the model is that the moment of inertia does not go to zero for spherical nuclei. In order to account for this, Trainor and Gupta (1971) proposed a governor model, in which it is assumed that a central spherical portion of radius equal to the semi-minor axis of the spheroid does not participate inrrotations (rotationally invariant core: RIC) and obtained satisfactory results. It is rather interesting to note that the two mass-point model and the governor model moments of inertia are obtainable as limiting cases of a generalised RIC model by considering the RIC to be of arbitrary radius (d) for a deformed nucleus of ellipsoidal shape ($a_3 > a_2 > a_1$). The distance between the centres of mass of the two fragments, obtained by dividing the portion of the RIC nucleus outside the RIC into two equal parts, is given by

$$r_L' = \frac{3}{4}\left(\frac{a_1 a_2 a_3^2 - d^4}{a_1 a_2 a_3 - d^3}\right) \qquad (26)$$

where $d \leqslant a_1 < a_2 < a_3$. The corresponding generalised two mass-point moment of inertia is

$$I = (M_{eff} / 4)\, r_L'^2 \qquad (27)$$

where $M_{eff} = M - M_s$, is the mass taking part in the rotation,

M_s is the mass of the RIC and M is that of the nucleus.

Clearly, eqs. (26) and (27) respectively go over to the case of the two-mass-point model and the governor model for $d = 0$, $a_1 = a_2$; and for $d = a_1 = a_2 < a_3$. Results obtained on the basis of the governor model (Trainor and Gupta 1971) are found to be in better agreement with the experiment. Hence, a quantum mechanical treatment of the generalised two mass-point model is expected to yield improved results. However, we have not included this work here, as it is more or less a repetition of the case of the simple two mass-point model already discussed in detail.

REFERENCES

Abou-Leila, H. and Darwish, S.M. (1971). Nucl. Phys. A175, 663.

Bohr, A. and Mottelson, B.R. (1953). Kgl. Danske. Videnskab. Selskab. Mat. Fys. Medd. 27, No. 16.

Davydov, A.S. and Chaban, A.A. (1960). Nucl. Phys. A20, 499.

Davydov, A.S. and Filippov, G.F. (1957). Sov. Phys. JETP 5, 676.

Diamond, R.M., Stephens, F.S. and Swiateckii, W.J. (1964). Phys. Letters 11, 315.

Duckworth, H.E. (1967). Bull. Am. Phys. Soc. 12, 1055.

Gupta, R.K. (1969). Can. J. Phys. 47, 299.

Hofstadter, R. (1957). Ann. Rev. Nucl. Sci. 7, 231.

Holzer, P., Mosel, U. and Greiner, W. (1964). Nucl. Phys. A138, 241.

Mariscotti, M.A.J., Goldhaber, G.S. and Buck, B. (1969). Phys. Rev. 178, 1864.

Merzbacher, E. (1961). 'Quantum Mechanics', John Wiley and Sons, INC. New York, P.66.

Morse, P.M. (1929). Phys. Rev. 34, 57.

Mosel, U. and Greiner, W. (1968). Z. Phyk. 217, 256.

Pauling, L. and Wilson, E.B. (1935). "Introduction to Quantum Mechanics," McGraw-Hill Book Co. Inc., New York, P. 273.

Pekeris, C.L. (1934). Phys. Rev. 45, 98.

Stephens, F.S., Lark, N. and Diamond, R.M. (1964). Phys. Rev. Letters, 12, 225.

Trainor, L.E.H. and Gupta, R.K. (1971). Can. J. Phys. 49, 133.

C H A P T E R - V

GENERAL FEATURES OF CONTINUUM MODEL

It is a widely accepted fact that the nuclear shell model provides a satisfactory explanation of a large number of experimental results for the ground and excited states of light nuclei ($A < 40$). But, for the nuclei in the region $150 < A < 190$ and $A > 220$ the shell model fails to account for the enormously large values of quadrupole moments, the properties of ground and excited states of doubly even nuclei, the magnetic moments of certain nuclei, the phenomenon of fission and so on. Such large effects may be expected to arise from the coordinated- both particle and surface- motion of a large number of nucleons inside the nucleus. Such a motion is usually termed as collective motion.

The close packing of the particles in the nucleus and the existence of a relatively sharp nuclear boundary have led to the comparison of a nucleus with a liquid drop the energy of which is expressed as a sum of surface energy, volume energy and electrostatic energy (Niels Bohr 1936; Niels Bohr and Kalckar 1937). Thus, an alternative to the shell model approach is the continuum model of the nucleus in which neither the nucleons themselves nor the interactions between them appear explicitly.

The continuum model explains the collective phenomenon more satisfactorily than the shell model. The model assumes the heavy nucleus to be a continuous, homogeneous, incompressible and uniformly charged liquid drop with a sharp boundary- a hydrodynamic concept. The change in various properties of the nuclei can then be attributed to changes in shape and curvature of the charged liquid drop. Such an approach was first used by Niels Bohr and Wheeler (1939) to explain the phenomenon of fission. Subsequently, Rainwater (1950), Bohr and Mottelson (1952-53), Hill and Wheeler (1953) and many others have used the hydrodynamic model for the study of deformed nuclei.

The rotational flow model presented in this thesis is based on the continuum model of the nucleus. Hence, the general principles underlying the dynamics of a fluid drop and the application of these principles for the study of nuclear hydrodynamics will be reviewed in this chapter.

V.1 DEFINITION AND BASIC PROPERTIES OF A FLUID

A fluid may be defined to be a continuous aggregation of molecules which readily yield to the slightest stress applied. The main difference between a fluid and a solid is that a fluid, no matter how viscous, will yield in time permanently to the slightest stress, whereas a solid no matter how plastic, requires a certain magnitude of stress before it will flow. A fluid may be either a liquid or a gas, the former is relatively incompressible whilst the latter is highly compressible.

A fluid particle is an infinitely small volume element of the fluid which is large enough compared to the size of the molecule, but small enough compared to the volume of the body under consideration. Fluids considered in practice contain an infinite number of such volume elements and hence possess infinite degrees of freedom.

A perfect fluid is a convenient idealization of the normal fluid and is helpful in achieving mathematical simplicity of the equations involved in obtaining a solution. In many cases, it is found to be a very good approximation to the actual fluid. A perfect fluid may be defined as one which is non-viscous, implying that there are no shearing stresses during the motion of the fluid, or incompressible, implying that the volume remains constant, or both.

V.2 BASIC FORMALISM

The basic problem in fluid dynamics is to find explicitly the velocity of a fluid particle in terms of its space-time coordinates. The formalism is based on the continuum model of fluid having appropriate continuum properties so defined as to ensure that on the macroscopic scale the behaviour of the model duplicates the behaviour of the actual fluid. In what follows, we will discuss the laws governing the kinematics of fluid motion and the corresponding forces in fluids, and the dynamical equations of motion.

V.2.1 'Lagrangian' and 'Eulerian' Modes of Description

The motion of a fluid may be investigated by two different methods; the Lagrangian method and the Eulerian or flux method.

In the Lagrangian method, we fix our attention upon an element of fluid whose initial position vector ($\bar{a}$) is specified at some given time t_o, and follow its motion throughout its history. The coordinates x_i and t are themselves functions of the a_i and t. Then any quantity F associated with the motion of fluid will be a function of $\bar{a}$ and t. The velocity component v_i and acceleration components f_i are then

$$v_i = \partial x_i/\partial t \; ; \qquad f_i = \partial v_i/\partial t = (\partial^2 x_i/\partial t^2).$$

In the Eulerian method, we fix our attention upon a particular point of space occupied by the fluid and observe what goes on there. The velocity components v_i are taken as functions of x_i and t. Then, any quantity F associated with the motion of the fluid is a function of two independent variables- the coordinates x_i of a point in space and of time t. It is easy to see that the total change in F with respect to time t is

$$dF/dt = \partial F/\partial t + \sum_{i=1}^{3} v_i(\partial F/\partial x_i). \qquad (1)$$

The dynamical equations obtained by the Eulerian method are relatively simple to handle, particularly for the case of steady motion. To pass from the Eulerian to the Lagrangian method, the equations $(dx_i/dt) = v_i$, with initial conditions $x_i = a_i$ would have to be solved. Throughout this thesis the Eulerian method has been used.

V.2.2 Descriptions in the Body (B) and Space (S) Fixed Systems

For studying pure rotations, it is convenient to choose the centre of mass as the common origin of both B and S and the axes of B to be along the principal axes of the body under consideration. Further, it can be shown (Goldstein 1950) that eq. (15) of Chapter III is valid even if the body is non-rigid. The equation is

$$(d/dt)_s = (d/dt)_b + \bar{w} \times \qquad (2)$$

The above equation is of prime importance in obtaining the components of a vector in terms of the coordinates either in B or in S.

(a) Velocity

Operating eq. (2) on the position vector $\bar{r}$ of a fluid element we get

$$\bar{u} = \bar{v} + \bar{w} \times \bar{r} \tag{3}$$

where $\bar{u}$ and $\bar{v}$ are respectively the velocities in S and B.

(b) Angular Momentum

Taking the vector product of eq. (3) with $\bar{r}$ and integrating over the total volume of the fluid, we obtain

$$\bar{L} = \bar{I} + \bar{R} \tag{4}$$

where $\bar{L}$ is the total angular momentum vector which consists of two parts, $\bar{I}$, the intrinsic angular momentum due to internal flow, and $\bar{R}$, the rotational angular momentum due to body-rotations. By internal flow we mean the motion of fluid elements with respect to B.

(c) Kinetic Energy

The total kinetic energy E in S can be obtained by taking the scalar product of eq. (3) with $\bar{u}$ and integrating over the total volume of the fluid. Doing this we get

$$E = \epsilon_{int} + (L^2 - I^2)/2I_R \tag{5}$$

where ϵ_{int} is the intrinsic energy of the system given by

$$\epsilon_{int} = \frac{1}{2} \iiint v^2 \, dx_1 \, dx_2 \, dx_3$$

and I_R is the rigid body moment of inertia.

(d) Acceleration and Force

The acceleration $\bar{a}_s$ in S of a fluid element can be obtained by the time differentiation of eq. (3) and a subsequent mathematical simplification. Doing this, we get

$$\bar{a}_s = \bar{a}_b + 2(\bar{w} \times \bar{v}) + \bar{w} \times (\bar{w} \times \bar{r}) \qquad (6)$$

In the above, the last two terms on the right hand side are respectively the Corioli's and the centrifugal terms. Also, eq. (6) gives the effective force acting on a fluid element of unit mass in the field of the remaining fluid elements.

The set of eqs. (3-6) are most useful in the study of dynamics of a fluid body.

V.3 PHYSICAL ASSUMPTIONS AND BASIC EQUATIONS

One of the fundamental physical assumptions is the conservation of mass leading to the 'equation of continuity' given by

$$(\partial \rho / \partial t) + \bar{\nabla} \cdot (\rho \bar{u}) = 0 \qquad (7)$$

where ρ is the fluid density. A fluid with an uniform density throughout its volume is said to be 'homogeneous'. Further, if

the density is constant in time for an homogeneous fluid, then eq. (7) reduces to

$$\bar{\nabla} \cdot \bar{u} = \bar{\nabla} \cdot \bar{v} = 0 \qquad (8)$$

the familiar divergenceless condition. The principle of conservation of mass requires the constancy of volume of the fluid under consideration and such a fluid is said to be 'incompressible'. We will be dealing only with such fluids.

Another important property of a fluid is the viscosity, property which arises basically out of the friction between the fluid particles in motion and results in the dissipation of kinetic energy. The most general formulation of classical fluid is completed by the inclusion of viscous effects. However, in our treatment, for simplicity, we have assumed the viscous effects to be negligibly small and hence, will not discuss this property here.

The third important property of a fluid is the 'vorticity' or 'circulation'. It gives an indication of the rotational character of fluid in motion at a given point in the body of the fluid.

The vorticity at any point inside a fluid with respect to S is the curl of the velocity field at that point and is denoted by $\bar{\xi}$

$$\bar{\xi} = \bar{\nabla} \times \bar{u} \qquad (9)$$

Thus, the vorticity represents for a deformable medium the generalization of the concept of angular velocity of a rigid body and is sometimes called as 'fluid rotation'. Using eq. (3) in eq. (9) we have

$$\bar{\xi} = \bar{\nabla} \times \bar{u} = \bar{\nabla} \times \bar{v} + 2\bar{w} \qquad (10)$$

The 'flux of vorticity' through the area bounded by the fluid is defined as

$$\iint \bar{\xi} \cdot \overline{dA} = \iint (\bar{\nabla} \times \bar{u}) \cdot \overline{dA}$$

where $\overline{dA}$ is an elementary surface area.

Applying Stoke's theorem to the above

$$\iint \bar{\xi} \cdot \overline{dA} = \oint \bar{u} \cdot \overline{dl} \; . \qquad (11)$$

The quantity on the right hand side of eq. (11) is defined as the 'circulation'. Thus, the circulation along a closed path is equal to the flux of vorticity through the area bounded by the closed path. It can be shown (Landau and Lifshitz 1959) that in a perfect fluid the circulation around a closed path is constant in time. This is called the 'Law of Conservation of Vorticity'. Thus, for a given velocity field, the vorticity is preserved for all time at each and every point in the body of a perfect fluid.

There are two types of motion of a fluid- the 'steady' motion and 'unsteady or turbulent' motion. The motion is said

to be steady only when the velocity at each point in the field is independent of time. Otherwise, it is said to be unsteady.

In a steady motion the lines of motion coincide with the paths of the fluid elements and will never intersect each other. In many problems the steady flow is a good approximation to the actual flow and helps to achieve mathematical simplicity of equations to be solved.

Lastly, since liquids always possess a sharp boundary, specification about the boundary will provide us with additional equations which are often useful in obtaining a solution of the problem under consideration.

V.3.1 Euler's Equations of Motion

The equations of motion for a fluid are obtained using Newton's second law of motion. Euler's equations of motions are obtained by equating the acceleration at any point inside the fluid to the sum total of forces acting on unit mass of the fluid situated at that point. The forces acting at any point inside the fluid can be classified into two; $\bar{F}_i$, the internal or the body force and $\bar{F}_e$, the external or impressed force. The acceleration at that point is given by eq.(1) with $\bar{u}$ in place of F. Hence, Euler's equations of motion are

$$(\partial\bar{u}/\partial t) + (\bar{u}\cdot\bar{\nabla})\,\bar{u} = \bar{F}_i + \bar{F}_e \qquad (12)$$

In the above, given $\bar{F}_i + \bar{F}_e$, one can solve for $\bar{u}$ and vice-vers

V.4 NATURE OF NUCLEAR FLUID

It was pointed out in the beginning of this Chapter that deformed heavy nuclei exhibit strong collective properties which are best explainable through a collective model approach wherein the nucleus is approximated to a liquid drop with a sharp boundary and the energy of which is written as a sum of volume energy, surface energy and electrostatic energy.

A consideration of the basic properties of nuclei will lead us to make some meaningful assumptions about the nature of nuclear fluid.

The nuclear density (ρ) is known to be fairly constant throughout the volume of a given nucleus except for a slight tapering near the surface and hence, for a given nucleus, it is assumed that $d\rho/dt = 0$ and the volume remains constant. This means that the nuclear fluid is homogeneous and incompressible.

The basic problem is to obtain the explicit form of interaction between the nucleons inside the nucleus in the absence of external forces. The internal forces which make a significant contribution are those arising out of nucleon and electrostatic interactions between the nucleons and the protons respectively. Further, as the nucleus does not dissipate energy, the frictional force between the nuclear fluid particles is assumed to be absent meaning thereby that the nuclear fluid is

'inviscid.' Also, a study of the available quadrupole moment data (see II.2.3) shows that a deformed nucleus, in the region of interest, can be assumed to be either spheroidal or ellipsoidal in shape.

The above assumptions about the nature of nuclear fluid lead us to the following equations which form the basis for the study of nuclear hydrodynamics.

$$
\begin{aligned}
&d\rho/dt = 0 && \text{(homogeneity)}\\
&\bar{\nabla}\cdot\bar{u} = \bar{\nabla}\cdot\bar{v} = 0 && \text{(incompressibility)}\\
&\bar{\zeta} = \bar{\nabla}\times\bar{v} + 2\bar{w} = \bar{\nabla}\times\bar{u} && \text{(vorticity)}\\
&\partial\bar{u}/\partial t + (\bar{u}\cdot\bar{v})\bar{u} = \bar{F}_i && \text{(absence of external forces)}\\
&\sum_{i=1}^{3} (x_i^2/a_i^2) = 1 && \text{(ellipsoidal boundary)}
\end{aligned}
\qquad (13)
$$

In the above a_i's correspond to the principal semi-axes of the ellipsoid and $\bar{F}_i$ correspond to the sum of effective nuclear and electrostatic forces at a given point in the body of nuclear fluid.

Thus, we conclude that the nuclear fluid has the properties of a perfect fluid- homogeneous, incompressible and inviscid- with a sharp boundary. Hence, the study of nuclear hydrodynamics should be relatively simple and straightforward.

V.5 TYPES OF FLOW GENERALLY CONSIDERED

Although the nuclear force is known to be short-range, strong and attractive, the explicit form of interaction is not

yet known. It is possible to obtain the effective force in the continuum model only when we know the velocity field $\bar{u}$ explicitly. On the other hand, one can make some physically valid assumptions about the nature of nuclear flow to obtain the velocity field $\bar{u}$ explicitly and subsequently use it to obtain the kinetic energy of the continuum and the effective force. The validity of the velocity field used is then confirmed by a direct comparison of the findings of the theory with experiment.

The vorticity condition leaves us with only two possible types of nuclear fluid flow, the first of which is a flow for which the vorticity ($\bar{\zeta}$) is zero called the 'irrotational or vortex free' flow and the other for which the vorticity is non-zero called the 'rotational or vortex' flow. Thus,

$$\begin{aligned} | \bar{\nabla} \times \bar{u} | &= 0 \qquad \text{'irrotational flow'} \\ \bar{\nabla} \times \bar{u} &= \bar{\zeta} \qquad \text{'rotational flow'} \end{aligned} \tag{14}$$

It is found that the nuclear moment of inertia obtained by assuming that the whole of the nucleus takes part in the rotation with a rigid flow ($\bar{v} = 0$), is about twice the experimental value (see II.4.1) which means that the effective mass taking part in the actual rotation is only about half of the total mass of the nucleus. Hence, it is necessary to assume flows which effectively decrease the value of model moment of inertia

from the rigid body value. Again, such flows can be either irrotational or rotational type.

V.5.1 Irrotational Flow

The nuclear fluid flow which is irrotational with respect to S should satisfy the following conditions

$$\begin{aligned} \bar{\nabla} \cdot \bar{u} &= \bar{\nabla} \cdot \bar{v} = 0 \\ \bar{\nabla} \times \bar{u} &= \bar{\nabla} \times \bar{v} + 2\bar{w} = 0 \end{aligned} \tag{15}$$

Clearly $\bar{u}$ can be written as the gradient of some scalar potential function ϕ called the velocity potential. Then, the velocity $\bar{u}$ is given by

$$\bar{u} = - \bar{\nabla} \phi \quad . \tag{16}$$

Combining eq. (16) with eq. (15) we obtain

$$\nabla^2 \phi = 0 \tag{17}$$

which is the familiar Laplace equation for ϕ. It is always possible to solve eq. (17) for a given boundary condition. For strongly deformed nuclei the ellipsoidal boundary condition may be used. Thus, knowing ϕ, one can explicitly know the velocity field $\bar{u}$ and hence the energy of the drop and the nature of effective force. However, the value of moment of inertia thus obtained (Bohr and Mottelson 1953) is found to be only one-fifth of the experimental value meaning that the effective mass taking part in the rotations due to irrotational flow is

much less than the actual nuclear mass contributing to the rotations.

V.5.2 Rotational Flow

We have seen that the value of nuclear moment of inertia lies between those predicted on the basis of the continuum model with irrotational flow and the rigid body model, and hence the nuclear flow is neither irrotational nor rigid. Nevertheless, it is possible to postulate other rotational flows (rigid flow being excluded) in order to reproduce the observed values of moments of inertia of the nuclei considered. A detailed discussion of flows of this type is given in Chapter VI wherein we have proposed a rotational flow with a constant vorticity for the study of rotational spectra of deformed even-even nuclei in the rare-earth region.

V.6 SEMI-CLASSICAL TREATMENT

The usual treatment is that one begins with the classical theory of a continuum in order to obtain the total energy or the collective Hamiltonian of the system and a subsequent quantization of the system by usual methods. In such an approach, fundamentally, it is necessary to postulate the nature of fluid motion within the continuum of known shape. In an actual problem as a first step one attempts to obtain the functional form of the energy and angular momentum at a given point inside the fluid drop by postulating a local velocity field at that point.

The total energy and total angular momentum as a function of shape parameters of the drop are obtained by integrating the corresponding local quantities over the volume of the continuum. The resultant Hamiltonian is what is termed as the 'Collective Hamiltonian' and is subsequently quantized by employing the usual quantum mechanical rules. The Schrödinger equation for the quantized Hamiltonian is then solved to obtain the eigenvalues and eigenfunctions of the system. It is always convenient to quantize the rotational part of the collective Hamiltonian in the angular momentum representations. The energy spectrum of such a Hamiltonian depends on the inertia and the stiffness parameters, and quite different nuclear spectrum is obtained for different values of these parameters. In the study of nuclear rotations, the success of a model is determined mainly by its ability to give the proper functional form of nuclear moment of inertia which can satisfactorily reproduce the experimental values. In fact, the extent of agreement of all theoretical predictions made on the basis of a model with experiments is a measure of the accuracy of the flow chosen and the quality of the Hamiltonian obtained.

REFERENCES

Bohr, A. (1952). Kgl. Danske. Videnskab. Selskab. Mat. Fys. Medd. 26, No. 14.

Bohr, A. and Mottelson, B.R. (1953). Kgl. Danske. Videnskab. Selskab. Mat. Fys. Medd. 27, No. 16.

Bohr, N. (1936). Nature 137, 344 (I; VI d).

Bohr, N. and Kalckar, F. (1937). Kgl. Danske. Videnskab. Selskab. Mat. Fys. Medd. 14, No. 10.

Bohr, N. and Wheeler, J.H. (1939). Phys. Rev., 56, 426.

Goldstein, H. (1950). 'Classical Mechanics,' Addison Wesley, New York, p.132.

Hill, D.L. and Wheeler, J.A. (1953). Phys. Rev., 89, 1102.

Landau, L.D. and Lifshitz, E.M. (1959). 'Fluid Mechanics', Pergamon Press, London.

Rainwater, J. (1950). Phys. Rev. 79, 432.

C H A P T E R - VI

ROTATIONAL FLOW MODEL (RFM)

It is well known that the empirical value of the ground state effective moment of inertia calculated using the usual L(L+1) rule for the deformed even-even nuclei are given neither by the rigid spheroid model nor by the irrotational flow model of Bohr and Mottelson (1953). In fact, the representation of a spheroidal nucleus by a two mass-point system, with and without a rotationally invariant core (RIC) (Trainor and Gupta 1971; Gupta 1969) are essentially attempts to parameterize the nuclear flow which, within the framework of the macroscopic model, is neither rigid nor irrotational. Krutov (1968) has used the concept of rotational flow by defining the collective rotational motion as the change of mass density distribution in time such that any motion which does not change the mass density distribution does not contribute to the energy of collective motion. Rowe (1970)

has interpreted the assumption of the RIC as the existence of a rotationally invariant superfluid core which remains as an inert spectator to the rotational flow of the remainder of the nucleus (the normal fluid) thus, referred to as the two-fluid model. He has shown that the adiabatic model, which assumes the separate existence of rotational and intrinsic particle excitations, with very little coupling between them, implies rotational flow, which is nothing but the rigid body flow except that the particles are not frozen in position but are free to execute any independent motion. Such a flow is found to lend support to the existence of clusters which participate in rotational flow as if they were elementary particles with their masses concentrated at their centres of mass thereby reducing the moment of inertia from its rigid body value. Recently, Gupta (1972) has shown that the linear dependence of the moment of inertia on the deformation parameter (β) is the characteristic feature of a system following the rotational flow motion and the RIC hypothesis, like the quadratic dependence is that of a hydrodynamical system.

In view of the above and in view of the fact that the nuclear flow is neither irrotational nor rigid, in this Chapter, we have attempted to propose a rotational flow model (RFM) based on the principles of continuum mechanics discussed in Chapter V. The model is developed using vortical flows in three dimensions obtained by extending the irrotational

flow model of Bohr and Mottelson (1953) to include rotational flow with finite but constant vorticity. The rigid spheroid and the irrotational flow models are obtained as limiting cases of the proposed RFM. The model is found to give more satisfactory results and is found to have many important physical implications. The outline of the model, theoretical formulation and its physical significance, calculations and results are discussed in the following sections.

VI.1 MODEL

The RFM is essentially based on the idea of extending the irrotational flow model of Bohr and Mottelson (1953) to include constant vorticity flows.

We have seen in Chapter II that the energies of the low-lying rotational levels of deformed even-even nuclei in the rare-earth region are approximately given by

$$E(L) = (\hbar^2/2I)\, L(L+1) \qquad (1)$$

where $L = 0, 2, 4$, etc., and I is the nuclear rotational moment of inertia in the state of angular momentum $\bar{L}$.

For a homogeneous, inviscid and incompressible fluid system with irrotational flow we have $\bar{\nabla} \cdot \bar{u} = 0$ and $\bar{\nabla} \times \bar{u} = 0$, where $\bar{u}$ is the velocity field in S. The corresponding moment of inertia (I_{Hi}) for a nucleus of ellipsoidal boundary with semi-axes a_i, a_j, a_k ($i, j, k = 1, 2, 3$ and cyclic) with

respect to the i^{th} principal axis is

$$I_{Hi} = I_{Ri}\left[(a_j^2 - a_k^2)/(a_j^2 + a_k^2)\right]^2 \qquad (2)$$

where a_i, a_j, a_k are given by eq. (5) of Chapter II, and I_{Ri} is the rigid body moment of inertia with respect to the i^{th} principal axis.

Experimental data indicates that

$$I_H < I_{expt} < I_R \qquad (3)$$

where I_{expt} is obtained from eq. (1) using the energy of L = 2 state in the ground state band.

It was shown in Chapter III that the velocity field ($\bar{v}$) in B is related to $\bar{u}$ in S by the equation

$$\bar{u} = \bar{v} + \bar{w} \times \bar{r} \qquad (4)$$

where $\bar{w}$ is the angular velocity of B. Taking the curl of eq. (4) we get

$$\bar{\nabla} \times \bar{u} = \bar{\nabla} \times \bar{v} + 2\,\bar{w} \qquad (5)$$

For irrotational flow eq. (5) reduces to

$$\bar{\nabla} \times \bar{u} = 0 \; ; \quad \text{and} \quad \bar{\nabla} \times \bar{v} = -2\bar{w} \qquad (6)$$

for rigid flow, it leads to

$$\bar{\nabla} \times \bar{u} = 2\bar{w} \; ; \quad \text{and} \quad \bar{\nabla} \times \bar{v} = 0 \qquad (7)$$

since $\bar{v}$ is zero. Eqs. (4), (7) and (8) suggest that it is possible to reproduce the values of I_{expt}, I_H and I_R assuming a flow with a constant vorticity condition, namely,

$$\bar{\nabla} \times \bar{u} = -2\bar{\Omega} \tag{8}$$

Combining eq. (5) with eq. (8) we obtain

$$\bar{\nabla} \times \bar{u} = 2(\bar{w} - \bar{\Omega}) \tag{9}$$

where $\bar{\Omega}$ is a constant vector. Note that $\bar{\Omega} \equiv 0$ gives the rigid flow (I_R) and $\bar{\Omega} \equiv \bar{w}$ gives the irrotational flow (I_H). We call $\bar{\Omega}$ as the 'vorticity vector'.

For a system performing pure rotations, the potential energy of the system does not change, and hence the Hamiltonian is given by just the kinetic energy. The Hamiltonian H and the angular momentum $\bar{L}$ of the continuum with density ρ are given in S by

$$H = \frac{1}{2} \int \rho u^2 \, d\tau \; ; \qquad \bar{L} = \int \rho (\bar{r} \times \bar{u}) \, d\tau \tag{10}$$

In the above, the integrations are over the entire volume of the system. By replacing $\bar{u}$ by $\bar{v}$ we get similar expressions for the Hamiltonian H_b and angular momentum $\bar{l}$ as measured in B. The relations between the quantities defined in S and in B, obtained from eq. (1) are

$$\bar{L} = \bar{l} + \bar{R} \tag{11}$$

$$H = H_b + \sum_{i=1}^{3} (L_i^2 - l_i^2)/2I_{Ri} \qquad (12)$$

where $i = 1,2,3$ correspond to the principal axes of the system; and $R_i = I_{Ri}\, w_i$.

Essentially, the problem at present is to obtain a velocity field which satisfies the vorticity condition given by eqs. (8) and (9) together with the incompressibility condition, $\bar{\nabla} \cdot \bar{v} = \bar{\nabla} \cdot \bar{u} = 0$. Then the total rotational kinetic energy could be obtained using this velocity field in eqs. (10), (11) and (12).

VI.2 THEORETICAL FORMULATION

The constant vorticity condition and the divergenceless condition in RFM are analogous to the basic differential laws of magnetostatics. Hence, the most general form of the velocity field must be obtainable, in principle, by solving the equations $\bar{\nabla} \times \bar{v} = -2\bar{\Omega}$ and $\bar{\nabla} \cdot \bar{v} = 0$ for a specified boundary. The usual method of approach is to exploit $\bar{\nabla} \cdot \bar{v} = 0$; and solve the Poisson equation for the vector potential of $\bar{v}$ by Green's function technique and hence obtain $\bar{v}$ explicitly in its analytical form (Jackson 1965). However, we dispense with this method, as there are simpler ways of proposing the velocity field satisfying all the required conditions.

VI.2.1 General Formulation in Three Dimensions

A rotational flow in three dimensions, in general, is characterised by the fact that each of the vectors $\bar{v}$, $\bar{u}$, $\bar{\Omega}$ and $\bar{w}$

will have non-vanishing components along the coordinate axes in B and in S. We look for a particular type of velocity field which would satisfy all the flow requirements in general, and which would reproduce the rigid body flow and the irrotational flow under appropriate limits of the vorticity vector. One such flow in B satisfying eqs. (8) and (9), and the divergenceless condition for an ellipsoidal boundary is given by

$$v_i = 2a_i^2 \left[\Omega_k x_j / (a_i^2 + a_j^2) - \Omega_j x_k / (a_i^2 + a_k^2) \right] \quad \ldots(13)$$

where i, j, k = 1,2,3, with two more equations with i, j, k cyclic. In fact, eq. (13) can be obtained for the case of irrotational flow ($\bar{\Omega} \equiv \bar{w}$) by solving the Laplace equation for the velocity potential with an ellipsoidal boundary condition (Basset 1961). Also, for $\bar{\Omega} \equiv 0$; we get the rigid flow ($\bar{v} \equiv 0$). Thus, eq. (13) satisfies all the flow requirements. It will be shown later that the velocity field given by eq. (13) is unique, and $\bar{\Omega}$ corresponds to the angular frequency of the fluid particle and has got important significance.

The velocity field defined by eq. (13) is used to obtain the intrinsic energy (H_b) and the intrinsic angular momentum ($\bar{I}$) using eq. (10) with $\bar{v}$ in place of $\bar{u}$. The two are given by

$$H_b = (2/5) M \sum_{i,j,k} \frac{a_i^2 a_j^2}{(a_i^2 + a_j^2)} \Omega_k^2 \qquad (14a)$$

$$l_i = -(4/5)\,[M\, a_j^2\, a_k^2/(a_j^2+a_k^2)]\,\Omega_i \qquad (14c)$$

where i, j, k are taken in cyclic order. Use of the above equations in eqs. (11) and (12) gives

$$H = \sum_{i=1}^{3} (A_i\, w_i^2 + B_i \Omega_i^2 + C_i\, w_i \Omega_i) \qquad (15a)$$

$$L^2 = \sum_{i=1}^{3} (A_i'\, w_i^2 + B_i' \Omega_i^2 + C_i'\, w_i \Omega_i) \qquad (15b)$$

where $A_i = \dfrac{\sqrt{A_i'}}{2} = I_{Ri}/2; \quad B_i = \dfrac{\sqrt{B_i'}}{2} = -\,C_i/2$

$$C_i = C_i'/(2I_{Ri}) = -4\, I_{Ri}\, a_j^2\, a_k^2/(a_j^2 + a_k^2)^2 \qquad (15c)$$

and $I_{Ri} = (M/5)\,(a_j^2 + a_k^2).$

Both eqs. (15a) and (15b) are in the standard form. In both the expressions the first term corresponds to pure rotations, the second to the intrinsic particle motion and the third to the rotation-intrinsic particle coupling. Clearly, for $\Omega \equiv 0$, the flow becomes rigid flow and eqs. (15a) and (15b) reduce to

$$H_R = \sum_{i=1}^{3} \frac{1}{2}\, I_{Ri}\, w_i^2 \qquad (15d)$$

$$L_R^2 = \sum_{i=1}^{3} I_{Ri}^2\, w_i^2 \qquad (15e)$$

and for $\Omega \equiv \bar{w}$, the flow becomes irrotational and eqs. (15a) and (15b) reduce to

$$l_i = -(4/5)\left[M\, a_j^2\, a_k^2/(a_j^2+a_k^2)\right]\Omega_i \qquad (14c)$$

where i, j, k are taken in cyclic order. Use of the above equations in eqs. (11) and (12) gives

$$H = \sum_{i=1}^{3} (A_i\, w_i^2 + B_i \Omega_i^2 + C_i\, w_i \Omega_i) \qquad (15a)$$

$$L^2 = \sum_{i=1}^{3} (A_i'\, w_i^2 + B_i' \Omega_i^2 + C_i'\, w_i \Omega_i) \qquad (15b)$$

where $A_i = \frac{\sqrt{A_i'}}{2} = I_{Ri}/2; \quad B_i = \frac{\sqrt{B_i'}}{2} = -C_i/2$

$$C_i = C_i'/(2I_{Ri}) = -4\, I_{Ri}\, a_j^2\, a_k^2/(a_j^2 + a_k^2)^2 \qquad (15c)$$

and $I_{Ri} = (M/5)\,(a_j^2 + a_k^2)$.

Both eqs. (15a) and (15b) are in the standard form. In both the expressions the first term corresponds to pure rotations, the second to the intrinsic particle motion and the third to the rotation-intrinsic particle coupling. Clearly, for $\vec{\Omega} \equiv 0$, the flow becomes rigid flow and eqs. (15a) and (15b) reduce to

$$H_R = \sum_{i=1}^{3} \frac{1}{2} I_{Ri}\, w_i^2 \qquad (15d)$$

$$L_R^2 = \sum_{i=1}^{3} I_{Ri}^2\, w_i^2 \qquad (15e)$$

and for $\vec{\Omega} \equiv \vec{w}$, the flow becomes irrotational and eqs. (15a) and (15b) reduce to

$$H_H = \sum_{i=1}^{3} \frac{1}{2} I_{Hi} w_i^2 \qquad (15f)$$

$$L_H^2 = \sum_{i=1}^{3} I_{Hi}^2 w_i^2 \qquad (15g)$$

where I_{Hi} is given by eq. (2) (Bohr and Mottelson 1953).

VI.2.2 Uniqueness of the Flow

The uniqueness of the proposed flow given by eq. (13) can be demonstrated in a very simple way.

Let $\bar{v}'$ and $\bar{v}''$ be two solutions satisfying all the flow requirements, the field $\bar{W} = \bar{v}' - \bar{v}''$ satisfies the conditions $\bar{\nabla} \cdot \bar{W} = \bar{\nabla} \times \bar{W} = 0$ everywhere, and $\bar{W} \cdot \bar{n} = 0$ on the surface, which leads to $\bar{W} = \bar{v}' - \bar{v}'' = 0$ and hence $\bar{v}$ is unique.

VI.2.3 Frequency of Intrinsic Motion

We will now show that the quantity $\bar{\Omega}$ occurring in eq. (13) corresponds to the frequency of the fluid element in motion.

Writing $\left[a_j^2/(a_j^2 + a_k^2) \right] \Omega_i$ as Ω_i' in eq. (13), we obtain $\bar{v} = \bar{\Omega}' \times \bar{r}$ which means $\bar{\Omega}'$ is the angular frequency of the fluid element with respect to B and hence $\bar{\Omega}$ is a measure of the frequency of intrinsic motion.

The relative magnitudes of $\bar{\Omega}$ and $\bar{w}$ will tell us whether the system is performing an adiabatic or a non-adiabatic motion. This will be discussed later.

VI.3 ROTATIONAL HAMILTONIAN OF THE SYSTEM

The deformed even-even nuclei in the rare-earth region show a characteristic rotational spectrum. Therefore, to a good approximation, it should be possible to write their Hamiltonian in the form

$$H = \sum_{i=1}^{3} L_i^2/2I_{Ei} \qquad i = 1,2,3 \qquad (16)$$

where I_{Ei} are the components of the effective moment of inert

The Hamiltonian and the angular momentum of the ellipsoi with the rotational flow given by eq. (13) are, in their most general form, given by eqs. (15a) and (15b) respectively.

The Hamiltonian as given by eq. (15a) can, in general, be put in the rotational form given by eq. (16) only if it is assumed that

$$\omega_i = k_i w_i \qquad (17)$$

where k_i's are dimensionless numbers called vorticity parameters. If all k_i's are equal to zero, eq. (13) gives the rigid body flow and if they are all equal to unity, we get the irrotational flow.

Since w_i's are the components of the angular velocity of the ellipsoid as a whole, eqs. (13) and (17) imply that the intrinsic motion as observed from B is directly coupled with the rotation of the ellipsoid as a whole, which can be considered

to be adiabatic compared to the intrinsic motion only if vorticity parameters are large compared to unity.

Using the form given by eq. (17) for ω_i's we get the rotational Hamiltonian in the form given by eq. (16) with the effective moment of inertia given by

$$I_{Ei} = I_{Ri}\left[1 + \left[4b_i^2(b_i^2-1)^2\right]/\left[4b_i^2-(b_i^2+1)^2/k_i\right]^2\right]^{-1} \quad \ldots(18)$$

where $b_i = a_j/a_k$ and is called the shape parameter of the ellipsoid. Note that both I_{Ei} and eq. (13) go over to the known values of the rigid body and the irrotational flow, as k_i goes to zero and unity respectively.

Thus, the kinetic energy of rotations and the form of rotational Hamiltonian compare closely with that of the rigid rotator with different expressions for the principal moments of inertia for a deformed nucleus. The L_i's occurring in eq. (16) are the projections of the total angular momentum $\bar{L}$ along the principal axes, and in the operator form they obey the commutation relations $\left[L_i, L_j\right] = -i\hbar L_k$. Hence, the Hamiltonian is quantized in the angular momentum representation Thus, the eigenfunctions of the Hamiltonian operator are nothin but the eigenfunctions of the angular momentum operators which are the usual D-functions, the properties of which are given in Appendix II.4.

In the next section we apply eqs. (16) and (18) for the study of rotations of a symmetric and an asymmetric nuclear liquid drop separately.

VI.4 THE CASE OF A SYMMETRIC AND AN ASYMMETRIC NUCLEAR DROP

The available energy and quadrupole moment data for even-even nuclei in the rare-earth region indicate that these nuclei can be assumed to be axially symmetric in their ground state, and the effect of asymmetry sets on gradually at higher excitations. Hence, for the study of these nuclei, it is essential to consider the case of a symmetric and an asymmetric drop separately.

The rotational Hamiltonian given by eq. (16) is exactly the same as the rigid rotator Hamiltonian (Chapter III), except that the quantity I_{Ei} occurs in place of I_{Ri} and hence all the results obtained in the case of the rigid rotator must also be valid in the present case.

VI.4.1 Symmetric Nuclear Drop

If we assume the deformed nucleus to be an axially symmetric (about the 3-axis in B) ellipsoidal drop, then $a_1 = a_2 < a_3$ and hence $I_{E1} = I_{E2} > I_{E3}$, and since $L_1^2 + L_2^2 = L^2 - K^2$, eq. (16) reduces to

$$H_s = (L^2/2I_{E1}) + (K^2/2)\,(1/I_{E3} - 1/I_{E1}) \qquad (19a)$$

where K is the projection of $\bar{L}$ along the symmetry axis of the nucleus. The corresponding eigenvalues are given by

$$E_s = L(L+1)\hbar^2/(2I_{E1}) + (K^2/2)\,(1/I_{E3} - 1/I_{E1}) \quad (19b)$$

The values of parameters k_1 and k_3 occurring in the above could be obtained using the known values of energies of states characterized by various values of L and K. It is interesting to know that in the case of rotation of a nucleus about an axis perpendicular to the symmetry axis ($K=0$), eqs. (19) will contain only the first term. This corresponds to the so-called ground state rotational band and will be discussed in detail in section VI.8.1.

VI.4.2 Asymmetric Nuclear Drop

In this case, $a_1 \neq a_2 \neq a_3$. Supposing $a_3 > a_2 > a_1$, then $I_{E1} > I_{E2} > I_{E3}$. It is not possible to obtain the eigenvalues of the rotational Hamiltonian given by eq. (16) exactly. However, we obtain them by treating the asymmetry as a small perturbation over the symmetric state (Davidson 1968), in which case eq. (16) can be written in the form

$$H = H_s + (L_2^2/2)\,(1/I_{E2} - 1/I_{E1}) \quad (20a)$$

For $I_{E1} \sim I_{E2}$, the last term in eq. (20a) can be treated as a perturbation over the symmetry. Hence,

$$\langle |L_2^2| \rangle = [L(L+1) - K^2]\hbar^2/2 \quad (20b)$$

Eq. (20b) combined with eq. (20a) will give the eigenvalues of H for an slightly asymmetric drop and the eigenfunctions are a linear combination of the eigenfunctions of the symmetri drop.

VI.5 ROTATIONAL FLOW IN TWO DIMENSIONS

It will be interesting to study the rotational flow in two dimensions, as it is much simpler to understand and as it gives rise to the rotational spectrum in the ground state rotational band (K=0).

VI.5.1 Two-Dimensional Flow as a Particular Case of the Flow in Three Dimensions

Consider a typical deformed nucleus of prolate spheroidal shape with x_3-axis as the axis of symmetry ($a_1 = a_2 < a_3$), and x_1-axis as the axis of rotation. The flow represented by eqs. (and (17) becomes two-dimensional flow when the fluid elements move in planes perpendicular to the axis of rotation which essentially means $w_2 = w_3 = 0$. This leads to

$$\begin{aligned} v_2 &= \left[2a_2^2 k_1 w_1/(a_2^2 + a_3^2)\right] x_3 \\ v_3 &= -\left[2a_3^2 k_1 w_1/(a_2^2 + a_3^2)\right] x_2 \qquad (21) \\ v_1 &= 0 \end{aligned}$$

with $$v_2/v_3 = -a_2^2 x_3 / (a_3^2 x_2) \qquad (22)$$

where a_3 and a_2 are respectively the semi-major and the

semi-minor axes of the prolate spheroid. It is clear from eq. (21) that only one vorticity parameter (k_1) occurs in the velocity field. Also, eq. (22) indicates that the flow lines are concentric ellipses in planes perpendicular to the axis of rotation. This will be discussed later.

In the following, we give an alternative method of obtaining the velocity field given by eq. (21).

VI.5.2 Alternative Method

It will be shown now that starting from anisotropic harmonic oscillator forces obtained by including non-rigidity in the rigid body forces, it is possible to derive the velocity field given by eq. (21).

Supposing the nuclear fluid rotated rigidly about the x_1-axis, the components of the force $\bar{F}$ acting on a fluid element of volume dv taken along the axes in B, are

$$F_{x_2} = - \rho\, dv\, w_1^2\, x_2 \; ; \quad F_{x_3} = - \rho\, dv\, w_1^2\, x_3 \; ; \quad F_{x_1} = 0 \qquad \ldots(23)$$

If, on the other hand, the fluid rotated non-rigidly, the velocity $\bar{v}$ of a fluid element measured in B is not necessarily zero. In this case, we assume that the force $\bar{F}$ on dv to be

$$F_{x_2} = - \eta_1\, \rho\, dv\, w_1^2\, x_2 \; ; \quad F_{x_3} = - \eta_2\, \rho\, dv\, w_1^2\, x_3 \; ; \quad F_{x_1} = 0 \qquad \ldots(24)$$

Eqs. (24) are identical to eqs. (23) for $\eta_1 = \eta_2 = 1$. Also, eqs. (24) give the acceleration of a fluid element in S, if S is chosen to coincide with B instantaneously.

For a steady flow of an incompressible fluid, we have

$$(\partial\bar{v}/\partial t) = 0 ; \qquad \bar{\nabla} \cdot \bar{v} = \bar{\nabla} \cdot \bar{u} = 0.$$

Hence,
$$(d\bar{v}/dt) = (\bar{v} \cdot \bar{\nabla})\bar{v} \tag{25}$$

The velocity field $\bar{v}$ in B satisfies the following equations obtained by the usual transformation of acceleration in S into B (eq. (6) of Chapter V)

$$\begin{aligned} (\bar{v} \cdot \bar{\nabla})v_2 &= -w_1^2 \eta_1 x_2 + 2w_1 v_3 + w_1^2 x_2 \\ (\bar{v} \cdot \bar{\nabla})v_3 &= -w_1^2 \eta_2 x_3 - 2w_1 v_2 + w_1^2 x_3 \end{aligned} \tag{26}$$

and $v_1 = 0$. These equations have to be solved to obtain v_2 and v_3 explicitly.

One of the simplest solutions of eqs. (18) satisfying the incompressibility condition is

$$v_2 = px_3 ; \qquad v_3 = qx_2 \tag{27}$$

The values of the coefficients p and q obtained using eq. (27) in eq. (26); and comparing eq. (27) with eq. (22), are

$$\begin{aligned} p &= w_1\left[1+(\eta_1-\eta_2)/4 - \sqrt{(\eta_1-\eta_2)^2+8(\eta_1+\eta_2)}\,/4\right] \\ &= 2a_2^2 k_1 w_1 /(a_2^2 + a_3^2) \end{aligned} \tag{28a}$$

$$q = w_1\left[1-(\eta_1-\eta_2)/4-\sqrt{(\eta_1-\eta_2)^2+8(\eta_1+\eta_2)}\,/4\right]$$

$$= 2a_3^2\, k_1\, w_1/(a_2^2 + a_3^2) \qquad (28b)$$

The algebraic sign before the radical is fixed by the rigid flow requirement, namely, for $\eta_1 = \eta_2 = 1$ we must have $v_2 = v_3 = 0$ and hence p and q must vanish. Solving for η_1 and η_2 we get

$$\eta_1 = 1 - 4\, k_1\, a_3^2/(a_2^2 + a_3^2) + 4\, k_1^2\, a_2^2\, a_3^2/(a_2^2 + a_3^2)^2$$

$$\eta_2 = 1 - 4\, k_1 a_2^2/(a_2^2 + a_3^2) + 4\, k_1^2\, a_2^2\, a_3^2/(a_2^2 + a_3^2)^2. \qquad (29)$$

Using eqs. (28) in eq. (27) and the resultant expression in eq. (4) we get

$$\bar{\nabla} \times \bar{u} = 2\left[\,1 - (p - q)/w_1\,\right]\bar{w} = 2(1 - k_1)\bar{w}. \qquad (30)$$

(a) Rigid Flow: In this case $\eta_1 = \eta_2 = 1$ and $v_2 = v_3 = 0$, which leads to $p = q = 0$ and hence eq. (22) gives the vorticity for the rigid flow.

(b) Irrotational Flow: Using eqs. (28) in eq. (30) we have

$$\bar{\nabla} \times \bar{u} = (\bar{w}/2)\sqrt{(\eta_1 - \eta_2)^2 + 8(\eta_1 + \eta_2)}\,.$$

For the flow to be irrotational the quantity on the right hand side must be zero and hence either η_1 or η_2 must be negative.

the shape parameters of the prolate spheroid obtained from the quadrupole moment data and the value of I_E obtained using the energy of $L = 2$ state in eq. (32).

The rotating non-rigid nucleus always undergoes a centrifugal stretching and hence the corresponding change in the potential energy has to be added to H given by eq. (31a) to get the total Hamiltonian of the system. The field experienced by a fluid element, represented by the force components given by eq. (24), is a conservative field since it satisfies $\bar{\nabla} \times \bar{F} = 0$. Hence, the force must be derivable from a scalar potential field. Thus, the total potential energy of the system obtained using the force components given by eq. (24), is

$$V = (M w^2/10) (\eta_1 a_2^2 + \eta_2 a_3^2) \qquad (32a)$$

where M is the mass of the nucleus and η_1 and η_2 are explicitly given by eqs. (29) in terms of a_2, a_3, k_1 and $w = w_1$. It will be shown in VI.8.1 that the potential energy of the nucleus as given by eq. (32a) has the familiar $C\beta^2/2$ form. Thus, if the drop is assumed to undergo uniform rotations with negligible centrifugal stretching, V remains a constant and hence H given by eq. (31a) can as well be taken as the total Hamiltonian of the system.

VI.6 STUDY OF VARIATION OF THE MODEL MOMENT OF INERTIA (I_E)

The model moment of inertia (I_{Ei}) given by eq. (18) depends on the vorticity parameter k_1 and the shape parameter

(c) Rotational Flow: For all values k_1, except 0 and 1, we obtain the rotational flow. But the experimental data indicate that

$$I_R > I_{expt} > I_H$$

and hence to obtain rotational flows which reproduce the experimental values of moments of inertia we must have $0 < k_1 < 1$.

VI.5.3 Study of Lines of Flow

The flow pattern is studied by plotting the velocity components given by eq. (21) with respect to $B(x_1x_2x_3)$ and is shown in Figure VI.1a. The intrinsic velocity $\bar{v}$ is zero at the origin and increases gradually as we go away from the origin and attains its maximum value at the boundary. As the direction of velocity field $\bar{v}$ (clockwise) is opposed to the direction of angular velocity $\bar{w}$ (anti-clockwise) of the whole spheroid, each fluid element in motion along concentric elliptic paths will experience a certain amount of drag which, in effect, results in a sort of slippage of the spheroid. Thus, $\bar{v}$ effectively decreases $\bar{w}$ from its rigid body value and hence causes a reduction in the rotational kinetic energy of the system.

To study the flow line pattern in S, we have plotted the velocity field $\bar{u}$ in S(XYZ) and is shown in Figure VI.1b. The ellipse undergoes a compression along one of the diameters of its director circle followed by a corresponding extension

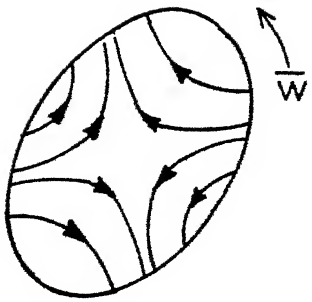

(b)

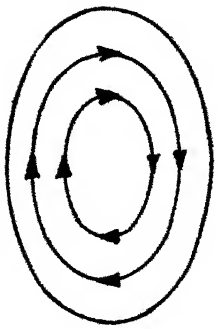

(a)

Fig.VI.1: Lines of flow in the space (b) and body (a) fixed coordinate systems.

along the other. Such a motion effectively introduces a change in the orientation of the ellipse in space. This is true for all other ellipses drawn in planes parallel to YZ-plane. Thus, the spheroid undergoes a net rotation in space about the X-axis.

VI.5.4 Rotational Hamiltonian in Two Dimensions

The constant vorticity rotational flow in two dimensions is characterized by $w_2 = w_3 = 0$ and the vorticity parameter k_1 for rotations about the x_1-axis. In this case, the rotational Hamiltonian reduces to the following form if we use eqs. (17), (15b) and (15c) in eq. (15a)

$$H = L^2/(2I_E) \tag{31a}$$

where

$$I_E = I_R \Big/ \left[1 + \frac{4\, k^2\, a_2^2 a_3^2 (a_3^2 - a_2^2)^2}{\left[(a_3^2 + a_2^2)^2 - 4\, k\, a_2^2\, a_3^2 \right]^2} \right] \tag{31}$$

and the energy eigenvalues are given by

$$E(L,0) = L(L+1)\hbar^2/(2I_E) \tag{32}$$

(In the above equations we have dropped the subscript 1 for the vorticity constant).

Thus, the rotational states in this case are characterized by $K = 0$ and $L = 0, 2, 4,$ etc., giving rise to the ground state rotational band. The value of the vorticity parameter (k) occurring in eq. (31) can be obtained using the known values of

$b_i = (a_j/a_k)$. It will be of theoretical interest to study the variation of (I_{Ei}/I_{Ri}) with k_i for a given b_i, and with b_i for a given k_i.

VI.6.1 Variation of (I_{Ei}/I_{Ri}) with k_i for a given b_i

The variation of (I_{Ei}/I_{Ri}) as a function of k_i, for various values of $b_i \leq 1$, is shown in Figure VI.2. For $b_i = 1$, $(I_{Ei}/I_{Ri}) = 1$ for all values of k_i. Also (I_{Ei}/I_{Ri}) goes to zero for those values of k_i for which

$$k_i = (1 + b_i^2)^2/(4\, b_i^2) \qquad (33)$$

is satisfied. It is clear from the graph that the values of k_i corresponding to the minima in the curve goes on increasing from 1 as we go from $b_i = 1$ to $b_i = 0$. The observed rotational spectrum of even-even nuclei in the rare-earth region indicate that the value of (I_{Ei}/I_{Ri}) is less than 0.55. The quadrupole moment data indicate that the range of the shape parameter b_i is 0.7 to 0.9. In this range of b_i, the values of the quantity (I_{Ei}/I_{Ri}) less than 0.55 are obtained for $0.8 < k_i < 1.9$. However, for $k_i > 1$ the effective moment of inertia (I_{Ei}) goes to zero for a finite deformation, which is contrary to what is observed. We, therefore, consider the valid range of k_i for the nuclei in the rare-earth region as $0.8 < k_i < 1$.

VI.6.2 Variation of (I_{Ei}/I_{Ri}) with b_i for a given k_i

The variation of (I_{Ei}/I_{Ri}) as a function of the shape parameter b_i for various values of k_i is shown in Fig. VI.3. Note that for $b_i = 1$, the effective moment of inertia has the rigid body value for rotational flow, and it has the value zero for the irrotational flow. However, small but finite values of effective moment of inertia are obtained for rotational flow with k_i and b_i slightly less than unity. Such small but finite values can also be obtained with the irrotational flow but with deformations which are much larger than those for the rotational flow. Further, the zero value of the effective moment of inertia can also be obtained with rotational flow, if k_i varies with b_i such that $k_i = 1$ when $b_i = 1$.

VI.7 NEED FOR THE INTRODUCTION OF ELLIPSOIDAL SHAPES

The deformed even-even nuclei in the rare-earth region show a rotational spectrum with band structure which closely resembles that expected of a spheroid. It is therefore assumed that the departure from spheroidal symmetry, if any, is small. To a first order in perturbation, the eigenvalues of the Hamiltonian given by eq. (16) are then given by eq. (20a). Since the expected departure from sphericity is small, we consider eq. (20a) in the approximation $(1/I_{E2} - 1/I_{E1}) \to 0$. The values of I_{E1} and I_{E3} can then be obtained from the energy level data of $L = 2$, $K = 0$ (in the ground state band)

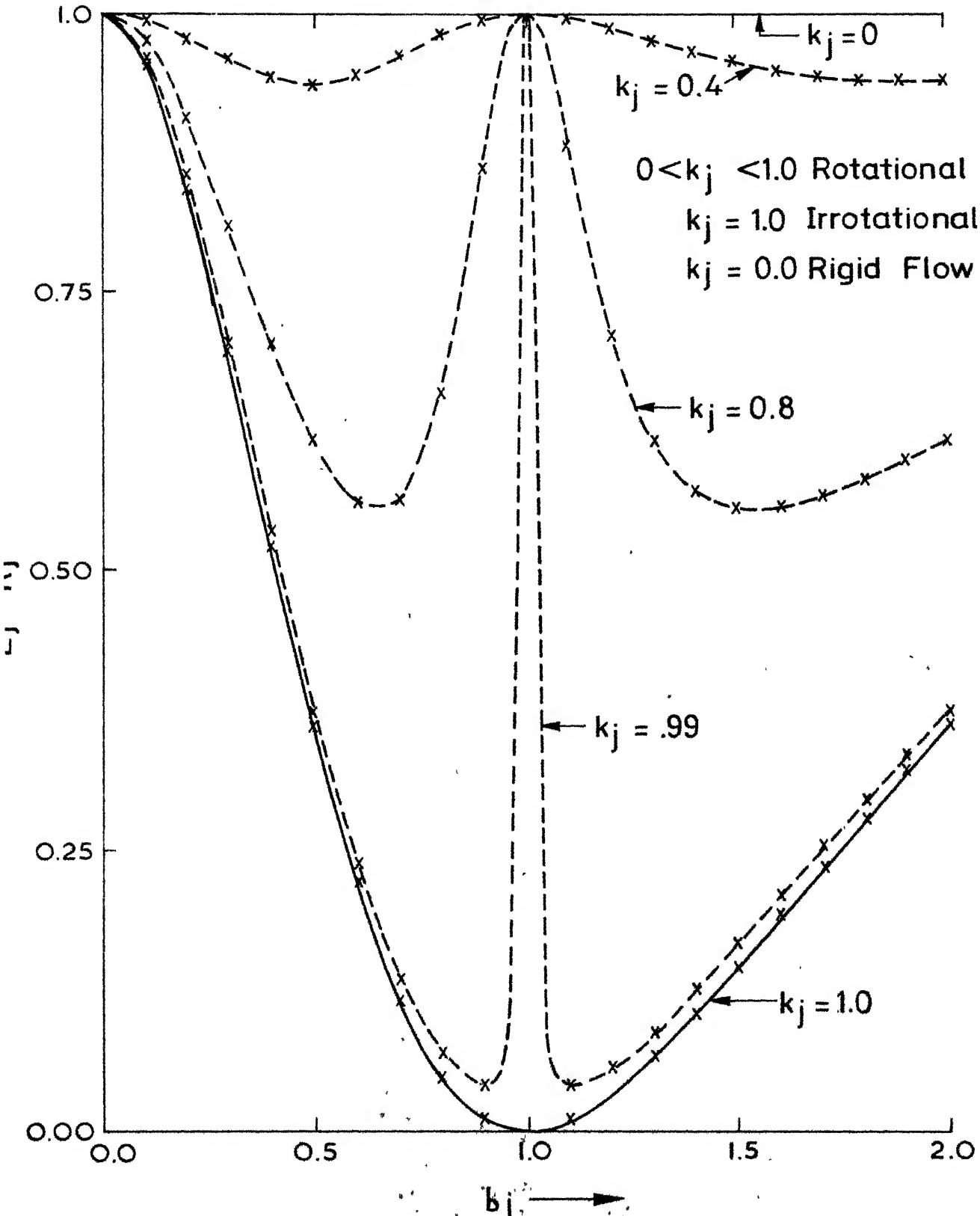

Fig. VI.3 Variation of (I_{Ei}/I_{Ri}) as a function of the shape parameter (b_i) for a given value of the vorticity constant (k_i).

and $L = K = 2$ states using eq. (19b). The values of I_{E3} obtained are small but finite as shown in Table VI.1. These small but finite values of I_{E3} imply that $b_3 = a_1/a_2$ is not unity as can be seen from Figure VI.3. The observed small values of I_{E3} can be reproduced by introducing ellipsoidal asymmetry, i.e., $b_1 \neq 1$. The asymmetry is large for $k_i = 1$ as compared to values of k_i slightly less than unity (see Figure VI.2).

Thus, if the higher rotational bands are assumed to be precessional bands, then according to the continuum model the nucleus must have ellipsoidal deformation.

VI.8 CALCULATIONS

It is clear from eqs. (19b), (20a) and (20b) that all the states in a deformed even-even nucleus can be accounted for in terms of either simple rotational motion of a spheroidal drop or in terms of the precessional motion of an ellipsoidal drop. Explicit calculations have been done for the rotational states in the ground state rotational band and in the excited state rotational band (the so-called β-vibrational band). Both these bands are characterized by $K = 0$.

VI.8.1 Ground State Rotational Band ($K = 0$)

Rotational states in this band are assumed to arise out of rotation of the spheroidal nucleus about an axis perpendicular

TABLE VI.1

Experimental Values of Energies of the L=2 state in the Ground State Band (K=0) and L=2 State in the K=2 Band, and the Corresponding Values of Moments of Inertia

Nucleus	E(2.0) (KeV)	I_{E1} (10^{-10} KeV sec.^{2})	E(2.2)* (KeV)	I_{E3} (10^{-19}KeV sec.^{2})
^{152}Sm	121.8	95.9	1084.0	7.18
^{154}Sm	82.1	142.4	1440.0	5.41
^{154}Gd	123.1	94.9	996.3	7.82
^{156}Gd	89.0	131.3	1154.1	6.75
^{158}Gd	79.5	146.9	1187.1	6.56
^{156}Dy	137.6	84.9	890.6	8.74
^{158}Dy	99.0	118.0	946.0	8.23
^{160}Dy	86.8	134.6	966.1	8.06
^{162}Dy	80.7	144.8	888.2	8.77
^{164}Dy	73.4	159.2	761.8	10.22
^{162}Er	102.0	114.5	901.0	8.64
^{164}Er	91.4	127.8	860.3	9.05
^{166}Er	80.6	145.0	787.0	9.89
^{168}Er	79.8	146.4	821.2	9.48
^{170}Er	79.3	147.3	930.0	8.37
^{168}Yb	88.0	132.7	986.0	7.90
^{170}Yb	84.3	138.6	1138.0	6.84
^{172}Yb	78.7	148.4	1466.0	5.31

TABLE VI.1 (Concluded)

^{176}Yb	82.1	142.3	1270.0	6.13
^{176}Hf	88.4	132.2	1341.2	5.81
^{178}Hf	93.2	125.4	1174.8	6.63
^{180}Hf	93.3	125.2	1200.2	6.49
^{180}W	103.6	112.8	828.0	9.41
^{182}W	100.1	116.7	1221.0	6.38
^{184}W	111.2	105.0	904.0	8.61
^{186}W	122.5	95.4	737.0	10.57
^{186}Os	137.2	85.1	767.4	10.15
^{188}Os	155.0	75.4	633.0	12.13
^{190}Os	180.7	62.6	557.9	13.96

*Mitsuo Sakai (1970).

to the symmetry axis and hence are characterized by $K = 0$ and $L = 0, 2, 4,$ etc. Thus, only one vorticity parameter appears in the calculations. The energy eigenvalues for rotations about the x_1-axis are given by eq. (32) and the corresponding moments of inertia are given by eq. (31).

For 32 even-even rare-earth nuclei the 2^+ state energies and the quadrupole moments are known (Mariscotti et. al. 1969). Assuming the centrifugal stretching to be small, the former data are used to calculate the value of I_E from eq. (32), and the latter is used to calculate the values of the parameters a_2 and a_3 of the spheroid using eq. (4) of Chapter II and the volume constancy condition. These are then used to calculate the value of k from eq. (31). The values of I_{expt}, a_2, a_3, β and k for various nuclei in the rare-earth region are given in Table VI.2. The vorticity parameter k is found to vary linearly with β^2 from nucleus to nucleus as shown in Figure VI.4. The empirical relationship found from this graph is

$$k = 1 - 1.5\,\beta^2 \qquad (34)$$

The above expression fits to $\pm$ 10 %. Notice that for spherical nuclei ($\beta \to 0$) k is unity which corresponds to the irrotational flow with no rotational spectrum. Eqs. (5) of Chapter II with $\gamma = 0$ and eq. (34) are used in eq. (31)

TABLE VI.2

Values of I_{expt}, a_2, a_3, β and k for Various Even-Even Nuclei with Spheroidal Shape in the Rare-Earth Region.

Nucleus	I_{expt} (10^{-19} KeV sec^2)	a_2 (fm)	a_3 (fm)	β	k
^{152}Sm	95.9	5.871	7.620	0.290	0.889
^{154}Sm	142.4	5.827	7.837	0.333	0.826
^{154}Gd	94.9	5.898	7.651	0.290	0.892
^{156}Gd	131.3	5.869	7.826	0.323	0.847
^{158}Gd	146.9	5.867	7.933	0.340	0.828
^{160}Gd	155.1	5.878	8.003	0.348	0.820
^{156}Dy	84.9	5.934	7.654	0.283	0.907
^{158}Dy	118.0	5.914	7.805	0.310	0.869
^{160}Dy	134.6	5.939	7.839	0.310	0.851
^{162}Dy	144.8	5.952	7.902	0.317	0.842
^{164}Dy	159.2	5.956	7.990	0.330	0.825
^{162}Er	114.5	5.975	7.841	0.303	0.878
^{164}Er	127.8	5.989	7.902	0.310	0.865
^{166}Er	145.0	5.990	7.994	0.323	0.848
^{168}Er	146.4	6.017	8.018	0.322	0.850
^{170}Er	147.3	6.057	8.007	0.312	0.852
^{168}Yb	132.7	6.048	7.936	0.303	0.865
^{170}Yb	138.6	6.065	7.986	0.308	0.862

TABLE VI.2 (Concluded)

^{172}Yb	148.4	6.079	8.044	0.313	0.855
^{174}Yb	152.7	6.119	8.030	0.303	0.854
^{176}Yb	142.3	6.157	8.021	0.295	0.869
^{174}Hf	128.5	6.152	7.943	0.284	0.881
^{176}Hf	132.2	6.173	7.981	0.286	0.879
^{178}Hf	125.4	6.239	7.903	0.262	0.891
^{180}Hf	125.2	6.268	7.916	0.258	0.893
^{180}W	112.8	6.286	7.872	0.249	0.904
^{182}W	116.7	6.324	7.863	0.240	0.905
^{184}W	105.0	6.376	7.822	0.225	0.917
^{186}W	95.4	6.407	7.830	0.220	0.926
^{186}Os	85.1	6.444	7.740	0.201	0.935
^{188}Os	75.4	6.491	7.710	0.188	0.944
^{190}Os	62.6	6.530	7.700	0.180	0.954

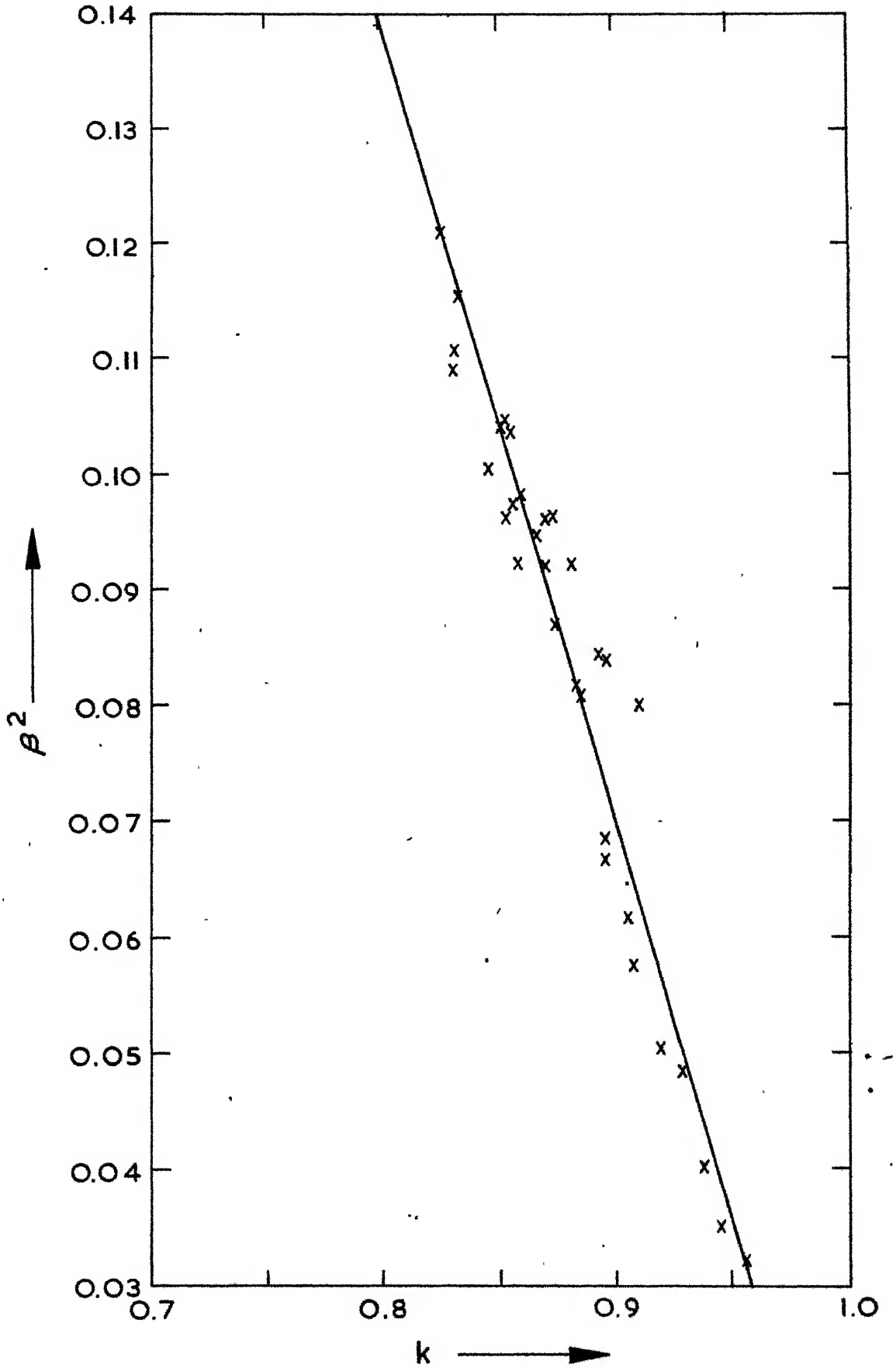

Fig. VI.4: Variation of the vorticity (k) with the square

to get I_E purely as a function of β :

$$I_E = 3B_R \beta^2 [1 + O(\beta)] \qquad (35)$$

where B_R is the mass parameter given by

$$B_R = [(15 + 8\pi)^2/600\pi] M R_o^2 .$$

The potential energy due to centrifugal stretching obtained using eqs. (5) of Chapter II with $\gamma = 0$, and eqs. (29) and (34) in eq. (32a) is approximately of the same form ($C\beta^2/2$) as that given by Bohr and Mottelson (1953) to a first order in β. Thus, the total energy of the system with respect to the ground state of the nucleus is given by (Eder 1970)

$$E(L,0) = [L(L + 1)\hbar^2/2I_E(\beta)] + C(\beta - \beta_o)^2/2 \qquad (36)$$

where β_o is the equilibrium deformation obtained by setting $(\partial E(L,0)/\partial\beta) = 0$ for each L. C is the usual stiffness parameter obtained by fitting the 4^+ state energy data. These values of β_o and C are used to calculate the energies of higher rotational states for fifty nuclei in the region $150 < A < 190$. The results are tabulated in Table VI.3. The maximum departure of the calculated value from the experimental value (Mariscotti et. al. 1969) usually occurred for the highest known level. The maximum departure $(\Delta E)_{max}$ was less than 1 % for 23 nuclei, less than 2 % for 8 nuclei and more than 2 %

Calculated and Experimental Values of Energies, and the Values of the Deformation Parameter β_{L^+} and the Stiffness C for the Rotational States in the Ground State Band (K=0).

Nucleus	L^π	2^+	4^+	6^+	8^+	10^+	12^+	14^+	16^+	18^+	β_{0^+}	C (MeV)	$(\Delta E)_{max}$ (%)
^{150}Nd	1:	132.0	397.0	760.0									
	2:	132.0	397.1	754.5	1183	1670	2209	2796	3428	4101			
	3:	0.2717	0.3001	0.3283	0.3548	0.3794	0.4023	0.4237	0.4439	0.4629	0.2522	40.00	0.9
^{152}Sm	1:	121.8	366.4	712.0	1122	1615							
	2:	121.8	366.3	696.4	1092	1544	2045	2592	3181	3812			
	3:	0.2813	0.3111	0.3406	0.3681	0.3937	0.4175	0.4398	0.4607	0.4805	0.2607	33.30	4.4
^{154}Sm	1:	81.99	267.0	545.0	927.0								
	2:	81.99	267.0	543.6	900.5	1328	1819	2368	2970	3623			
	3:	0.3444	0.3546	0.3678	0.3825	0.3977	0.4129	0.4278	0.4424	0.4565	0.3394	72.00	2.9
^{154}Gd	1:	123.1	371.2	718.1	1146	1644	(2189)						
	2:	123.1	371.2	706.6	1109	1568	2077	2631	3227	3865			
	3:	0.2756	0.3039	0.3322	0.3588	0.3835	0.4065	0.4281	0.4484	0.4675	0.2563	37.00	4.6
^{156}Gd	1:	88.97	288.2	584.5	966.0	1417	1924						
	2:	88.97	288.2	583.4	960.4	1410	1923	2492	3115	3788			
	3:	0.3228	0.3340	0.3481	0.3635	0.3792	0.3947	0.4099	0.4246	0.4388	0.3172	77.00	0.6
^{158}Gd	1:	79.51	261.4	539.0	898.2								
	2:	79.51	261.4	538.6	902.5	1345	1858	2438	3077	3774			
	3:	0.3406	0.3465	0.3548	0.3645	0.3751	0.3861	0.3972	0.4083	0.4193	0.3379	130.00	0.4

^{164}Er	1:	91.20	299.0	608.0	1014	1512							
	2:	91.20	299.0	613.5	1024	1519	2090	2730	3433	4194			
	3:	0.3007	0.3066	0.3148	0.3243	0.3345	0.3451	0.3557	0.3663	0.3767	0.2979	177.00	1.0
^{166}Er	1:	80.60	264.9	545.0	910.0	(1343)							
	2:	80.60	264.9	545.3	913.0	1359	1877	2459	3092	3799			
	3:	0.3204	0.3259	0.3337	0.3428	0.3528	0.3631	0.3736	0.3842	0.3944	0.3178	154.00	0.3
^{168}Er	1:	79.80	264.0	549.0									
	2:	79.80	264.0	548.2	926.9	1393	1941	2565	3259	4020			
	3:	0.3177	0.3207	0.3251	0.3305	0.3367	0.3435	0.3507	0.3580	0.3654	0.3164	300.00	0.1
^{170}Er	1:	79.00	261.0	542.0									
	2:	79.00	261.0	541.2	912.9	1369	1904	2511	3185	3925			
	3:	0.3159	0.3194	0.3244	0.3305	0.3374	0.3449	0.3527	0.3607	0.3685	0.3144	258.00	0.1
^{162}Yb	1:	166.5	486.7	922.9	1444	2013							
	2:	166.5	486.6	904.1	1393	1939	2535	3176	3857	4580			
	3:	0.2240	0.2516	0.2780	0.3022	0.3245	0.3452	0.3645	0.3827	0.3999	0.2033	60.00	3.7
^{164}Yb	1:	122.5	384.0	758.0	1219	1748	2354	(2928)	(3398)				
	2:	122.4	384.0	752.6	1205	1726	2308	2942	3624	4350			
	3:	0.2562	0.2726	0.2911	0.3096	0.3273	0.3445	0.3607	0.3762	0.4350	0.2468	86.00	2.0
^{166}Yb	1:	101.8	329.7	667.1	1097	1604	2172	(2928)	(3803)				
	2:	101.8	329.7	666.8	1097	1606	2185	2825	3522	4266			
	3:	0.2790	0.2882	0.2999	0.3128	0.3259	0.3390	0.3519	0.3644	0.3758	0.2750	134.00	0.5
^{168}Yb	1:	87.90	287.0	582.0	967.0	1427	(1932)						
	2:	87.90	287.0	586.1	972.9	1437	1970	2564	3214	3916			
	3:	0.3004	0.3078	0.3176	0.3288	0.3406	0.3525	0.3644	0.3761	0.3876	0.2969	135.00	0.8
^{170}Yb	1:	84.20	277.7	572.0	962.0	1439	(1986)						
	2:	84.20	277.7	574.3	966.1	1445	2000	2635	3334	4095			
	3:	0.3039	0.3077	0.3133	0.3201	0.3277	0.3357	0.3442	0.3525	0.3609	0.3021	255.00	0.5

TABLE VI.3 (Contd.)

^{172}Yb	1:	78.70	260.3	540.0	910.0	1352							
	2:	78.70	260.3	539.9	911.5	1368	1904	2513	3189	3929			
	3:	0.3127	0.3159	0.3206	0.3264	0.3329	0.3400	0.3475	0.3551	0.3628	0.3113	281.00	1.1
^{174}Yb	1:	76.50	252.0	527.0	892.0								
	2:	76.50	252.0	520.3	873.7	1304	1806	2372	2996	3653			
	3:	0.3149	0.3195	0.3260	0.3338	0.3425	0.3516	0.3609	0.3703	0.3797	0.3128	184.00	2.0
^{176}Yb	1:	82.10	270.0	564.0	947.0								
	2:	82.10	270.0	556.3	932.0	1389	1918	2513	3169	3882			
	3:	0.2981	0.3029	0.3098	0.3175	0.3263	0.3355	0.3448	0.3542	0.3635	0.2959	205.00	1.5
^{166}Hf	1:	158.7	470.7	897.6	1407	1971	2565	(3178)					
	2:	158.7	470.7	883.3	1370	1915	2512	3153	3836	4558			
	3:	0.2235	0.2483	0.2726	0.2953	0.3164	0.3359	0.3543	0.3715	0.3879	0.2060	68.50	3.0
^{168}Hf	1:	123.9	385.0	756.1	1212	1734	2304	(2854)					
	2:	123.9	385.0	748.6	1191	1698	2261	2873	3530	4227			
	3:	0.2495	0.2676	0.2873	0.3068	0.3254	0.3430	0.3598	0.3757	0.3914	0.2388	78.40	2.0
^{170}Hf	1:	100.0	320.6	641.1	1041	1503	2013	2564	3147	(3761)			
	2:	100.0	320.	639.0	1039	1508	2037	2618	3247	3921			
	3:	0.2765	0.2891	0.3043	0.3202	0.3361	0.3515	0.3664	0.3808	0.3946	0.2699	91.00	3.1
^{172}Hf	1:	94.50	307.9	627.0	1036	1519	2063	2651	3273	(3915)			
	2:	94.50	307.9	627.0	1038	1529	2090	2714	3395	4129			
	3:	0.2811	0.2884	0.2982	0.3092	0.3207	0.3324	0.3439	0.3553	0.3664	0.2775	138.00	4.0
^{174}Hf	1:	90.90	298.0	609.0	1010	1502							
	2:	90.90	298.0	610.8	1018	1510	2077	2712	3400	4166			
	3:	0.2839	0.2895	0.2972	0.3061	0.3158	0.3257	0.3357	0.3459	0.3555	0.2813	204.00	0.8
^{176}Hf	1:	88.30	290.0	596.6	998.0								
	2:	88.30	290.0	596.5	997.2	1483	2044	2673	3365	4133			
	3:	0.2854	0.2903	0.2972	0.3054	0.3142	0.3235	0.3328	0.3422	0.3515	0.2831	225.00	0.1

TABLE VI.3 (Contd.)

^{178}Hf	1:	93.20	306.8	632.5	1059								
	2:	93.20	306.8	632.6	1061	1582	2187	2867	3615	4428			
	3:	0.2732	0.2771	0.2828	0.2895	0.2970	0.3048	0.3129	0.3211	0.3292	0.2714	320.00	0.2
^{180}Hf	1:	93.33	308.7	641.1	1085								
	2:	93.33	308.7	640.7	1083	1626	2263	2969	3791	4669			
	3:	0.2696	0.2721	0.2757	0.2802	0.2853	0.2910	0.2969	0.3030	0.3093	0.2685	504.00	0.1
^{172}W	1:	122.7	377.2	727.2	1147	1616	2129	2677	(3252)	(3849)			
	2:	122.7	377.3	727.2	1150	1631	2164	2741	3361	4019			
	3:	0.2463	0.2665	0.2880	0.3087	0.3284	0.3469	0.3646	0.3811	0.3968	0.2337	67.00	2.4
^{174}W	1:	111.9	355.0	704.2	1137	1635	2186	(2780)					
	2:	111.9	355.0	703.2	1135	1636	2197	2810	3470	4175			
	3:	0.2539	0.2673	0.2830	0.2992	0.3150	0.3304	0.3451	0.3592	0.3727	0.2467	103.50	0.5
^{176}W	1:	108.7	348.9	699.4	1140	1648	2206	(2801)	(3425)				
	2:	108.7	348.9	689.6	1138	1654	2233	2869	3576	4294			
	3:	0.2545	0.2649	0.2779	0.2917	0.3055	0.3191	0.3323	0.3449	0.3572	0.2490	135.00	1.2
^{178}W	1:	104.0	342.0	697.0	1152	1679	2264	2894					
	2:	104.0	342.0	704.2	1179	1755	2422	3170	3992	4881			
	3:	0.2564	0.2603	0.2659	0.2725	0.2798	0.2875	0.2953	0.3032	0.3111	0.2546	390.00	8.8
^{180}W	1:	103.6	337.5	690.0	1147	1667	2252						
	2:	103.6	337.5	687.0	1136	1672	2283	2960	3698	4491			
	3:	0.2549	0.2614	0.2701	0.2800	0.2903	0.3008	0.3112	0.3214	0.3314	0.2517	223.00	1.4
^{182}W	1:	100.1	329.4	680.4	1144	(1712)							
	2:	100.1	329.4	679.1	1138	1696	2342	3068	3866	4730			
	3:	0.2565	0.2602	0.2655	0.2719	0.2789	0.2864	0.2940	0.3017	0.3094	0.2548	396.00	0.5
^{184}W	1:	111.2	364.0	748.2									
	2:	111.2	364.0	745.5	1240	1835	2518	3278	4107	5002			
	3:	0.2395	0.2442	0.2507	0.2583	0.2665	0.2749	0.2834	0.2919	0.3002	0.2373	370.00	0.4

TABLE VI.3 (Concluded)

$^{186}_{W}$	1:	122.5	399.6	818.0									
	2:	122.5	399.7	815.0	1350	1988	2715	3523	4401	5323			
	3:	0.2248	0.2300	0.2370	0.2451	0.2536	0.2624	0.2711	0.2797	0.2886	0.2223	394.00	0.4
$^{178}_{0s}$	1:	131.6	397.7	760.8	1194	1682	2218						
	2:	131.6	397.6	756.9	1183	1666	2196	2766	3376	4023			
	3:	0.2308	0.2530	0.2756	0.2971	0.3172	0.3360	0.3537	0.3705	0.3863	0.2161	66.00	1.0
$^{180}_{0s}$	1:	132.2	408.5	795.1	1257	1767	2308	2875					
	2:	132.3	408.4	786.5	1250	1774	2352	2975	3645	4351			
	3:	0.2259	0.2432	0.2618	0.2800	0.2974	0.3139	0.3294	0.3443	0.3584	0.2155	97.60	3.4
$^{182}_{0s}$	1:	126.9	400.2	793.9	1277	1871							
	2:	126.9	400.2	787.0	1263	1811	2421	3083	3794	4548			
	3:	0.2272	0.2402	0.2553	0.2706	0.2855	0.2998	0.3136	0.3267	0.3393	0.2200	136.00	3.1
$^{184}_{0s}$	1:	119.8	383.6	773.9	1275	1871							
	2:	119.8	383.6	766.1	1245	1804	2432	3118	3857	4644			
	3:	0.2311	0.2409	0.2529	0.2656	0.2783	0.2908	0.3029	0.3146	0.3259	0.2261	181.00	3.8
$^{186}_{0s}$	1:	137.2	433.9	868.7	1420	(2068)							
	2:	137.2	433.9	856.4	1377	1978	2645	3370	4147	4970			
	3:	0.2131	0.2245	0.2378	0.2514	0.2648	0.2778	0.2903	0.3022	0.3137	0.2070	187.00	3.0
$^{188}_{0s}$	1:	155.0	477.9	939.8	1514	2170							
	2:	155.0	477.9	922.0	1456	2061	2725	3441	4202	5005			
	3:	0.1992	0.2148	0.2307	0.2467	0.2620	0.2765	0.2902	0.3033	0.3157	0.1901	153.00	5.2
$^{190}_{0s}$	1:	186.7	547.8	1050	1662								
	2:	186.7	547.7	1018	1565	2172	2827	3527	4264	5037			
	3:	0.1820	0.2031	0.2236	0.2426	0.2602	0.2766	0.2919	0.3064	0.3201	0.1668	118.00	6.0

In the above, the rows 1 and 2 respectively denote the calculated and experimental values of energies, and 3 denotes the value of the superfluous parameter β_{L^+}.

for 19 nuclei. The values of stiffness constant that we obtain are found to be comparable to those of Mosel and Greiner (1968) and are considerably greater than those obtained by Mariscotti et. al. (1969). Just as the case of the two mass-point model, the stiffness C increases rapidly with the addition of neutron pairs and decreases gradually with the addition of prot. pairs.

VI.8.2 First Excited Rotational Band (β-Vibrational Band)

Rotational states belonging to this band are also characterized by $K = 0$ and $L = 0, 2, 4$, etc., but they are higher up in energy with respect to the ground state. Hence, in the calculations we have used eq. (36) and the corresponding energy minimization condition obtained by putting $(\partial E/\partial\beta) = 0$ for each L. As there is no quadrupole moment data available for states belonging to this rotational band, the dependence of vorticity parameter k on β was taken to be the same as given by eq. (34).

In the actual calculations we have used the experimental values of $E(0^{+'})$ and $E(2^{+'})$ respectively to obtain the stiffness (C) of the harmonic potential, and equilibrium deformation $\beta_{0^{+'}}$ for the band by exactly fitting the experimental energies. Using these values of the parameters, the energies of higher rotational states belonging to this band have been calculated. The results, for twenty nuclei in the

rare-earth region for which the experimental values of $E(0^{+'})$ and $E(2^{+'})$ are available, are tabulated in Table VI.4. The predicted energies for nuclei in the middle of the region are found to be in excellent agreement with the experimental values. Not very good agreement is obtained for the nuclei in the transition region and for neutron deficient nuclei, implying thereby that these nuclei do not undergo pure rotations. However, slight changes in the fitting of the $E(0^{+'})$ and $E(2^{+'})$ values are found to change the predicted energies of higher rotational states noticeably, and hence a least squares fitting would lead to better results.

The scarcity of data in this band did not enable us to draw any conclusion about the systematics of the stiffness constant C as a function of the neutron number and the proton number.

VI.8.3 Other Higher Rotational Bands and the Determination of the Shape Parameters of the Nucleus of Ellipsoidal Shape

The type of calculations given in the last two sections can be carried on for the rotational states belonging to other higher rotational bands ($K \neq 0$) assuming them to arise out of the precissional motion of the nucleus of ellipsoidal shape. To do this one has to know the values of k_i for values of $b_i = a_j/a_k$ (i,j,k cyclic). Except for $K = 2$ band, the experimental data for other $K \neq 0$ bands is very scarce.

TABLE VI.4

Calculation of the Energies of the Rotational Levels in the First Excited β-vibrational Band of Deformed even-even Nuclei in the Rare-Earth Region

Nucleus	$L^{\pi'}$	$0^{+'}$	$2^{+'}$	$4^{+'}$	$6^{+'}$	$8^{+'}$	$10^{+'}$	$E(0^{+'})$ (KeV)	C (MeV
^{150}Nd	1:	0.0	165.0	465.0					
	2:	0.0	165.0	455.1	820.3	1243	1714	675.0	26.
	3:	0.2050	0.2442	0.2857	0.3220	0.3542	0.3840		
^{150}Sm	1:	0.0	305.7	708.9					
	2:	0.0	305.7	725.7	1208	1738	2310	740.4	31.
	3:	0.1200	0.1900	0.2378	0.2762	0.3092	0.3384		
^{152}Sm	1:	0.0	126.0	341.0					
	2:	0.0	126.0	369.6	691.6	1074	1507	685.0	27.
	3:	0.2438	0.2700	0.3042	0.3365	0.3661	0.3932		
^{154}Sm	1:	0.0	77.8	271.1					
	2:	0.0	77.8	254.1	519.3	865.1	1281	1099.8	73.
	3:	0.3454	0.3498	0.3591	0.3713	0.3850	0.3993		
^{152}Gd	1:	0.0	315.2	666.9	1054				
	2:	0.0	315.2	707.5	1148	1629	2148	615.4	22.4
	3:	0.0993	0.1926	0.2461	0.2885	0.3246	0.3565		
^{154}Gd	1:	0.0	135.0	367.0	685.0	1076	1514		
	2:	0.0	135.0	390.5	723.6	1116	1559	681.0	28.
	3:	0.2320	0.2610	0.2968	0.3299	0.3599	0.3873		
^{156}Gd	1:	0.0	79.7	248.2					
	2:	0.0	79.7	260.8	534.0	889.7	1318	1050.0	92.
	3:	0.3353	0.3391	0.3472	0.3579	0.3702	0.3832		
^{156}Dy	1:	0.0	153.1	412.3					
	2:	0.0	153.1	428.7	779.1	1186	1641	675.6	28.2
	3:	0.2089	0.2435	0.2823	0.3168	0.3475	0.3754		
^{158}Dy	1:	0.0	92.0	287.0	(559.0)				
	2:	0.0	92.0	294.8	589.9	962.3	1400	991.0	62.1
	3:	0.2997	0.3072	0.3215	0.3387	0.3566	0.3744		

TABLE VI.4 (Concluded)

^{164}Er	1: 0.0	68.0	223.9	(457)				
	2: 0.0	68.0	223.0	453.4	750.0	1098	1246.0	
	3: 0.3496	0.3554	0.3670	0.3819	0.3982	0.4128		
^{168}Er	1: 0.0	59.5	194.1	401.0				
	2: 0.0	59.5	196.6	407.5	687.8	1033	1217.0	1
	3: 0.3774	0.3795	0.3842	0.3910	0.3992	0.4084		
^{168}Yb	1: 0.0	77.0	235.0					
	2: 0.0	77.0	251.0	513.3	852.3	1260	1156.0	
	3: 0.3163	0.3203	0.3285	0.3363	0.3519	0.3648		
^{170}Yb	1: 0.0	75.0	159.0					
	2: 0.0	75.0	245.1	501.2	833.3	1233	1069.0	
	3: 0.3178	0.3215	0.3294	0.3399	0.3519	0.3644		
^{172}Yb	1: 0.0	74.9	240.1					
	2: 0.0	74.9	243.8	495.8	820.6	1209	1043.0	
	3: 0.3136	0.3182	0.3276	0.3399	0.3535	0.3675		
^{174}Hf	1: 0.0	72.0	236.0	482.0	805.0	(1185)		
	2: 0.0	72.0	232.1	467.8	767.6	1123	827.0	
	3: 0.3167	0.3234	0.3365	0.3526	0.3697	0.3869		
^{176}Hf	1: 0.0	76.7						
	2: 0.0	76.7	250.0	509.7	844.7	1246	1150.0	
	3: 0.3019	0.3059	0.3141	0.3249	0.3371	0.3498		
^{178}Hf	1: 0.0	78.0	253.5					
	2: 0.0	78.0	254.5	518.9	860.7	1270	1198.0	
	3: 0.2954	0.2991	0.3068	0.3171	0.3287	0.3408		
^{182}W	1: 0.0	119.0	372.0					
	2: 0.0	119.0	372.5	728.6	11164	1665	1138.0	
	3: 0.2229	0.2314	0.2464	0.2632	0.2800	0.2962		
^{184}W	1: 0.0	117.0						
	2: 0.0	117.0	362.0	701.5	1113	1583	1003.0	
	3: 0.2217	0.2322	0.2447	0.2686	0.2872	0.3049		
^{186}W	1: 0.0	123.0						
	2: 0.0	123.0	371.7	707.2	1107	1558	883.0	
	3: 0.2112	0.2255	0.2471	0.2692	0.3098			

(In the above, 1 and 2 denote the experimental and calculated values, respectively of the energies $E(L^{+'})-E(0^{+'})$ and E_{calc} in KeV and 3 denotes the value of the deformation parameter $\beta_{L^{+'}}$. Values within the parentheses involve a lot of experimental uncertainty

However, no quadrupole moment data is available for these states. Hence, we adopt a slightly different method to obtain the values of k_i as a function of b_i in a self-consistent way. For this, it is necessary to estimate the values of shape parameters b_1 , b_2 and b_3.

In order to obtain b_1 , b_2 and b_3 we follow an iterative process starting with initial values obtained from the limiting case of $(1/I_{E2} - 1/I_{E1}) \to 0$. In this case, the values of I_{E1} and I_{E3} can be obtained as mentioned in VI.7 (refer to Table VI.1). Assuming that the nuclear volume is given by $(1.2)^3 A$ fm^3 and using the quadrupole moment data, the shape parameters of the spheroid are obtained. With such values of b_1 for various nuclei, values of k_1 were determined to reproduce values of I_{E1} using eq. (31). Values of k_1 and b_1 so obtained could be fitted with the expression

$$k_i = 1 - \alpha (1 - b_i^2)^2 \qquad (37)$$

where $i = 1$ and α was found to be equal to 0.71 to within $\pm$ 10 %. Note that eq. (37) when expressed in terms of β is of the same form as eq. (34). The values of b_3 to fit the experimental values of I_{E3} are obtained assuming eq. (37) to be valid for $i = 3$ and using eq. (31).

Thus, by considering the limiting case with $(1/I_{E2} - 1/I_{E1}) \to$ we have obtained the relationship between the vorticity constant

and the shape parameter, and an estimate of the value of b_3.

We now consider the case where $(1/I_{E2} - 1/I_{E1})$ is small but finite. For an ellipsoid, the quadrupole moment can be expressed in terms of any two shape parameters such as b_1 , b_3 or b_2 , b_3 using eq. (6) of Chapter II and the volume constancy condition, in the following form

$$Q/e = 0.29\ Z\ (A\ b_1/b_3)^{2/3}\ [(2/b_1^2 - b_3^2 - 1) + \sqrt{6}\ (b_3^2 - 1)] \quad (38a)$$

$$Q/e = 0.29\ Z\ (A\ b_3/b_2)^{2/3}\ [(2b_2^2 - 1/b_3^2 - 1) + \sqrt{6}\ (1 - 1/b_3^2)] \quad (38b)$$

Thus, from the estimate of b_3 , estimates of b_1 and b_2 are obtained using eqs. (38a) and (38b). In the iteration, these values of b_1 , b_2 , b_3 and the parameter $\alpha = 0.71$ are used as the initial values.

In the case $I_{E1} = I_{E2}$, the energy $E(2,0)$ of the ground state band is a function of I_{E1} and I_{E2} according to Eq. (20a). Using eq. (31) and eq. (37), it can be expressed as a function of b_1 , b_2 and α. Using estimates of b_1 and b_2 a new value of α is obtained to fit the observed $E(2,0)$ value. The energy $E(2,2)$ is a function of I_{E1} , I_{E2} and I_{E3} according to eq. (20a). Using eqs. (31) and (38) with the new value of α , it can be expressed as a function of b_1 , b_2 , b_3. Using the estimates of b_1 and b_2 , a new value of b_3 is obtained to fit the value of $E(2,2)$. With the new value of b_3 , new values of b_1 and b_2 are found using eqs. (38).

We have thus obtained new estimates of b_1 , b_2 , b_3 and α. The process was repeated until self-consistency was achieved. The procedure was carried out for 29 nuclei in the rare-earth region for which the energy of $K = L = 2$ state was known. The values obtained are tabulated in Table VI.5.

The self-consistent values of b_1 , b_2 , b_3 and α can be used to calculate the energies of various states in the $K \neq 0$ bands.

Thus, the RFM can also be applied for studying rotational states in all the excited state rotational bands. However, the data is very scarce for bands with $K \neq 0$, except for $K=2$.

VI.9 RESULTS AND THEIR COMPARISON WITH OTHER MODELS

The energies of rotational states belonging to the ground state and the $K=0$ excited state rotational bands (β-vibrational band), calculated on the basis of the rotational flow model are in quite good agreement with the experimental values as compared to other models. Since slight changes in the fitting of lowest levels introduces significant changes in the energy of higher states, a least squares fitting would give better results. However, exact fitting procedure gives proper systematics of the vorticity constant and the stiffness parameter. Also, unlike other phenomenological and empirical models (Diamond, et. al. 1964, Mariscotti et. al. 1969, Sood 1968, Gupta 1969), in the present model, the known correlation

TABLE VI.5

Values of Shape Parameters b_1 , b_2 , b_3 and the Parameter α for Ellipsoidal Shape

Nucleus	Shape Parameters			α
	b_1	b_2	b_3	
^{152}Sm	0.759	1.404	0.938	0.584
^{154}Sm	0.745	1.400	0.959	0.829
^{154}Gd	0.759	1.411	0.934	0.560
^{156}Gd	0.743	1.418	0.948	0.720
^{158}Gd	0.732	1.439	0.950	0.748
^{156}Dy	0.764	1.415	0.925	0.498
^{158}Dy	0.752	1.415	0.940	0.653
^{160}Dy	0.746	1.420	0.944	0.713
^{162}Dy	0.745	1.423	0.942	0.756
^{164}Dy	0.742	1.428	0.943	0.810
^{162}Er	0.754	1.418	0.936	0.606
^{164}Er	0.745	1.432	0.937	0.636
^{166}Er	0.743	1.432	0.940	0.711
^{168}Er	0.745	1.426	0.942	0.710
^{170}Er	0.748	1.413	0.946	0.715
^{168}Yb	0.756	1.395	0.948	0.687
^{170}Yb	0.754	1.392	0.952	0.699
^{172}Yb	0.752	1.388	0.959	0.730

TABLE VI.5 (Concluded)

^{176}Yb	0.765	1.366	0.957	0.727
^{176}Hf	0.769	1.357	0.958	0.690
^{178}Hf	0.783	1.337	0.955	0.701
^{180}Hf	0.784	1.334	0.956	0.691
^{180}W	0.796	1.328	0.946	0.671
^{182}W	0.800	1.306	0.957	0.710
^{184}W	0.805	1.311	0.947	0.649
^{186}W	0.808	1.321	0.937	0.587
^{186}Os	0.820	1.300	0.938	0.582
^{188}Os	0.826	1.306	0.928	0.531
^{190}Os	0.818	1.343	0.910	0.412

between the quadrupole moment and the energy level data has been taken into account in a consistent way. The values of stiffness constant needed to fit the rotational states in the ground state rotational band are comparable to those obtained by Mosel and Greiner (1968) and the variation of the same with the neutron number and the proton number has approximately the same trend as those obtained on the basis of other models, like the two mass-point model, the variable moment of inertia model, etc. The difference in the value of stiffness in the ground state band and the $K=0$ excited state band may be due to the difference in energies of the $L=2$ state and the corresponding $L=0$ state in the respective bands. Further, it is rather interesting to note that a flow with constant vorticity gives a quadratic dependence of the vorticity on the deformation parameter β or the shape parameter b_i such that for spherical nuclei we obtain irrotational flow with no rotational spectrum. The self-consistent calculations give the universal dependence of vorticity on the shape parameter although it fits only to within 20 %.

VI.10 DISCUSSION

The constant vorticity flow given by eq. (13) is unique and hence the corresponding Hamiltonian H given by eq. (15a) is also unique. In fact, the Hamiltonian in its most general form contains a pure rotational energy term, an intrinsic particle

energy term and the coupling between the two, and it goes over to the rigid body case (H_R) for $\vec{\Omega} \equiv 0$ and the irrotational flow case (H_H) for $\vec{\Omega} \equiv \vec{w}$. The relative magnitudes of $\vec{\Omega}$ and $\vec{w}$ determine the strength of rotation-intrinsic particle coupling. The assumption that the frequency of intrinsic particle motion is directly proportional to the rotational frequency (refer to eq. (17)) in order to put the general Hamiltonian H given by eq. (15a) into the familiar rotational form given by eq. (16), leads to the conclusion that the intrinsic motion is directly coupled to the rotational motion meaning thereby that the intrinsic motion always accompanies rotational motion or vice-versa. The vorticity parameters (k_i) which are introduced as proportionality constants play an important role in identifying the type of motion. Thus, when k_i's are comparable to unity, the motion is non-adiabatic and becomes adiabatic only if k_i's are very large compared to unity. However, for $k_i > 1$ the effective moment of inertia I_{Ei} goes to zero for a finite deformation which is contrary to what is observed. Thus, adiabatic motion seems to be unphysical in case of a rotational flow with constant vorticity.

Another important outcome of the RFM is that small but finite values of effective moment of inertia are obtainable with k_i and b_i slightly less than unity (refer to Figures VI.3 and VI.4). Thus, it is possible to account for the observed

values of moments of inertia along all the principal axes of the ellipsoid.on the basis of the RFM. Although, in case of a spheroidal nucleus, the model gives the rigid body moment of inertia along the x_3-axis which remains to be explained, introduction of slight asymmetry about the x_3-axis decreases the moment of inertia considerably from its rigid body value. On the other hand, the irrotational flow model gives a zero value of moment of inertia along the x_3-axis of a spheroidal nucleus, and requires relatively large asymmetry along the x_3-axis to get the same value of moment of inertia. Thus, we conclude that a spheroidal nucleus can undergo rotations about its symmetry axis giving rise to a finite value of moment of inertia, and in the case of a flow with constant vorticity, such rotations give rise to the rigid body moment of inertia. The observed small but finite values of moment of inertia (I_{E3}) about the symmetry axis can be reproduced by introducing slight ellipsoidal asymmetry, i.e., $b_1 \neq 1$. However, the zero value of momcnt of inertia for spherical nuclei is always obtained since the variation of k_i with b_i is such that $k_i = 1$ when $b_i = 1$.

Further, it is clear from eq. (35) that for axially symmetric nuclei rotating about an axis perpendicular to the symmetry axis, the RFM moment of inertia depends quadratically on the deformation parameter β. The same result was obtained

by Bohr and Mottelson (1953) for the case of irrotational flow. However, in case of the RFM the terms in higher powers of β make a significant contribution to the value of I_E. In fact, a comparison of the mass parameter (B_R) obtained on the basis of the rotational flow model with that of the hydrodynamic mass parameter (B_H) gives $(B_R/B_H) = 7.1$. Thus, the RFM has been successful in increasing the value of the hydrodynamic mass parameter, thereby implying that the effective mass participating in the rotation with a rotational flow is about seven times the mass participating in the rotation with an irrotational flow.

Another interesting consequence of the RFM is that it gives the potential energy due to centrifugal stretching in the form $(\beta-\beta_o)^2$ which is in accordance with that obtained by Bohr and Mottelson (1953) and Diamond et. al. (1964), but is contrary to the $(\beta^2-\beta_o^2)^2$ dependence of Mariscotti et. al. (1969). However, the contribution of the potential energy to the total energy is relatively small and hence does not make much of a difference in the calculations. Lastly, for the general three dimensional flow the nature of the effective force and the corresponding potential energy function are quite complicated.

Thus, the RFM provides an energy Hamiltonian for axially symmetric nuclei purely in terms of its deformation or its shape parameter, in the form

$$H(\beta) = \frac{L^2}{2I_E(\beta)} + \frac{C}{2}\beta^2$$

where $I_E(\beta) = 3\left[(15 + 8\pi)^2/600\pi\right]MR_o^2\beta^2\left[1 + O(\beta)\right]$.

REFERENCES

Basset, A.E. (1961). 'A Treatise on Hydrodynamics with Numerous Examples', Dover Publications, New York, p.16.

Bohr, A. and Mottelson, B.R. (1953). Kgl. Danske Videnskab. Selskab. Mat. Fys. Medd. 27, No. 16.

Davidson, J.P. (1968). 'Collective Models of the Nucleus', Academic Press, New York, p. 29.

Diamond, R.M., Stephens, F.S. and Swiatecki, W.J. (1964). Phys. Letters. 11, 315.

Eder, G. (1965). 'Nuclear Forces', Translated by Kaplan, I. (1968). The M.I.T. Press, Massachusetts, p. 220.

Gupta, R.K. (1969). Can. J. Phys. 47, 299, (1972). Phys. Rev. C6, 426.

Jackson, W.D. (1965). 'Classical Electrodynamics', John Wiley and Sons, Inc., New York, p. 139.

Krutov, V.A. (1968). Ann. Physik. 21, 263.

Mariscotti, M.A.J., Goldhaber, G.S. and Buck, B. (1969). Phys. Rev. 178, 1864.

Mosel, U. and Greiner, W. (1968). Z. Physik. 217, 256.

Rowe, D.J. (1970). Nucl. Phys. A152, 273.

Sood, P.C. (1968). Can. J. Phys. 46, 1419.

Trainor, L.E.H. and Gupta, R.K. (1971). Can. J. Phys. 49, 133.

C H A P T E R - VII

SUMMARY

The quantum mechanical treatment of the simple two mass-point model gives the rotational-vibrational energy of a deformed even-even rare-earth nucleus in a closed form with an L-dependent zero-point energy term which contributes considerably to the energy of high spin states with no break-down in the rotational structure. The model successfully correlates the intrinsic quadrupole moment data with the moment of inertia more satisfactorily than the rigid spheroid or the hydrodynamic models. The two mass-point mass parameter (B_T) is about half of the hydrodynamic value (B_H), and the corresponding moment of inertia (I_T) is about a third of the

rigid spheroid value (I_R), for values of $\beta \simeq 0.3$. However, unlike I_H, I_T does not go to zero with β. Further, the model gives proper values of intrinsic quadrupole moments and $B(E2; 4^+ \rightarrow 2^+)/B(E2; 2^+ \rightarrow 0^+)$ for transitions of the type $L + 2 \rightarrow L$. The variation of the stiffness (C) of the harmonic potential with the neutron number and with the proton number are in accordance with those found on the basis of various other models.

Use of the anharmonic Morse potential with exactly the same stiffness as that of the harmonic potential did not give any noticeable improvement in the fitting of energy levels.

Both the potentials give almost the same values of the parameters (I_o and C), and the largest value of the stiffness is obtained for ^{180}Hf, an almost 'rigid rotor'. Both the potentials yield excellent results when a least squares fitting procedure is adopted.

The states belonging to the first excited β-vibrational band can also be analysed on the basis of the two mass-point model. However, the data available is scarce.

The two mass-point model fails to account for the S-type systematics observed for the nuclei of interest. The main drawback of the model is that it does not give zero moment of inertia for the case of spherical nuclei. However,

this has been taken care of in the generalised two mass-point model with a rotationally invariant core of variable radius, and a quantum mechanical treatment of the same would, perhaps, yield improved results as compared to the simple two mass-poimt model.

The rotational flow model (RFM) based on the principles of continuum mechanics with a constant vorticity flow in three dimensions gives satisfactory values of energies and deformations for the even-even nuclei in the rare-earth region. The proposed rotational flow in three dimensions is unique and hence the corresponding Hamiltonian is also unique. The Hamiltonian (H) and the angular momentum (L) thus obtained, in their most general form, contain three terms corresponding to pure rotational motion, the intrinsic-particle motion and the coupling between the two, and they go over to the rigid body case and the irrotational flow case under appropriate limits of the vorticity. The general Hamiltonian can be put into the familiar rotational form ($L^2/2I$) only if it is assumed that the frequency of intrinsic-particle motion is directly coupled to the rotational frequency through the vorticity parameters. Thus, the velocity field directly depends on the rotational frequency of the ellipsoidal boundary and hence the adiabatic motion seems to be not possible in this case.

By far the most interesting aspect of the RFM is the study of variation of (I_{Ei}/I_{Ri}) as a function of k_i for a given b_i, and as a function of b_i for a given k_i. Whereas the former gives the physically valid range of vorticity constant (k) for the nuclei of interest as $0.8 < k < 1$, the latter shows that small but finite values of moment of inertia along the symmetry axis could be obtained for values of k_i and b_i slightly less than unity. Both the graphs indicate if the higher rotational bands are assumed to be precessional bands, then according to the continuum model the nucleus must have ellipsoidal deformation. Thus, the rotational states in the higher rotational bands can be analysed on the basis of the RFM. Further, the graphs indicate that within the framework of the RFM, a spheroidal nucleus can undergo rotations about its symmetry axis giving rise to a finite value of moment of inertia, and in the case of a flow with constant vorticity, such rotations give rise to the rigid body moment of inertia. The observed small but finite values of moment of inertia (I_{E3}) about the symmetry axis can be reproduced by introducing slight ellipsoidal asymmetry. However, the zero value of moment of inertia for spherical nuclei is always obtained since the variation of k_i with b_i is such that $k_i = 1$ when $b_i = 1$.

Also, for axially symmetric nuclei rotating about an axis perpendicular to the symmetry axis, the RFM moment of

inertia depends quadratically on the deformation parameter β. However, the terms in higher powers of β make a significant contribution to the value of I. In fact, the RFM mass parameter, thus obtained, is about seven times the hydrodynamic mass parameter implying thereby that the effective mass participating in the rotational motion with rotational flow is about seven times the mass participating in the rotational motion with an irrotational flow.

In the case of a simple two dimensional flow, the RFM is found to give a β^2 dependent potential energy term arising out of the centrifugal stretching of the rotating nucleus. Thus, the RFM provides an energy Hamiltonian for axially symmetric nuclei purely in terms of its deformation or its shape parameter.

The RFM fails to account for the S-type systematics observed for the nuclei of interest and an attempt to reproduce the same is desirable. Application of the RFM to the study of deformed nuclei in other regions of the periodic table may be of interest while examining the validity of the model in general. As an extension of the work presented in this thesis, it will be interesting to study the nature of the effective force and the corresponding potential energy function in the case of the general three dimensional constant vorticity flow. Further, as the deformed nuclei can not only rotate but also vibrate, it

will be of use to investigate the possibility of including shape vibrations of the ellipsoidal drop by considering its shape parameters to be time dependent. This will be useful to account for the spectra of spherical nuclei on the basis of the rotational flow model.

APPENDIX I

It is known that the energy of rotational states in the ground state rotational band increases with the angular momentum L of the state in accordance with the L(L+1) rule. In this case the moment of inertia is defined as

$$\frac{2I}{\hbar^2} = \left[\frac{dE}{d\{L(L+1)\}} \right]^{-1} \qquad (I.1)$$

and the corresponding rotational frequency is defined as

$$\hbar w = \frac{dE}{d\sqrt{L(L+1)}} \qquad (I.2)$$

In order to investigate the variation of $(2I/\hbar^2)$ with $\hbar^2 w^2$, the quantities on the right hand side of eqs. (I.1) and (I.2) are obtained by replacing the derivative with the corresponding differential quotient evaluated between the spin values L and L-2. Thus, using

$$dE = E(L) - E(L-2)$$

$$d\{L(L+1)\} = L(L+1) - (L-2)(L-1) = 2(2L-1)$$

we obtain

$$\hbar^2 w^2 = \frac{L^2-L+1}{(2L-1)^2} \left[E(L) - E(L-2) \right]^2 \text{ KeV}^2$$

and

$$\frac{2I}{\hbar^2} = \frac{2(2L-1)}{E(L) - E(L-2)} \text{ KeV}^{-1}$$

which are eqs. (8) and (9) of Chapter II.

APPENDIX - II

II.1 To obtain the angular momentum components in their operator form

We have the correspondence relation

$$(\alpha_1 \ \alpha_2 \ \alpha_3) \longleftrightarrow (\phi \ \theta \ \psi) \longleftrightarrow (\alpha_X \ \alpha_Y \ \alpha_Z)$$

So one can write

$$\alpha_j = \alpha_j (\phi \ \theta \ \psi)$$

Taking the time derivative

$$\dot{\alpha}_j = w_j = \frac{\partial \alpha_j}{\partial \phi} \dot{\phi} + \frac{\partial \alpha_j}{\partial \theta} \dot{\theta} + \frac{\partial \alpha_j}{\partial \psi} \dot{\psi}$$

Now, by comparing these w_j's with those given by eq. (3a), we get

$$\frac{\partial \alpha_1}{\partial \phi} = \text{Sin } \theta \ \text{Sin } \psi \ ; \quad \frac{\partial \alpha_1}{\partial \theta} = \text{Cos } \psi \ ; \quad \frac{\partial \alpha_1}{\partial \psi} = 0$$

$$\frac{\partial \alpha_2}{\partial \phi} = \text{Sin } \theta \ \text{Cos } \psi \ ; \quad \frac{\partial \alpha_2}{\partial \theta} = -\text{Sin } \psi \ ; \quad \frac{\partial \alpha_2}{\partial \psi} = 0$$

$$\frac{\partial \alpha_3}{\partial \phi} = \text{Cos } \theta \ ; \quad \frac{\partial \alpha_3}{\partial \theta} = 0 \ ; \quad \frac{\partial \alpha_3}{\partial \psi} = 1 \ .$$

Writing $\phi = \phi (\alpha_1 \ \alpha_2 \ \alpha_3)$ yields

$$\frac{\partial}{\partial \phi} = \frac{\partial \alpha_1}{\partial \phi} \cdot \frac{\partial}{\partial \alpha_1} + \frac{\partial \alpha_2}{\partial \phi} \cdot \frac{\partial}{\partial \alpha_2} + \frac{\partial \alpha_3}{\partial \phi} \cdot \frac{\partial}{\partial \alpha_3}$$

Using the above equations, we get

$$\frac{\partial}{\partial\phi} = \text{Sin}\,\theta\ \text{Sin}\,\psi\ \frac{\partial}{\partial\alpha_1} + \text{Sin}\,\theta\ \text{Cos}\,\psi\ \frac{\partial}{\partial\alpha_2} + \text{Cos}\,\theta\ \frac{\partial}{\partial\alpha_3}$$

Similarly one can obtain

$$\frac{\partial}{\partial\theta} = \text{Cos}\,\psi\ \frac{\partial}{\partial\alpha_1} - \text{Sin}\,\psi\ \frac{\partial}{\partial\alpha_2} \quad \text{and} \quad \frac{\partial}{\partial\psi} = \frac{\partial}{\partial\alpha_3}$$

Solve for $(\partial/\partial\alpha_j)$ to get eqs. (19a). Similarly, we can write

$$\alpha_X = \alpha_X\,(\phi\ \theta\ \psi)$$

Taking the time derivative

$$\dot{\alpha}_X = w_X = \frac{\partial\alpha_X}{\partial\phi}\ \dot{\phi} + \frac{\partial\alpha_Y}{\partial\theta}\ \dot{\theta} + \frac{\partial\alpha_Z}{\partial\psi}\ \dot{\psi}$$

Now, comparing these $w_{X,Y,Z}$ with those given by eqs. (3b) we have

$$\frac{\partial\alpha_X}{\partial\phi} = 0\ ; \quad \frac{\partial\alpha_X}{\partial\theta} = \text{Cos}\,\phi\ ; \quad \frac{\partial\alpha_X}{\partial\psi} = \text{Sin}\,\theta\ \text{Sin}\,\phi$$

$$\frac{\partial\alpha_Y}{\partial\phi} = 0\ ; \quad \frac{\partial\alpha_Y}{\partial\theta} = \text{Sin}\,\phi\ ; \quad \frac{\partial\alpha_Y}{\partial\psi} = -\text{Sin}\,\theta\ \text{Cos}\,\phi$$

$$\frac{\partial\alpha_Z}{\partial\phi} = 1\ ; \quad \frac{\partial\alpha_Z}{\partial\theta} = 0\ ; \quad \frac{\partial\alpha_Z}{\partial\psi} = \text{Cos}\,\theta\ .$$

Following the same procedure as before we get eqs. (19b).

Consider $L^2 = L_1^2 + L_2^2 + L_3^2 = \hbar^2 \left[\frac{\partial^2}{\partial\alpha_1^2} + \frac{\partial^2}{\partial\alpha_2^2} + \frac{\partial^2}{\partial\alpha_3^2}\right]$

Using eqs. (19a) we get

$$\frac{\partial^2}{\partial\alpha_1^2} = \frac{\text{Sin}^2\psi}{\text{Sin}^2\theta}\ \frac{\partial^2}{\partial\phi^2} + \text{Cos}^2\psi\ \frac{\partial^2}{\partial\theta^2} + \text{Sin}^2\psi\ \text{Cot}^2\,\theta\ \frac{\partial^2}{\partial\psi^2} - \frac{2\text{Sin}\,\psi\ \text{Cos}\,\psi\ \text{Cot}}{\text{Sin}\,\theta}$$

$$+ \text{Sin}^2\psi\ \text{Cot}\,\theta\ \frac{\partial}{\partial\theta} + \text{Sin}\,\psi\ \text{Cos}\,\psi\ \frac{(1+\text{Cos}^2\,\theta)}{\text{Sin}^2\,\theta}\ \frac{\partial}{\partial\psi}\ .$$

Similarly,

$$\frac{\partial^2}{\partial\alpha_2^2} = \frac{\mathrm{Cos}^2\psi}{\mathrm{Sin}^2\theta}\frac{\partial^2}{\partial\phi^2} + \mathrm{Sin}^2\psi\frac{\partial^2}{\partial\theta^2} + \mathrm{Cos}^2\psi\,\mathrm{Cot}^2\theta\frac{\partial^2}{\partial\psi^2} + \frac{2\mathrm{Sin}\,\psi\,\mathrm{Cos}\,\psi\,\mathrm{Cot}\,\theta}{\mathrm{Sin}\,\theta}$$

$$+ \mathrm{Cos}^2\psi\,\mathrm{Cot}\,\theta\frac{\partial}{\partial\theta} - \mathrm{Sin}\,\psi\,\mathrm{Cos}\,\psi\frac{(1+\mathrm{Cos}^2\theta)}{\mathrm{Sin}^2\theta}\frac{\partial}{\partial\psi}$$

and

$$\frac{\partial^2}{\partial\alpha_3^2} = \frac{\partial^2}{\partial\psi^2}.$$

Adding the three leads to

$$L^2 = -\hbar^2\left[\frac{1}{\mathrm{Sin}^2\theta}\frac{\partial^2}{\partial\phi^2} + \frac{1}{\mathrm{Sin}\,\theta}\frac{\partial}{\partial\theta}\left(\mathrm{Sin}\,\theta\frac{\partial}{\partial\theta}\right) + \frac{1}{\mathrm{Sin}^2\theta}\frac{\partial^2}{\partial\psi^2}\right] \quad (20).$$

Similarly, working with α_X, α_Y, α_Z we will end up with the same result for L^2.

II.2 Commutation Relations

Using the operator form of L_1, L_2, L_3 and L_X, L_Y, L_Z the following relations can easily be verified

$$\left[L_1, L_2\right] = -i\hbar L_3 \quad \text{and cyclic in } 1,2,3$$

and (21)

$$\left[L_X, L_Y\right] = +i\hbar L_Z \quad \text{and cyclic in } X,Y,Z.$$

The above relations are used to verify

$$\left[L_1^2, L_3\right] = +i\hbar\left[L_1, L_2\right]_+$$

$$\left[L_2^2, L_3\right] = -i\hbar\left[L_1, L_2\right]_+$$

and

$$\left[L_X^2, L_Z\right] = -i\hbar\left[L_X, L_Z\right]_+$$

$$\left[L_Y^2, L_Z\right] = +i\hbar\left[L_X, L_Z\right]_+$$

where the subscript '+' indicates that the quantity is an anti-commutator.

From the above it follows that

$$\left[L^2, L_3\right] = \left[L^2, L_Z\right] = 0$$

and

$$\left[L^2, L_j\right] = \left[L^2, L_{X,Y,Z}\right] = 0 \qquad (21a)$$

Also the above relations can be used to verify

$$\left[L^2, L_1^2\right] = \left[L^2, L_2^2\right] = \left[L^2, L_3^2\right] = 0$$

and

$$\left[L^2, L_X^2\right] = \left[L^2, L_Y^2\right] = \left[L^2, L_Z^2\right] = 0 \,. \qquad (21b)$$

II.3 To Obtain the Rotation Operator $\bar{R}(\phi\ \theta\ \psi)$ Explicitly

In order to obtain $\bar{R}(\phi\ \theta\ \psi)$ explicitly, it is necessary to study the effect of rotation on a given function $f(XYZ)$. Consider a rotation of a point fixed in $B(x_1 x_2 x_3)$ frame through an angle α about the common Z-x_3 axes. Then

$$x_1 = X \text{ Cos } \alpha + Y \text{ Sin } \alpha$$
$$x_2 = -X \text{ Sin } \alpha + Y \text{ Cos } \alpha$$
$$x_3 = Z \,.$$

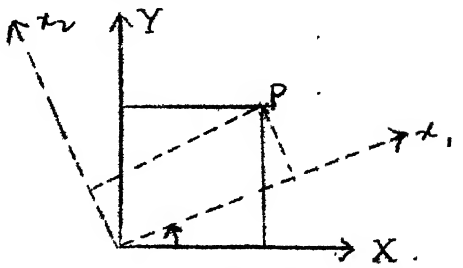

Now $\bar{R}(\alpha)\ f(XYZ) = f(x_1 x_2 x_3) = f(X \text{ Cos } \alpha + Y \text{ Sin } \alpha, -X \text{ Sin } \alpha + Y \text{ Cos }$

For infinitesimal rotation α is small and hence a Taylor expansion of f can be made about $\alpha = 0$, which is much easier

if we work in spherical polar coordinates ($r\ \theta\ \phi$), where

$$X = r \sin\theta \cos\phi$$
$$Y = r \sin\theta \sin\phi$$
$$Z = r \cos\theta$$

Then $R\, f(XYZ) = R\, f(r, \theta, \phi) = f(r, \theta, \phi - \alpha) = e^{-\alpha \frac{\partial}{\partial \phi}} f(r\ \theta\ \phi)$ where the exponential is the well-known symbolic form of the infinite Taylor series.

If $\bar{L}$ is the orbital angular momentum then

$$L_Z = \frac{\hbar}{i} \frac{\partial}{\partial \phi}$$

Thus

$$R(\alpha)\, f(XYZ) = e^{\frac{-i\alpha}{\hbar} L_Z} f(XYZ) .$$

If $\bar{e}_Z$ is the unit vector along the Z-axis, then

$$R(\alpha)\, \Psi = e^{\frac{-i\alpha}{\hbar} (\bar{L} \cdot \bar{e}_Z)} \Psi$$

where Ψ is the wave function describing the system. This can be written in a more general form

$$R(\alpha)\, \Psi = e^{\frac{-i\alpha}{\hbar} (\bar{L} \cdot \bar{n})} \Psi$$

where $R(\alpha)$ symbolizes a rotation through an angle α about any axis and $\bar{n}$ is a unit vector along that axis.

If α is small, we can expand the above equation

$$R(\alpha)\psi = \left[1 - \frac{i\alpha}{\hbar} (\bar{L}.\bar{n}) + O(\alpha^2) \right] \psi$$

giving the first order change in ψ due to $R(\alpha)$ as $-\frac{i\alpha}{\hbar} (\bar{L}.\bar{n})\psi$. For this reason the three angular momentum operators L_X, L_Y, L_Z are also referred to as the infinitesimal rotation operators. $(\bar{L}.\bar{n})$ will simply be some linear combination of these operators, the coefficients depending on the direction of $\bar{n}$ of the axis of rotation. Thus, it is possible to write the individual rotations $R(\phi)$, $R(\theta)$, $R(\psi)$ explicitly.

$$R(\phi) = e^{\frac{-i\phi}{\hbar} L_Z}$$

$$R(\theta) = e^{\frac{-i\theta}{\hbar} L_{x'_1}}$$

$$R(\psi) = e^{\frac{-i\psi}{\hbar} L_3}$$

so that

$$R(\phi\ \theta\ \psi) = R(\psi)\ R(\theta)\ R(\phi) = e^{\frac{-i\psi}{\hbar} L_3} \quad e^{\frac{-i\theta}{\hbar} L_{x'_1}} \quad e^{\frac{-i\phi}{\hbar} L_Z}.$$

A simple geometrical argument (Rose, 1957) leads to

$$R(\phi\ \theta\ \psi) = e^{\frac{-i\phi}{\hbar} L_Z} \quad e^{\frac{-i\theta}{\hbar} L_x} \quad e^{\frac{-i\psi}{\hbar} L_Z}$$

which is equation (23).

II.4 Properties of D-functions

Here, we will list some important properties of the D-functions without going into the details of derivation.

(a) Taking the complex conjugate of eq. (25) of the text

$$D^{L}_{MK}(\mathcal{R}) = \langle LM|\, e^{\frac{-i}{\hbar}(\phi L_Z + \theta L_X + \psi L_Z)} |LK\rangle^*$$

$$= \left(\psi(LM),\ e^{\frac{-i}{\hbar}(\phi L_Z + \theta L_X + \psi L_Z)}\ \psi(LK) \right)^* \quad \text{(Change of notatio}$$

$$= \left(e^{\frac{i\phi}{\hbar} L_Z}\ \psi(LM),\ e^{\frac{-i}{\hbar}(\theta L_X + \psi L_Z)}\ \psi(LK) \right)^* \quad \text{(Since } e^{\frac{-i\phi}{\hbar} L_Z} \text{ is unitary)}$$

$$= e^{iM'\phi}\ (LM|\, e^{\frac{-i\theta}{\hbar} L_X} |LK)^*\ e^{iK\psi}$$

$$D^{L}_{MK}(\mathcal{R}) = e^{iM\phi}\ d^{L}_{MK}(\theta)\ e^{iK\psi} \qquad (25a)$$

where $$d^{L}_{MK}(\theta) = (LM|\, e^{\frac{-i\theta}{\hbar} L_X} |LK) \qquad (25b)$$

By group theoretical methods Wigner has shown that

$$d^{L}_{MK}(\theta) = \sqrt{(L+M)!\ (L+K)!\ (L-M)!\ (L-K)!}$$

$$\cdot \sum_p \frac{(-1)^p\ (\cos\tfrac{\theta}{2})^{2L+K-M-2p}\ (\sin\tfrac{\theta}{2})^{M-K+2p}}{p!(L-M-p)!\ (L+K-p)!\ (p+M-K)!}$$

where the summation extends over all integral values of p for which the arguments of the factorials are non-negative. Notice that $d^{L}_{MK}(\theta)$ is real, that is why the complex conjugation in eq. (25b) has been omitted. Thus, our definition of $d^{L}_{MK}(\theta)$ is in accordance with definition given by Rose, although our $D^{L}_{MK}(\mathcal{R})$ is the complex conjugate of $D^{L}_{MK}(\mathcal{R})$ given by Rose (1957).

(b) Properties of $d^L_{MK}(\theta)$

Since the inverse of rotation $\exp(-i\theta L_X)$ is $\exp(i\theta L_X)$, a rotation about X through $-\theta$ means

$$d^L_{MK}(\theta) = d^L_{MK}(-\theta)$$

which leads to

$$d^L_{MK}(\theta) = (-1)^{M-K} \; d^L_{-M,-K}(\theta) \tag{25c}$$

For the particular case of $\theta = \pi$ we have the very simple result

$$d^L_{MK}(\pi) = (-1)^{L-K} \; \delta(M+K, 0) \tag{25d}$$

In terms of $D^L_{MK}(\gamma)$ we have

$$D^L_{MK}(\gamma)^* = (-1)^{M-K} \; D^L_{-M,-K}(\gamma) \tag{25e}$$

The rotation matrices possess the usual orthonormality properties

$$\begin{aligned} \sum_K D^L_{MK}(\gamma)^* \; D^L_{M'K}(\gamma) &= \delta_{M,M'} \\ \sum_K D^L_{KM}(\gamma) \; D^L_{KM'}(\gamma) &= \delta_{M,M'} \end{aligned} \tag{25f}$$

Coupling rules for the $D^{(L)}$ are given by

$$D^{L_1}_{M_1K_1}(\gamma) \; D^{L_2}_{M_2K_2}(\gamma) = \sum_L (L_1L_2M_1M_2|LM)(L_1L_2K_1K_2|LK) \; D^L_{MK} \tag{25g}$$

where $L = L_1+L_2$, $M = M_1+M_2$ and $K = K_1+K_2$.

Using orthogonality relations we can invert (25g) to give

$$D^{L}_{MK}(\nu) = \sum_{M_1 K_1} (L_1 L_2 M_1\ M-M_1 | LM)(L_1 L_2 K_1\ K-K_1 | LK) D^{L_1}_{M_1 K_1}(\nu)\ D^{L_2}_{M-M_1, K-K_1}$$

...(25h)

In eq. (24) of the text, the functions Ψ will in general consists of a radial and angular part which are simply the spherical harmonics Y_{LM}. In the case of pure rotations the radial part does not change and hence can be dropped out of the equation (24). Thus, we get

$$Y_{LM}(\theta'\ \phi') = \sum_{K} D^{L}_{MK}(\nu)^{*}\ Y_{LK}(\theta\ \phi) \qquad (25i)$$

where (θ, ϕ) indicate the spherical polar coordinates in the S-frame and (θ', ϕ') in the B-frame.

Integrals of products of D-functions over an unit sphere are given by

$$\int D^{L_1}_{M_1 K_1}(\nu)^{*}\ D^{L_2}_{M_2 K_2}(\nu)\, d\nu = \frac{8\pi^2}{2L_1+1}\ \delta(L_1 L_2)\ \delta(M_1 M_2)\ \delta(K_1 K_2)$$

... (25j)

and

$$\int D^{L_1}_{M_1 K_1}(\nu)^{*}\ D^{L_2}_{M_2 K_2}(\nu)\ D^{L_3}_{M_3 K_3}(\nu)\, d\nu =$$

$$= \frac{8\pi^2}{2L_1+1}\ \delta(M_1, M_2+M_3)\ \delta(K_1, K_2+K_3)\ (L_2 L_3 M_2 M_3 | L_1 M_1)\ (L_2 L_3 K_2 K_3 | L_1 K_1)$$

...(25k)

For either M or K = 0 the $D^{L}_{MK}(\nu)$ reduce to spherical harmonics

$$D^{L}_{M0}(\phi\ \theta\ 0) = \left[\frac{4\pi}{2L+1}\right]^{\frac{1}{2}} Y_{LM}(\theta\ \phi) \qquad (25l)$$

$$D^L_{0K}(0\ \theta\ \phi) = (-1)^K \left[\frac{4\pi}{2L+1}\right]^{\frac{1}{2}} Y_{LK}(\theta\ \phi) \qquad (25m)$$

II.5 To determine the action the relabeling transformations T_1, T_2 of III.5.5 have upon these functions, we use

$$T_1(\phi_1, \phi_2, \phi_3)\ D^L_{MK}(\gamma) = \sum_{K'} D^L_{MK'}(\gamma)\ D^L_{K'K}(\gamma)$$

(a) Since the operation T_1 is the rotation π about the 2-axis

$$\phi_1 = \phi_3 = 0 \quad \text{and} \quad \phi_2 = \pi$$

and using $$D^L_{MK}(0, \pi, 0) = (-1)^{L+K} \delta_{M,-K}$$

we get

$$T_1\ D^L_{MK}(\gamma)^* = (-1)^{L-K}\ D^L_{M,-K}(\gamma) \qquad (25n)$$

(b) Since T_2^2 is two successive rotations of $\pi/2$ about the 3-axis clearly

$$D^L_{MK}(0\ 0\ \pi) = e^{-iK\pi} \delta_{K,M}$$

and hence

$$T_2^2\ D^L_{MK}(\gamma)^* = e^{iK\pi}\ D^L_{MK}(\gamma)^* \qquad (25p)$$